

# **Improving the cathode of a Microbial Fuel Cell for efficient electricity production**

*Annemiek ter Heijne*

### **Thesis committee**

#### **Thesis supervisor**

Prof.dr. C.J.N. Buisman  
Professor of Biological Recycling Technology  
Wageningen University

#### **Thesis co-supervisor**

Dr.ir. H.V.M. Hamelers  
Assistant professor  
Sub-department of Environmental Technology

#### **Other members**

Prof.dr. G. Eggink, Wageningen University  
Prof.dr. U. Schröder, Technical University Braunschweig, Germany  
Prof.dr.ir. W. Verstraete, Ghent University, Belgium  
Prof.dr.ir. M.C.M. van Loosdrecht, Delft University of Technology

This research was conducted under the auspices of the Graduate School SENSE (Socio-Economic and Natural Sciences of the Environment).

# Improving the cathode of a Microbial Fuel Cell for efficient electricity production

Annemiek ter Heijne

## **Thesis**

submitted in fulfilment of the requirements for the degree of doctor

at Wageningen University

by the authority of the Rector Magnificus

Prof.dr. M.J. Kropff,

in the presence of the

Thesis Committee appointed by the Academic Board

to be defended in public

on Friday 3 December 2010

at 1:30 p.m. in the Aula

Annemiek ter Heijne

Improvement of the cathode of a Microbial Fuel Cell for efficient electricity production,  
161 pages.

Thesis, Wageningen University, Wageningen, NL (2010)

With references, with summaries in Dutch and English

ISBN: 978-90-8585-821-8

For my parents



# Table of contents

Chapter 1	Introduction	3
Chapter 2	Performance of non-porous graphite and titanium-based anodes in Microbial Fuel Cells	25
Chapter 3	A bipolar membrane combined with ferric iron reduction as an efficient cathode system in Microbial Fuel Cells	43
Chapter 4	Microbial Fuel Cell operation with continuous biological ferrous iron oxidation of the catholyte	61
Chapter 5	Cathode potential and mass transfer determine performance of oxygen reducing biocathodes in Microbial Fuel Cells	79
Chapter 6	Copper recovery combined with electricity production in a Microbial Fuel Cell	95
Chapter 7	Improvement of the cathode of a scaled-up Microbial Fuel Cell	113
Chapter 8	General discussion and outlook	129
	Summary/Samenvatting	149
	List of publications	157
	Acknowledgements	161
	About the author	165



# Chapter 1

## Introduction

Chapter 1.2 is partly based on:

Hamelers, H. V. M.; Ter Heijne, A.; Sleutels, T. H. J. A.; Jeremiasse, A. W.; Strik, D. P. B. T. B.; Buisman, C. J. N. 2010. New applications and performance of bioelectrochemical systems. *Appl. Microbiol. Biotechnol.* 85, 1673-1685.

## 1.1 Introduction

This thesis describes the improvement of electricity production in the Microbial Fuel Cell (MFC). The Microbial Fuel Cell is a new technology, in which microorganisms produce electricity from a renewable energy source in the form of biomass. In this introduction, we describe the need for production of electricity from renewable sources. Furthermore, we explain that Microbial Fuel Cells are a promising technology because of their high efficiency, and finally, we discuss four basic concepts for describing performance of a Microbial Fuel Cell.

### 1.1.1 Energy use is linked to income

There is a huge and increasing energy demand in the world. Worldwide, total final energy consumption has increased from 4675 Mtoe in 1973 to 8286 Mtoe in 2007, and is expected to further increase to 11405 Mtoe in 2030 (IEA, 2009). The increasing energy consumption is a result of the increasing wealth: there is a clear relationship between income and energy use. In countries where >95% of the people live above the poverty line of \$2 per day, the energy consumption per capita is four times higher than in countries where >75% of the people is poor (IEA, 2008). At the same time, access to affordable and reliable energy is essential for improving quality of life and for economic development. Figure 1 shows the relationship between income and energy use per capita. Increase in energy use is accompanied with an increase in income. Rapidly industrializing countries like China and India are still at the start of their climb onto the energy ladder, and their energy consumption will rise as incomes increase.

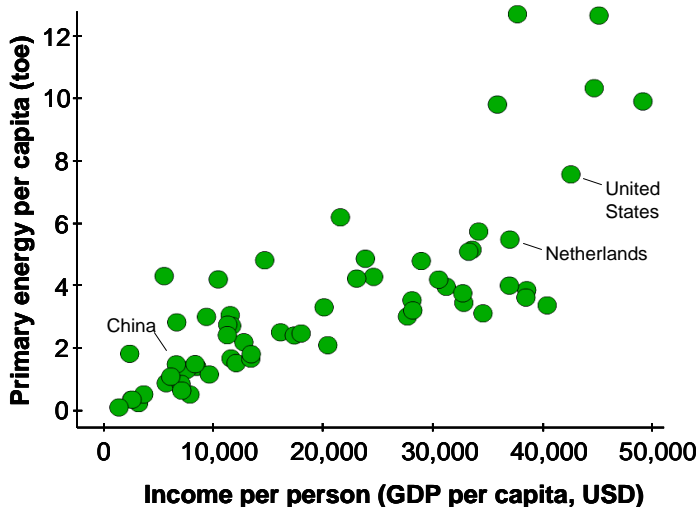


**Figure 1.** Energy use per capita increases with increasing income, data for 2008 (Gapminder, 2010).

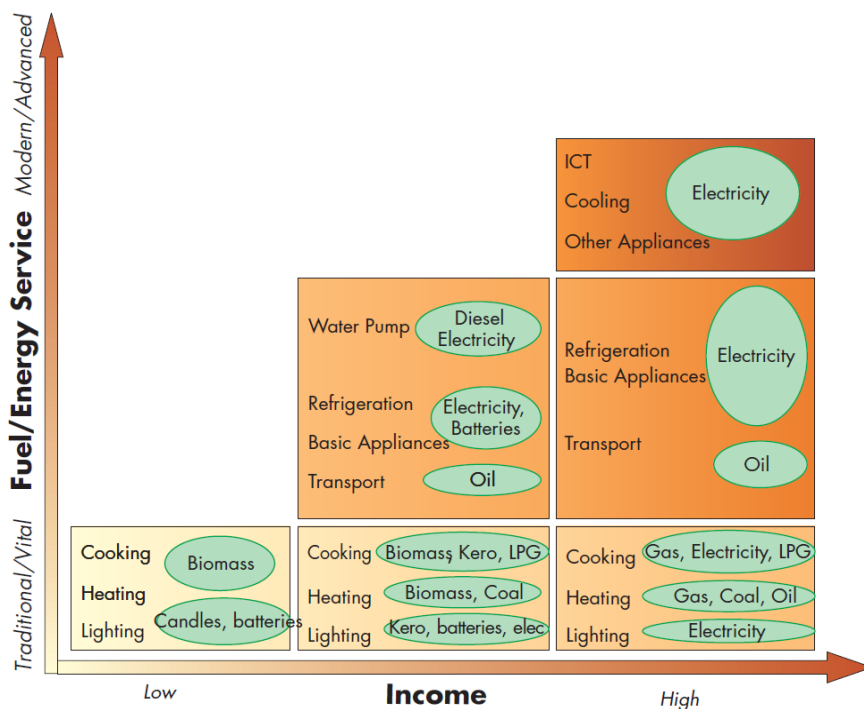


Figure 2. Energy poverty: household fuel transition (source: IEA, 2002).

Besides the relationship between income and total energy use, there is also a link between income and type of energy used. Energy is available in many different sources and forms. The energy sources (e.g. coal, gas, biomass, hydropower) can be either directly used or converted before use. For example, biomass, coal, and gas can be directly used for heating and cooking, while oil is converted into liquid fuel before use, and part of the coal, gas, and biomass is converted into electricity before being used. The energy source and the form in which energy is used are mainly dependent on income (Figure 2). Whereas low incomes depend on the use of biomass for cooking and heating, higher incomes move their energy use from biomass to gas, coal, oil, and finally electricity as the most modern and advanced form of energy.

While modern energy services, and electricity in particular, are a key enabler of economic and social development, it is estimated that today, 1.6 billion people have no access to electricity (IEA, 2008). Furthermore, worldwide electricity consumption is expected to rise from 15665 TWh in 2006 to 28141 TWh in 2030. Therefore, an increase in electricity production capacity is needed.

### 1.1.2 Energy sources for electricity production

Energy sources can be divided into fossil sources (oil, coal and gas) and renewable sources (for example sun, biomass, wind and hydropower). This distinction between fossil and renewable sources is made based on the time scale during which the energy has been stored. Most energy originates from the sun, which drives the uptake of CO<sub>2</sub> via photosynthesis, in this way storing energy in the form of carbohydrates. In fossil sources, the sun's energy has been fixed millions of years ago, while the sun's energy in renewable sources has been fixed on a much shorter time-scale in the order of decades (for biomass). Besides being fixed in biomass, the sun's energy can also be used indirectly as wind and hydropower, or directly as solar power.

When considering the energy sources used for electricity, we see that 68% of the electricity is produced from the fossil sources coal, oil, and gas together, whereas biomass currently contributes to only 2.6% of the electricity production (Figure 3). For production of electricity, efficiency is an issue of major interest, as it indicates which part of the energy present in the source ends up as electricity. While most electricity is derived from fossil fuels, the conversion into electricity via combustion has the drawback of low efficiency. During combustion of particularly coal, large part of the energy is lost as unused heat. The average efficiency of coal-fired electricity production is 36%, while conversion of gas into electricity reaches higher efficiencies of on average 48% (data for 2008, IEA, 2010).

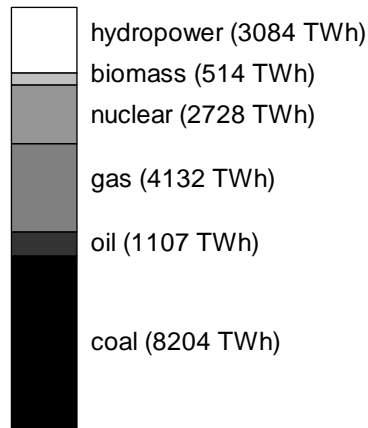


**Figure 3.** Contribution of the different energy sources to electricity production in 2007. The total electricity generation was 19771 TWh, of which 68% originated from fossil sources. Based on IEA (2008).

### 1.1.3 Extraction and use of fossil energy sources have major drawbacks

Although fossil sources can still comply with the current need, their extraction and use can have serious negative social and environmental impacts. Easily accessible sources of oil and gas are being, or have already been, exploited. As a result, extraction will become increasingly difficult, giving higher costs and leading to environmental and social risks.

Two recent catastrophes related to gas and oil extraction are the Sidoarjo mud volcano and the oil leak in the Gulf of Mexico. The mud volcano in Sidoarjo (East Java, Indonesia) has started on May 29, 2006, and was caused by the blow-out of a natural gas drill. The mud flow increased from 5,000 m<sup>3</sup> a day to 50,000 m<sup>3</sup> per day by the end of 2006, and during 2007 further increased to 100,000-120,000 m<sup>3</sup> per day (Wibowo and Williams, 2009), destroying the homes of many people in the surroundings of Sidoarjo. Mud flowing from the volcano has displaced over 35,000 people in more than a dozen villages (McMichael, 2009). Although dikes have been built to contain the mud, there are still regular floodings. Attempts to stop the outbreak have not been successful until now, and the mud will continue to flow possibly for years to come (McMichael, 2009). The recent oil leak in the Gulf of Mexico is another example of the large environmental risks related to deep well oil drilling. Started as a result of an explosion after a blowout at the Deepwater Horizon oil rig on April 20, 2010, vast amounts of oil have been flowing into the sea, having dramatic effects on the ecosystems: birds, sea animals, and coral reefs have been damaged. Scientific teams have estimated that the amount of oil that has leaked into the sea started at 10,000 m<sup>3</sup> per day immediately after the explosion to 8,400 m<sup>3</sup> per day just before the well has been closed (Deepwater horizon response, 2010). Overall, it has been estimated that 780,000 m<sup>3</sup> of oil have been released from the well. It is assumed to be the largest offshore oil spill in history.

As the accessible amount of fossil sources become more limited, it will become more difficult to exploit these sources, and this may lead to more catastrophes in the near future. Besides accessibility, three other arguments that plead for restriction of the use of fossil fuels are climate change, air pollution, and political instability.

Climate is changing as a result of increased greenhouse gas concentrations in the atmosphere. One of the main constituents of greenhouse gases is CO<sub>2</sub>. The increased concentration of CO<sub>2</sub> in the atmosphere comes, to a great extent, from human activities and their use of fossil fuels. Because the carbon present in fossil sources has been sequestered millions of years ago, the CO<sub>2</sub> released during combustion results in an increase in CO<sub>2</sub> concentration in the atmosphere. During the last two centuries, CO<sub>2</sub> concentrations in the atmosphere have risen from 275 ppm to 375 ppm (IPCC, 2007) as a result of the use of fossil

fuels. The Intergovernmental Panel of Climate Change predicts that the emission of greenhouse gases will result in worldwide temperature increases and sea level rises during the coming centuries.

Combustion of fossil fuels not only emits CO<sub>2</sub> into the atmosphere, but also leads to air pollution with SO<sub>2</sub> and fine particulates. Increased levels of both air pollutants have adverse affects for humans as they may lead to heart disease, breathing problems and lung cancer. SO<sub>2</sub> in the air is a main precursor of acid rain, which damages the environment by acidification.

Finally, countries that have major reserves of fossil fuels can use this advantage to exercise power. Alternative energy sources would empower less advantageous countries and enable them to develop according to their own insights.

Because all of the above mentioned reasons, it is of major importance that alternatives for fossil fuels are developed.

#### 1.1.4 Renewable energy sources

Renewable sources are the alternative for fossil sources. These renewable energy sources are solar energy, wind energy, biomass, geothermal, wave-tidal, hydropower, and blue energy: the energy from the salinity gradient between fresh water (river mouths) and the receiving saline reservoirs (seas and oceans) that can be used to generate renewable electrical power (Post et al., 2008). The energy derived from renewable sources is referred to as renewable energy. Renewable energy is abundant: it can supply >3000 times the worldwide energy consumption (Figure 4).

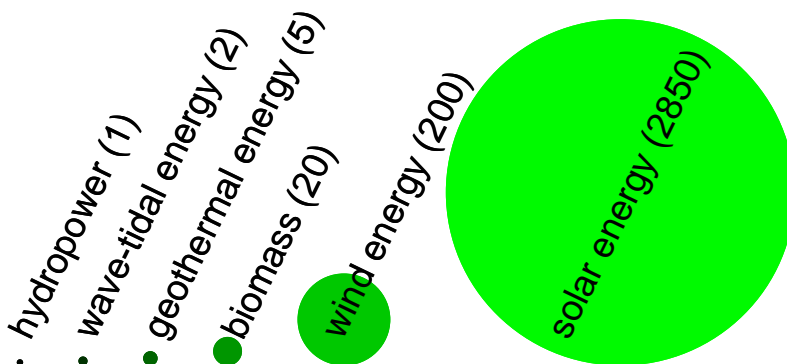


**Figure 4.** Abundance of renewable energy sources in the world according to Greenpeace (2010). The numbers between brackets indicate the number of times that this source can provide the current global energy need. All renewable sources together can provide 3078 times the global energy need.

When comparing renewable sources to fossil sources, their major advantage is that, ideally, they do not emit greenhouse gasses (CO<sub>2</sub>), which makes them carbon neutral. For wind and water this may be evident, but also biomass, where CO<sub>2</sub> is released when the energy is used, is considered carbon neutral. The reason for this is that the CO<sub>2</sub> they emit has been taken up only recently (via photosynthesis), and thus has a short recycle time compared to fossil fuels, where the CO<sub>2</sub> was taken up millions of years ago. This carbon neutrality however, does not make renewable sources directly more advantageous or environmentally sustainable than fossil sources. To assess if the use of renewable sources is more environmentally sustainable than the use of fossil sources, each source should be judged separately based on their adverse effects.

### **1.1.5 Biomass is the most important renewable energy source**

Biomass is currently the mostly used renewable energy source, contributing to 9.8% of the total primary energy supply in 2007 (IEA, 2008). Moreover, it is expected to stay the most important primary source of renewable energy for the decades to come (IEA, 2008). When we compare biomass to fossil sources, the sustainability of its use strongly depends on the type of biomass feedstock (Tilman et al., 2009). It has been argued that some of these biomass feedstocks might even be less sustainable than fossil fuels because of the competition with food production and the CO<sub>2</sub> emissions as a result of land clearing for crop growth (Fargione et al., 2008).

It is estimated that as much as 61% of the total global biomass is used in the traditional way (IEA, 2008), mostly in developing countries. This traditional use of biomass, i.e. burning of wood, dung and harvest residues for cooking and heating, has serious negative effects on health and the environment. More people die prematurely in poor countries from the health impacts related to indoor air quality as a result of burning of biomass, than from malaria (IEA, 2008). It is thus important to convert biomass as efficiently and as clean as possible. More efficient conversion of biomass will reduce the amount of biomass that is required, so that energy accessibility is improved, and at the same time reduces health risks. Modern energy in the form of electricity is a desired form of energy, as access to electricity is a key driver for social and economical development. Therefore, simple and cost-effective technologies are needed for efficient conversion of biomass into modern energy in developing countries. Whereas in developing countries, the conversion of biomass into electricity can contribute to social and economical development, in industrialized countries, production of electricity from biomass will be more oriented towards climate change mitigation. In this sense, replacing coal with biomass for electricity production is an effective strategy for greenhouse gas reduction, as coal has the highest specific CO<sub>2</sub> emissions of all fossil energy carriers (WBGU, 2009).

The potential of biomass is enormous: the estimated global biomass consumption in 2006 was 1186 Mtoe (IEA, 2008). When assuming that this total amount of biomass can be converted into electricity at an efficiency of 50%, this would result in 593 Mtoe (6879 TWh) of electricity. This means that biomass has the potential to replace 85% of all coal that is currently used for electricity production (Figure 3).

### 1.1.6 Efficient conversion of biomass into electricity by Microbial Fuel Cells

It is generally accepted that the biomass that is considered to be waste, like municipal and industrial organic wastes, are an attractive and sustainable biomass feedstock, because these can not be used for any food or feed production. Municipal and industrial organic wastes are water containing waste streams consisting of a mixture of proteins, lipids, carbohydrates and organic acids. These organic materials can be broken down by microorganisms under anaerobic conditions into smaller organic components. Acetate, being the end product in this conversion, has the lowest energy content. Nevertheless, it still contains sufficient energy to be converted into methane or electricity. Therefore, acetate is the biomass source used in this thesis.

The challenge is to convert these wet organic waste streams in an efficient manner into electricity. Wet waste streams need a low temperature conversion if they are to be efficiently converted, as heating the water would lead to major energy losses. Currently, the only available technology for converting these wet streams into electricity is anaerobic digestion. Anaerobic digestion is a process that uses microorganisms to convert biomass under anaerobic conditions in several steps into methane gas, which can be used to produce electricity in a gas motor. This gas motor is a major limitation in the efficiency of the process, as the combustion of methane to produce electricity has a maximum efficiency of 43%, even when part of the heat is reused (Weiland, 2010). Overall, the conversion from biomass into electricity via anaerobic digestion occurs in several steps: first the biomass is biochemically converted into methane gas, secondly the formed gas needs to be cleaned from  $H_2S$  before being combusted. This makes the overall conversion from biomass to electricity via anaerobic digestion complex and expensive.

In the search for efficient conversion technologies of biomass into electricity, the new Microbial Fuel Cell technology has recently drawn much attention. Research on Microbial Fuel Cells is still in an early stage, however, Microbial Fuel Cells have already shown to offer potential advantages: (i) they can convert biomass to electricity at high efficiency in one step, (ii) they operate at ambient temperatures, and (iii) they are robust, as they can operate in a stable way for extended time, and (iv) they are environmentally sustainable, because they do

not contain heavy metals. Therefore, the expectations for Microbial Fuel Cells as a future electricity producing technology from biomass are high, and there is a need to further investigate and develop this technology.

It should be noted, that biomass is present in many forms, like wood, crop residues, animal manure, and municipal waste. Not all of these sources have the same suitability for electricity production in a Microbial Fuel Cell. While wet organic waste streams (municipal organic wastes, animal slurries) are particularly interesting, they likely need pretreatment before being used for electricity generation. At the same time, pretreatment may also enable the use of other forms of biomass for conversion into electricity.

### **1.1.7 Aim of this thesis**

This thesis aims at efficient electricity production in Microbial Fuel Cells. Focus lies on improving the reduction reaction at the cathode, because the cathode is the main limiting factor in the power production in Microbial Fuel Cells (Logan, 2009).

## **1.2 Microbial Fuel Cells for renewable electricity production**

In Microbial Fuel Cells, electrons are generated from biomass by microorganisms. A Microbial Fuel Cell consists of an anode and a cathode, often separated by a membrane (Figure 5). At the bio-anode, microorganisms catalyze the oxidation of organic materials and produce CO<sub>2</sub>, protons, and electrons. This reaction only happens under anaerobic conditions: if oxygen is present in the system, oxygen is used as an electron acceptor instead of the electrode as this is energetically more favorable. The produced electrons flow from anode to cathode, where a reduction reaction takes place, usually the reduction of oxygen to water. At the same time, positively charged ions, for example K<sup>+</sup> or Na<sup>+</sup>, migrate through the membrane from anode to cathode to maintain electroneutrality in the solutions. On their way from anode to cathode, the electrons release their energy (for example at a light bulb) so that useful energy can be gained. An additional advantage is that this electron transfer takes place as a result of the breakdown of organic material at the anode, and when wastewater is used, this means that the wastewater is purified at the same time.

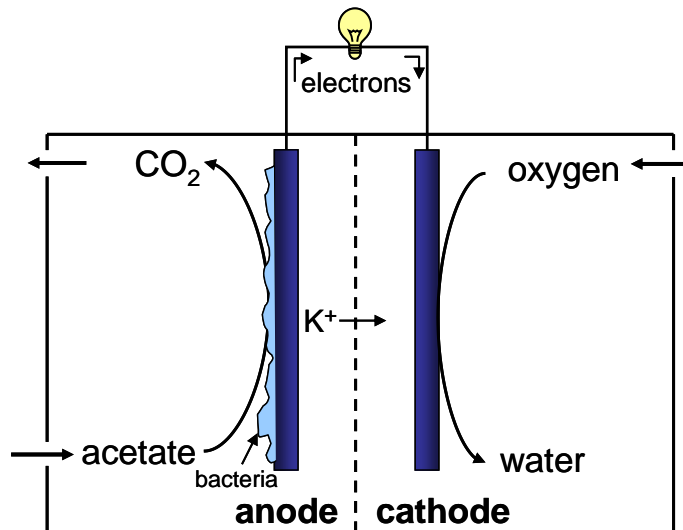


**Figure 5.** Principle of the Microbial Fuel Cell, where biomass (in the form of acetate) is oxidized into CO<sub>2</sub>, protons and electrons at the anode. The electrons flow from bio-anode to the cathode where oxygen is reduced to water. To maintain electroneutrality, positively charged ions, for example K<sup>+</sup>, flow from anode to cathode.

Bioelectrochemical system (BES) is the general term for this type of system consisting of two electrodes, where one or both electrode reactions are catalyzed by microorganisms. A bioelectrochemical system is called a Microbial Fuel Cell (MFC) if electrical energy (electricity) is harvested and is called a Microbial Electrolysis Cell (MEC) if electrical energy is supplied to drive an otherwise non-spontaneous reduction reaction at the cathode. Historical breakthroughs towards the current bioelectrochemical systems are the first discovery of electricity generation by the microorganism *Escherichia coli* (Potter, 1912), mediatorless direct electron transfer and oxidation of lactate by *Shewanella putrefaciens* (Kim et al., 2002), and mediatorless carbohydrate oxidation by *Rhodospirillum rubrum* in an Microbial Fuel Cell (Chaudhuri and Lovley, 2003). These results provide the fundamental groundwork of numerous applications for bioelectrochemical systems, like wastewater treatment and electricity generation by microorganisms, since toxic soluble mediators were not needed anymore (Logan, 2005).

The popularity of research on bioelectrochemical systems is increasing rapidly as illustrated by the amount of peer reviewed papers on bioelectrochemical systems like the Microbial Fuel Cells which doubled over the year 2007 to 2008 (Scopus, 2009). Currently, it is estimated that world wide over 100 research groups are working on bioelectrochemical systems, investigating

systems from fundamentals towards new applications (Proceedings of the 2<sup>nd</sup> international Microbial Fuel Cell Conference 2009).

To facilitate operation of bioelectrochemical systems, a primary electron donor must be supplied to the anode and a final electron acceptor must be supplied to the cathode. The advantage of bioelectrochemical systems when using two compartments is that they not solely convert compounds, but also separate oxidation and reduction processes, which makes it possible to extract useful products out of wastes. Nowadays, bioelectrochemical systems with bio-anodes use electron donors that are derived from wastes (e.g. wastewaters) (Logan, 2005), sediments (Reimers et al., 2001), processed energy crops (as cellulose) (Niessen et al., 2005; Ren et al., 2007; Rezaei et al., 2009) photosynthetic microorganisms (Strik et al., 2008a; Chiao et al., 2006; Fu et al., 2009) or in-situ photosynthesized plant rhizodeposits (Strik et al., 2008b; De Schampelaire et al., 2008).

BESs with microorganisms at the bio-anode or biocathode generally may be combined with any other known bio- or chemical half-reaction at the other electrode. Recently, Microbial Fuel Cells were developed with mediatorless biocathodes using various final electron acceptors like oxygen (Bergel et al., 2005), and nitrate (Clauwaert et al., 2007). The last years bioelectrochemical systems research has also moved in the direction from producing electricity in Microbial Fuel Cells to Microbial Electrolysis Cell applications using microorganisms as novel biocatalysts that produce all kinds value added products like H<sub>2</sub> (Rozendal et al., 2006), CH<sub>4</sub> (Cheng et al., 2009), H<sub>2</sub>O<sub>2</sub> (Rozendal et al., 2009) or ethanol (Steinbusch et al., 2009), while using final electron acceptors like protons, CO<sub>2</sub> and acetate.

### **1.3 Energy efficiency as a key parameter for Microbial Fuel Cells**

To make Microbial Fuel Cells an attractive electricity producing technology, its efficiency in converting the energy available in biomass into the energy available as electricity (i.e. its energy efficiency), is of utmost importance and should be maximized. In this chapter, four basic concepts that are used to be able to define energy efficiency in Microbial Fuel Cells will be discussed. These concepts are: (1) electrode potentials, (2) polarization curves, (3) overpotentials, and (4) coulombic and voltage efficiency. These four concepts will be used throughout this thesis to determine and compare performance of Microbial Fuel Cells and cathodes.

### 1.3.1 Electrode potentials

Electrode potentials express the energy level of the electrons. Anode and cathode potentials are determined by thermodynamics of the anode and cathode reactions.

Because a potential has no meaning by itself and should be expressed compared to another potential, a reference electrode is needed, for example an Ag/AgCl reference electrode. This reference electrode has a fixed value, which enables us to express anode and cathode potentials versus a constant value. The lower the electrode potential (versus the reference electrode), the more energy the electrons contain. Electrons will spontaneously flow from high to low energy level, i.e. from low to high electrode.

Figure 6A shows the theoretical electrode potentials for the Microbial Fuel Cell with acetate oxidation in the anode and oxygen reduction in the cathode. These electrode potentials are calculated from thermodynamic laws. The energy difference between anode and cathode is  $+0.62 - -0.47 = 1.09$  V. This is the maximum theoretic voltage that can be extracted from the Microbial Fuel Cell. When a current is produced, the measured voltage is considerably lower than 1.09 V; cell voltages of  $<0.5$  V are generally observed. The reason that the measured cell voltage is lower than the theoretical voltage is that energy losses occur in several parts of the system (Figure 6B), especially at the cathode. These energy losses will be further discussed in chapter 2.1.2.

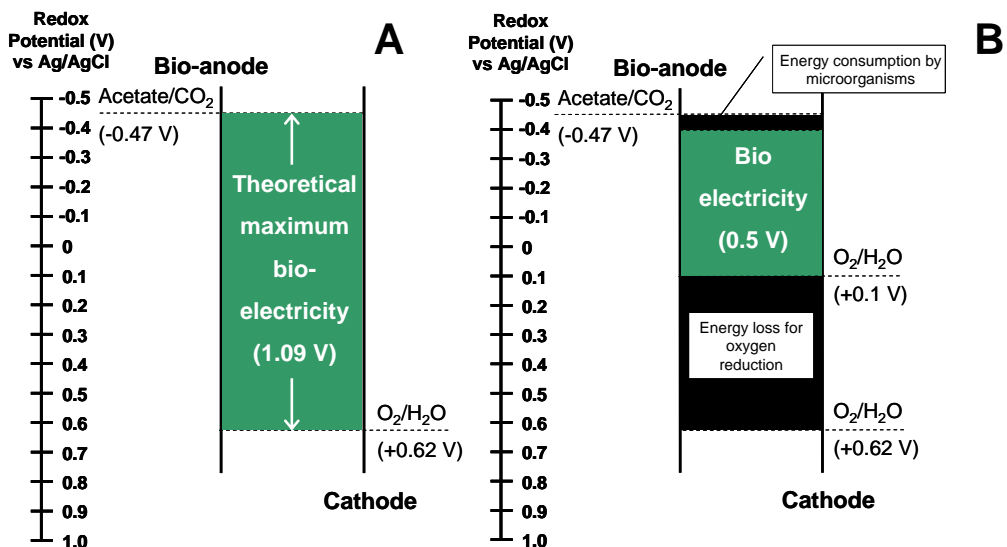
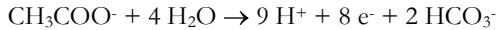


Figure 6. Energy gain from the microbial fuel cell, in theory (A) and practice (B).

Electrode potentials can be calculated based on the Gibbs's free energy (kJ/mol) of the reaction. This Gibbs's free energy is a measure of the maximal work that can be derived from the reaction. For example for oxidation of acetate at the anode, we have the reaction:



The standard Gibbs's free energy ( $\Delta G^0$ ) for this anodic reaction can be calculated from tabulated energies of formation for the different compounds in the reaction and can be for example taken from Amend and Shock (2001). This is done by subtracting the formation energies of the oxidized components from the formation energies of the reduced components, taking into account the stoichiometry. The standard procedure is to write the reaction as a reduction reaction:  $9 \text{H}^+ + 8 \text{e}^- + 2 \text{HCO}_3^- \rightarrow \text{CH}_3\text{COO}^- + 4 \text{H}_2\text{O}$

The standard Gibbs's free energy ( $\Delta G^0$ ) is then calculated as:

$$\Delta G^0 = \Delta G_{\text{prod}} - \Delta G_{\text{react}} = \Delta G_{\text{CH}_3\text{COO}^-} + 4 \cdot \Delta G_{\text{H}_2\text{O}} - (9 \cdot \Delta G_{\text{H}^+} + 2 \cdot \Delta G_{\text{HCO}_3^-})$$

The standard Gibbs's free energy reflects the reaction energy under standard conditions, i.e. pH=0, all concentrations are 1 M and all gas pressures are 1 atm). To assess the reaction energy under actual conditions, the standard Gibbs's free energy can be converted to the actual Gibbs's free energy ( $\Delta G_a$ ) using the equation:

$$\Delta G_a = \Delta G^0 - \frac{RT}{nF} \ln \Pi,$$

Where

R = gas constant (8,314 kJ/mol.K)

T = temperature (K)

n = mol of electrons in reaction

F = Faraday constant (96485 C eq<sup>-1</sup>)

$\Pi$  = the reaction quotient, taking into account the activity of the species. In case of acetate

oxidation for example, 
$$\Pi = \frac{[\text{CH}_3\text{COO}^-]}{[\text{H}^+]^9 \cdot [\text{HCO}_3^-]^2}$$

The actual Gibbs's free energy can then be converted to an electrode potential E according

to:  $E = \frac{\Delta G}{nF}$ . This electrode potential is then expressed vs Normal Hydrogen Electrode

(NHE). Similarly, the standard potential of a reaction  $E^0$  can be calculated from the standard Gibbs's free energy and can be converted to the actual potential using the Nernst equation:

$$E = E^0 - \frac{RT}{nF} \ln \Pi.$$

**Table 1.** Overview of typical reactions in bioelectrochemical systems with their standard potential ( $E^0$ ) and actual potential ( $E$ )

Anodic Oxidation Reaction		$E^0$	$E$
		(V vs NHE)	(V vs NHE)
Acetate	$C_2H_3O_2^- + 4 H_2O \rightarrow 2 HCO_3^- + 9 H^+ + 8 e^-$	0.187	-0.289
Glucose	$C_6H_{12}O_6 + 12 H_2O \rightarrow 6 HCO_3^- + 30 H^+ + 24 e^-$	0.104	-0.429
Cathodic Reduction Reaction		$E^0$	$E$
		(V vs NHE)	(V vs NHE)
Oxygen to water	$O_2 + 4 H^+ + 4 e^- \rightarrow 2 H_2O$	1.229	0.805
Oxygen to hydrogen peroxide	$O_2 + 2 H^+ + 2 e^- \rightarrow H_2O_2$	0.694	0.269
Protons to hydrogen	$2 H^+ + 2 e^- \rightarrow H_2$	0	-0.414

Actual conditions:  $[HCO_3^-]=0.05$  M, Acetate, glucose = 0 .05 M,  $[H_2O] = 1$  M,  $[H^+]: 10^{-7}$  M,  $pO_2 = 0.2$  atm,  $pH_2 = 1$  atm,  $T=298$  K

This calculation can be done for both the oxidation and the reduction reactions. Some typical anode and cathode reactions and their potentials are listed in Table 1 (Hamelers et al, 2010). For example, the potential of acetate oxidation is -0.289 V vs NHE under actual conditions. When combining this with oxygen reduction (+0.805 V vs NHE), there is a driving force for electrons to flow from anode to cathode and electricity is produced. When combining acetate oxidation with reduction of protons to hydrogen however, we see that the reduction potential is lower than the oxidation potential, which means that energy input is needed to drive the reactions.

### 1.3.2 Polarization curves

Performance of Microbial Fuel Cells is usually presented in polarization curves. Polarization curves express the cell voltage and power density as a function of the current density. They can be produced in two ways: using an external resistance, of which the value is changed in several steps and measuring the cell voltage, or using a potentiostat, which can control the cell voltage or potentials at a desired level and measures the current. While a potentiostat measures the current directly, the use of an external resistance requires conversion of the measured cell voltage  $V$  (V) to current  $I$  (A) by  $I=V/R$ , where  $R$  = resistance ( $\Omega$ ).

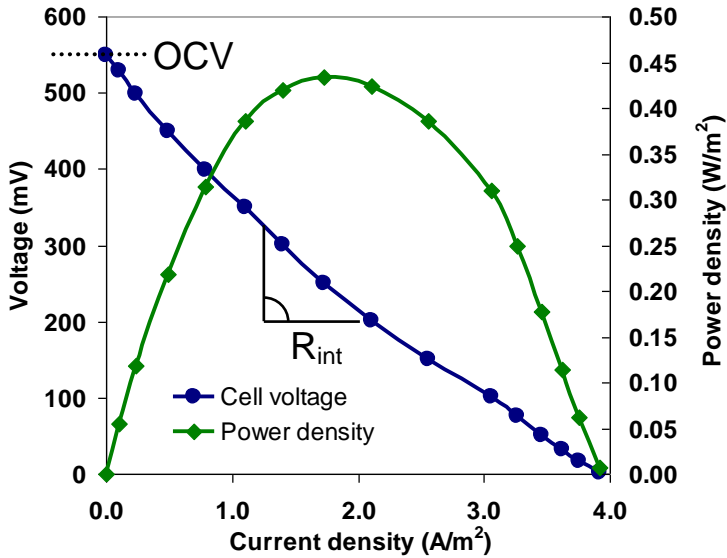


**Figure 7.** A typical polarization curve for a Microbial Fuel Cell. The open circuit voltage (OCV) is the maximum cell voltage, found when no current flows. Cell voltage decreases with increasing current density as a result of increasing losses. Power density shows a maximum at a certain current density. The internal resistance can be determined from the slope of the cell voltage curve.

Figure 7 shows a typical polarization curve for a Microbial Fuel Cell. When no current flows (intersect with x-axis), no losses occur and we find the maximum cell voltage, which is called the open cell voltage (OCV). As current increases, we see a decrease in cell voltage. This decrease in cell voltage is a result of increasing losses with increasing current. For example, if the solution has low conductivity, the ions that migrate from anode to cathode meet a certain resistance. This resistance leads to a voltage loss that is dependent on the current  $I$  ( $V=I \cdot R$ ), and is called an ohmic loss. Besides ohmic losses, other examples of energy losses are activation losses, and concentration losses. Where ohmic losses represent the energy loss as a result of resistance in all conductive parts of the cell (electrodes, solution, electrical connections), activation losses are caused by activation energy that is needed to start the reaction, and concentration losses are caused by concentration gradients close to the electrode as a result of the reactions occurring. All these losses are a result of resistances that exists in several parts of the Microbial Fuel Cell. The higher the current density, the higher the voltage loss in the system. Therefore, we find a decrease in cell voltage with increasing current density.

A useful way to compare different systems is by calculating the slope of the polarization curve, we find the internal resistance  $R_{\text{int}}$  of the system. When the current is expressed as current density ( $\text{A}/\text{m}^2$  or  $\text{A}/\text{m}^3$ ) the resistance is calculated in  $\Omega\cdot\text{m}^2$  or  $\Omega\cdot\text{m}^3$ . This resistance is a useful metric to compare performance of systems that have different surface area or volume (Clauwaert et al., 2008; Sleutels et al., 2009).

Power is defined as  $P=VI$ . The different combinations of  $V$  and  $I$  are characteristic for each Microbial Fuel Cell and determine at which point the maximum power of the system is produced.

### 1.3.3 Overpotentials

The performance of an electrode is determined by its overpotential as a function of the current density. The overpotential indicates the amount of energy lost at the electrode. Energy losses at the electrode can occur as a result of ohmic losses, activation losses, and concentration losses. While polarization curves generally only show the relationship between current density and cell voltage, it is also useful to express the current density versus the electrode potentials. In this way, the contribution of anode and cathode to the total resistance can be quantified. For this, overpotentials are an important measure. As an example, we will discuss the cathode overpotential here.

The cathode overpotential is defined as the difference between the cathode potential and the theoretical cathode potential. The theoretical cathode potentials as calculated above via the Gibb's free energy of the reaction, describes a situation in which the cathode is in equilibrium with the electron acceptor, i.e. the energy level of the electrons in the cathode equals that of the electron acceptor (for example oxygen). This theoretical cathode potential is in practice comparable to the open cell potential (OCP). The OCP is the potential of an electrode when no current is produced. In that case, no load is applied to the system and the energy losses at the electrodes should be zero. When the cathode potential is decreased from the equilibrium situation, a current may flow from the cathode to the electron acceptor due to the potential difference. This electron flow will occur only in the presence of a suitable catalyst. The overpotential is then both a measure of the energy lost in the electron transfer reaction and a measure of the driving force of the reaction. The amount of energy lost at the electrode, i.e. the overpotential, is dependent on the current density and the charge transfer resistance: the higher the current density, the more energy is lost and the higher the overpotential is.

Similar to total internal resistance in  $\Omega\cdot\text{m}^2$  or  $\Omega\cdot\text{m}^3$ , anode and cathode resistance can also be expressed in order to compare different systems. This is done by dividing anode or cathode overpotential by the current density.

### 1.3.4 Coulombic efficiency and voltage efficiency

The energy efficiency of Microbial Fuel Cells describes which part of the energy present in the substrate ends up as electrical energy. The overall energy efficiency is a combination of two efficiencies in the Microbial Fuel Cell: Coulombic efficiency and voltage efficiency.

Coulombic efficiency indicates the extent to which the produced electrons end up in the desired product. At the anode for example, the Coulombic efficiency indicates which part of the electrons present in the biomass end up as electrons in the electrical circuit. Coulombic efficiency decreases when other electron acceptors than the electrode are present, e.g. oxygen, nitrate, or sulphate, or when there is competition with other microorganisms for the substrate, e.g. with methanogens that convert acetate into methane instead of electricity.

Voltage efficiency represents the actual measured voltage compared to the theoretical maximum voltage and thus compares the energy produced as cell voltage relative to the maximum energy that can be produced in the Microbial Fuel Cell. Voltage efficiency decreases as a result of increasing losses due to internal resistances.

Finally, energy efficiency is defined as the product of Coulombic efficiency and voltage efficiency, as the combination of both determines which part of the energy present in the substrate ends up as electrical energy.

## 1.4 Thesis outline

The aim of this thesis is to increase power density in the Microbial Fuel Cell by means of improving the cathode reaction.

**Chapter 2** starts with investigation of bio-anodes. It describes the performance of bio-anodes using different electrode materials and characterized the different bio-anodes using polarization curves and electrochemical impedance spectroscopy. It was shown that bio-anodes were capable of producing considerable current densities up to 4.6 A/m<sup>2</sup> at a flat electrode. Because bio-anodes need to be combined with a suitable cathode that can accept electrons at a similar rate, we show how the reaction rate at the cathode can be improved in **Chapter 3**.

The mostly used catalyst for oxygen reduction is Pt, however, its high cost requires development of other cheap and renewable catalysts. As an alternative for oxygen reduction, we studied the reduction of Fe<sup>3+</sup> to Fe<sup>2+</sup> at low pH on a graphite electrode. To enable this process, a bipolar membrane was used to separate anode and cathode compartment. This bipolar membrane could maintain a pH difference between both compartments, needed to sustain current production as neutral pH is required at the anode, and low pH is required at the

cathode to keep  $\text{Fe}^{3+}$  soluble. Because the formed  $\text{Fe}^{2+}$  needs to be regenerated to  $\text{Fe}^{3+}$  to make the cathode renewable.

As chemical  $\text{Fe}^{2+}$  oxidation at low pH proceeds only at low rate, **Chapter 4** studies the performance of the Microbial Fuel Cell, in which the formed  $\text{Fe}^{2+}$  was regenerated to  $\text{Fe}^{3+}$  by the microorganism *Acidithiobacillus ferrooxidans* using oxygen as the final electron acceptor. A maximum power density of  $1.2 \text{ W/m}^2$  was reached. It was found however, that the membrane was not 100% efficient which resulted in the need to supply the cathode with sulphuric acid to maintain the required low pH.

Another alternative for the cathode was investigated in **Chapter 5**, where we studied whether microorganisms could catalyze oxygen reduction when directly attached to the cathode (biocathode). It was found that indeed, oxygen reduction was catalyzed compared to the plain graphite electrode. The current density produced however, was one order of magnitude lower compared to the reduction of  $\text{Fe}^{3+}$ , and it was found that both charge transfer and mass transfer limited biocathode performance.

In **Chapter 6**, we studied a completely new process in the cathode of the Microbial Fuel Cell, namely the reduction of  $\text{Cu}^{2+}$  to metallic Cu. We found that electricity was produced while copper was recovered in its pure form. When oxygen was added to the cathode, copper seemed to act as a catalyst, because electricity production increased compared to the anaerobic situation.

In **Chapter 7**, we continued the study on the first reported scaled-up Microbial Fuel Cell in the world with a total volume of 5 L and a surface area of  $0.5 \text{ m}^2$ , in order to gain more insight in the factors affecting Microbial Fuel Cell performance on a larger scale. To improve the cathode reaction, we used the system with a bipolar membrane and a cathode with reduction of  $\text{Fe}^{3+}$  and biological oxidation of the formed  $\text{Fe}^{2+}$ . The maximum power was  $2.0 \text{ W/m}^2$  ( $200 \text{ W/m}^3$ ) and we demonstrated that better or similar performance can be reached in scaled-up systems compared to lab-scale systems.

Finally, in **Chapter 8** we discuss the factors limiting Microbial Fuel Cell performance as encountered in this thesis. We estimate the maximum power and energy efficiency that can be produced in Microbial Fuel Cells and compare current and estimated performance to anaerobic digestion.

## 1.5 References

- Amend, J. P.; Shock, E. L. 2001. Energetics of overall metabolic reactions of thermophilic and hyperthermophilic Archaea and Bacteria. *FEMS Microbiol. Rev.* 25, 175-243.
- Bergel, A.; Féron, D.; Mollica, A. 2005. Catalysis of oxygen reduction in PEM fuel cell by seawater biofilm. *Electrochem. Commun.* 7, 900-904.
- Chaudhuri, S.K.; Lovley, D.R. 2003. Electricity generation by direct oxidation of glucose in mediatorless microbial fuel cells. *Nature Biotechnol.* 21, 1229-1232.
- Cheng, S.; King, D.; Call, D.F.; Logan, B.E. 2009. Direct biological conversion of electrical current into methane by electromethanogenesis. *Environ. Sci. Technol.* 43, 3953-3958.
- Chiao, M.; Lam, K.B.; Lin, L. 2006. Micromachined microbial and photosynthetic fuel cells. *J. Micromech. Microeng.* 16, 2547-2553.
- Clauwaert, P.; Rabaey, K.; Aelterman, P.; De Schampelaire, L.; Pham, T.H.; Boeckx, P.; Boon, N.; Verstraete, W. 2007. Biological denitrification in microbial fuel cells. *Environ. Sci. Technol.* 41, 3354-3360.
- Clauwaert, P.; Aelterman, P.; Pham, T.H.; De Schampelaire, L.; Carballa, M.; Rabaey, K.; Verstraete, W. 2008. Minimizing losses in bio-electrochemical systems: The road to applications. *Appl. Microbiol. Biotechnol.* 79, 901-913.
- De Schampelaire, L.; Van Den Bossche, L.; Hai, S.D.; Höft, M.; Boon, N.; Rabaey, K.; Verstraete, W. 2008. Microbial fuel cells generating electricity from rhizodeposits of rice plants. *Environ. Sci. Technol.* 42, 3053-3058.
- Deepwater horizon response, 2010. <http://www.deepwaterhorizonresponse.com/go/doc/2931/840475/>. Accessed on August 4, 2010.
- Fargione, J.; Hill, J.; Tilman, D.; Polasky, S.; Hawthorne, P. 2008. Land clearing and the biofuel carbon debt. *Science.* 319, 1235-1238.
- Fu, C.C.; Su, C.H.; Hung, T.C.; Hsieh, C.H.; Suryani, D.; Wu, W.T. 2009. Effects of biomass weight and light intensity on the performance of photosynthetic microbial fuel cells with *Spirulina platensis*. *Bioresour. Technol.* 100, 4183-4186.
- Gapminder, 2010. <http://www.gapminder.org>
- Greenpeace, 2010. Energy [R]evolution: a sustainable world energy outlook. <http://www.greenpeace.org/international/Global/international/publications/climate/2010/fullreport.pdf>
- Hamelers, H. V. M.; Ter Heijne, A.; Sleutels, T. H. J. A.; Jeremiasse, A. W.; Strik, D. P. B. T. B.; Buisman, C. J. N. 2010. New applications and performance of bioelectrochemical systems. *Appl. Microbiol. Biotechnol.* 85, 1673-1685.
- IEA, 2002. World Energy Outlook 2002. International Energy Agency, <http://www.iea.org/textbase/nppdf/free/2000/weo2002.pdf>
- IEA, 2008. World Energy Outlook 2008. International Energy Agency, <http://www.worldenergyoutlook.org/docs/weo2008/WEO2008.pdf>
- IEA, 2009. Key World Energy Statistics. International Energy Agency, [http://www.iea.org/textbase/nppdf/free/2009/key\\_stats\\_2009.pdf](http://www.iea.org/textbase/nppdf/free/2009/key_stats_2009.pdf)

- IEA, 2010. Opportunities to transform the electricity sector in major economies. International Energy Agency, [http://www.iea.org/papers/2010/electricity\\_sector\\_opportunities.pdf](http://www.iea.org/papers/2010/electricity_sector_opportunities.pdf)
- IPCC, 2007. Climate change 2007: the physical science basis. In: Solomon, S., Qin, D., Manning, M.; Chen, Z.; Marquis, M.; Averyt, K.B.; Tignor, M.; Miller, H.L. (Ed). Contribution of working group I to the fourth assessment report of the Intergovernmental Panel on Climate Change, Cambridge, United Kingdom and New York, USA.
- Kim, H.J.; Park, H.S.; Hyun, M.S.; Chang, I.S.; Kim, M.; Kim, B.H. 2002. A mediator-less microbial fuel cell using a metal reducing bacterium, *Shewanella putrefaciens*. *Enzyme Microb. Technol.* 30, 145-152.
- Logan, B.E. 2005. Simultaneous wastewater treatment and biological electricity generation. *Water Sci. Technol.* 52, 31-37.
- Logan, B. E. 2009. Exoelectrogenic bacteria that power microbial fuel cells. *Nature Rev. Microbiol.* 7, 375-381.
- McMichael, H. 2009. The lapindo mudflow disaster: Environmental, infrastructure and economic impact. *Bull. Indon. Econ. Stud.* 45, 73-83.
- Niessen, J.; Schröder, U.; Harnisch, F.; Scholz, F. 2005. Gaining electricity from in situ oxidation of hydrogen produced by fermentative cellulose degradation. *Lett. Appl. Microbiol.* 41, 286-290.
- Post, J. W.; Hamelers, H. V. M.; Buisman, C. J. N. 2008. Energy recovery from controlled mixing salt and fresh water with a reverse electrodialysis system. *Environ. Sci. Technol.* 42, 5785-5790.
- Potter, M.C. 1912. Electrical effects accompanying the decomposition of organic compounds. *Proc. R. Soc. London, Ser. B.* 84, 260-267.
- Proceedings of the 2<sup>nd</sup> Microbial Fuel Cell Conference, June 10th-12th 2009, GIST, Gwangju, Korea.
- Reimers, C.E.; Tender, L.M.; Fertig, S.; Wang, W. 2001. Harvesting energy from the marine sediment - Water interface. *Environ. Sci. Technol.* 35, 192-195.
- Ren, Z.; Ward, T.E.; Regan, J.M. 2007 Electricity production from cellulose in a microbial fuel cell using a defined binary culture. *Environ. Sci. Technol.* 41, 4781-4786.
- Rezaei, F.; Xing, D.; Wagner, R.; Regan, J.M.; Richard, T.L.; Logan, B.E. 2009 Simultaneous cellulose degradation and electricity production by *Enterobacter cloacae* in a microbial fuel cell. *Appl. Environ. Microbiol.* 75, 3673-3678.
- Rozendal, R.A.; Hamelers, H.V.M.; Euverink, G.J.W.; Metz, S.J.; Buisman, C.J.N. 2006. Principle and perspectives of hydrogen production through biocatalyzed electrolysis. *Int. J. Hydrogen Energy.* 31, 1632-1640.
- Rozendal, R.A.; Leone, E.; Keller, J.; Rabaey, K. 2009. Efficient hydrogen peroxide generation from organic matter in a bioelectrochemical system. *Electrochem. Comm.* 11, 1752-1755
- Scopus, <http://www.scopus.com>. Elsevier BV, The Netherlands. Accessed August 18, 2009.
- Sluets, T. H. J. A.; Hamelers, H. V. M.; Rozendal, R. A.; Buisman, C. J. N. 2009. Ion transport resistance in microbial electrolysis cells with anion and cation exchange membranes. *Int. J. Hydrogen Energy.* 34, 3612-3620.
- Steinbusch, K.J.J.; Hamelers, H.V.M.; Schaap, J.D.; Kampman, C.; Buisman, C.J.N. 2009. Bio-electrochemical ethanol production through mediated acetate reduction by mixed cultures. *Environ. Sci. Technol.* 44, 513-517.

- Strik, D.P.B.T.B.; Terlouw, H.; Hamelers, H.V.M.; Buisman, C.J.N. 2008a. Renewable sustainable biocatalyzed electricity production in a photosynthetic algal microbial fuel cell (PAMFC). *Appl. Microbiol. Biotechnol.* 81, 659-668.
- Strik, D.P.B.T.B.; Hamelers, H.V.M.; Snel, J.F.H.; Buisman, C.J.N. 2008b. Green electricity production with living plants and bacteria in a fuel cell. *Int. J. Energy Res.* 32, 870-876.
- Tilman, D.; Socolow, R.; Foley, J. A.; Hill, J.; Larson, E.; Lynd, L. 2009. Beneficial biofuels - the food, energy, and environment trilemma. *Science.* 325, 270-271.
- WBGU, 2009. German Advisory Council on Global Change. Factsheet 1: Bioenergy.  
[http://www.wbgu.de/wbgu\\_publications\\_facts.html](http://www.wbgu.de/wbgu_publications_facts.html)
- Weiland, P. 2010. Biogas production: Current state and perspectives. *Appl. Microbiol. Biotechnol.* 85, 849-860.
- Wibowo, H.T.; Williams, V. 2009. Sidoarjo mudflow phenomenon and its mitigation efforts. *Am. Geophys. Union*, Fall Meeting 2009, abstract #NH51A-1055.



## Chapter 2

# Performance of non-porous graphite and titanium-based anodes in microbial fuel cells

2

This chapter has been published as:

Ter Heijne, A.; Hamelers, H.V.M.; Saakes, M.; Buisman, C. J. N. 2008. Performance of non-porous graphite and titanium-based anodes in Microbial Fuel Cells. *Electrochim. Acta.* 53, 5697-5703.

## Abstract

Four non-porous materials were compared for their suitability as bio-anode in microbial fuel cells (MFCs). These materials were flat graphite, roughened graphite, Pt-coated titanium, and uncoated titanium. The materials were placed in four identical MFCs, of which the anode compartments were hydraulically connected in series, as well as the cathode compartments. The MFCs were operated with four resistors. The anode kinetics at these electrode materials were studied by means of dc-voltammetry and electrochemical impedance spectroscopy (EIS). Both techniques were compared and showed that the bio-anode performance decreased in the order roughened graphite > Pt-coated titanium > flat graphite > uncoated titanium. Uncoated titanium was unsuitable as anode material. For the other three materials, specific surface area was not the single variable explaining the differences in current density for the different materials. All polarization curves showed a clear limiting current. This limit could not be attributed to mass transfer of the substrate and reflected the maximum biomass activity. The current density of the non-porous bio-anodes, except for the uncoated titanium anode, was comparable to the reported current densities of porous materials when normalized to the projected surface area. The high current densities that were recorded by dc-voltammetry however, could not be maintained in a stable way for a longer period. This shows that polarization curves of MFCs should be evaluated critically.

## 2.1 Introduction

The microbial fuel cell (MFC) is a promising technology to convert biodegradable materials, e.g. organic materials present in wastewater, into electricity. The technology is based on electrochemically active microorganisms that grow by oxidizing the biodegradable material to CO<sub>2</sub> and protons while transferring the electrons to a solid electrode (Logan et al., 2006). Electron transfer from the microorganisms to the electrode can occur via several mechanisms (Lovley, 2006; Schröder, 2007). When using a mixed culture in a system with continuous flow, it is likely that the current is produced by a thin biofilm attached to the surface of the electrode, as the electrochemically active microorganisms close to the electrode have a competitive advantage.

The power output of the MFC is amongst others influenced by the electrochemical performance of the bio-anode. The bio-anode is defined here as the assembly of the biofilm and the solid electrode to which it is attached. The electrochemical performance of the bio-anode can be expressed in a polarization curve, i.e. the relationship between the current density and the anode potential. Two main processes can be distinguished that influence the polarization curve of the bio-anode: (i) the microbial kinetics of substrate oxidation and the associated electron transfer and (ii) the mass transfer of substrate and products. To study the microbial kinetics of the bio-anode, a polarization curve can only be useful if mass transfer is not determining the current density. The effect of mass transfer on the current density can be eliminated or decreased by proper design of the MFC, such that the bio-anode has a thin diffusion layer.

Until now, mainly porous carbon-based materials, like graphite felt, graphite granules, carbon cloth, and reticulated vitreous carbon (RVC, porous glassy carbon) have been used as anodes (Ter Heijne et al., 2006; Rabaey et al., 2005; Cheng and Logan, 2007; He et al., 2005). Carbon-based materials are attractive because they are relatively cheap. Porous materials are of major practical importance because they have a high specific surface area which is expected to lead to high volumetric activity. To study specific materials however, a non-porous electrode is beneficial because mass transfer can be quantified. For porous materials on the other hand, mass transfer is difficult to quantify, because of the unknown thickness of the diffusion layer. This unknown mass transfer makes interpretation of measurement data for porous materials more difficult. Platinum has been tested as anode material in MFCs because of its catalytic activity for hydrogen oxidation (Niessen et al., 2004; Schröder et al., 2003).

An electrode material needs to have certain properties to be suitable as a bio-anode: it should (i) have good bio-compatibility to support microbial growth, (ii) have high electrical

conductivity, and (iii) be electrochemically inert (Rosenbaum et al., 2007). Based on the properties mentioned above, four electrode materials were selected: flat graphite, roughened graphite, Pt-coated titanium, and uncoated titanium. The objective of this study was to study the bio-anode kinetics at these non-porous electrode materials. The materials were placed in four identical MFCs, of which the anode compartments were hydraulically connected in series to ensure an equal anolyte composition, including dispersed biomass. The microbial kinetics were studied by means of dc-voltammetry and electrochemical impedance spectroscopy (EIS).

## 2.2 Materials and methods

### 2.2.1 Microbial fuel cell design and setup

The experimental setup consisted of four identical MFCs. All four anode compartments were hydraulically connected in series, as well as all four cathode compartments. Each MFC consisted of two plexiglass plates with a single flow channel, two electrodes, and two plexiglass support plates (Figure 1). The two plates with a flow channel were separated by a cation exchange membrane (Fumasep FKB, Fumatech, St. Ingbert, Germany). The other side of the flow channel faced the electrode.

The anodes were made of four different materials: flat graphite,  $\text{Al}_2\text{O}_3$ -blasted graphite (further called: roughened graphite) (both MR200, gas tight impregnated, from Müller & Rössner GmbH & Co., Troisdorf, Germany), Pt-coated titanium, and uncoated titanium (both from Magneto Special Anodes BV, Schiedam, the Netherlands).

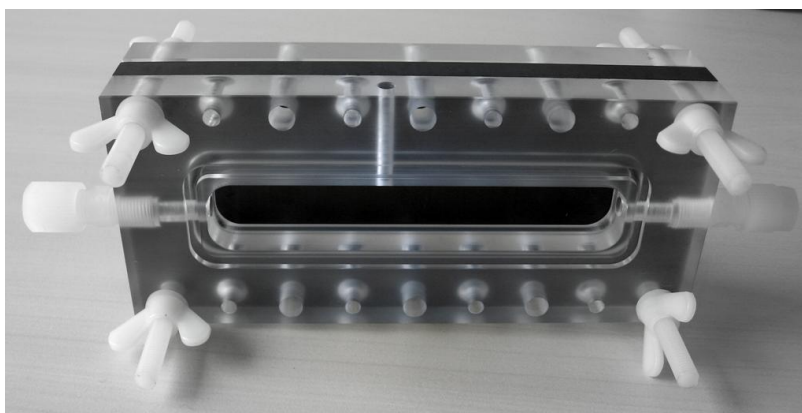


**Figure 1.** MFC design: the assembly of flow channel, flat graphite electrode, and support plate of one side of the MFC.

Although Pt-coated titanium has electrochemical catalytic activity for e.g. oxidation of hydrogen gas to protons, initial experiments showed that Pt-coated titanium had no catalytic activity for oxidation of Ac<sup>-</sup>. All four cathodes were flat graphite plates (Müller & Rössner GmbH & Co., Troisdorf, Germany). The surface area of the flow channel, and thus the projected surface area of the electrodes in contact with solution, was 22 cm<sup>2</sup>, and the volume of the flow channel was 33 mL (11.2 cm length x 2 cm width x 1.5 cm height).

### 2.2.2 Microbial fuel cell operation

The anolyte was inoculated with the effluent of another MFC run on acetate (Ter Heijne et al., 2007). Both anode and cathode compartments were equipped with Ag/AgCl, 3 M KCl reference electrodes (+205 mV vs NHE). Potentials of anode vs. reference electrode and cell voltages of each MFC were collected every 60 seconds via a Fieldpoint FP-AI-110 module connected to a PC. The MFCs were operated in a temperature controlled chamber at 30 °C.

The MFCs were each started with a resistance of 1000 Ω and with a 0.020 M phosphate buffer at pH=7 in the cathode. After two weeks of operation, the catholyte was replaced with a Fe(III)[CN]<sub>6</sub><sup>3-</sup> solution (0.050 M) in 0.020 M buffer (pH=7) for a fast cathode reaction (reduction of Fe(III)[CN]<sub>6</sub><sup>3-</sup> to Fe(II)[CN]<sub>6</sub><sup>4-</sup>). Four resistors with a range of 0 – 1000 Ω were used. Fresh anolyte, consisting of 0.020 M potassium acetate solution in 0.020 M phosphate buffer at pH 7, was fed at a rate of 0.15 L/d. Anolyte pH was controlled at 7. Anolyte and catholyte were recirculated at a flow rate of 10 L/h.

The MFCs were operated at three different resistances with Fe(III)[CN]<sub>6</sub><sup>3-</sup> in the cathode: first R=1000 Ω during 9 days, second R=250 Ω during 5 days, and third R=100 Ω during 6 days, except for the MFC with the uncoated titanium anode, which was operated with a resistance of 500 Ω instead of 250 Ω for 5 days, and was changed back to R=1000 Ω due to its bad performance (anode potential > +100 mV vs Ag/AgCl). At the end of each period, when anode potential was stable (difference in anode potential between two days < 10 mV, and daily standard deviations < 10 mV), each MFC was characterized with a potentiostat (IVIUMStat, Ivium Technologies, Eindhoven, the Netherlands) by EIS and dc-voltammetry. After the third resistance (R=100 Ω), anode potential did not become stable. To be able to measure at a stable situation, the resistor was increased to R=250 Ω for 16 hours before EIS and dc-voltammetry measurements, was kept at 250 Ω during the following 7 days, and was finally increased to R=1000 Ω during 6 days.

The anolyte was supplied with nutrients and vitamins in batch. At the start, and after each change in resistance, the following solutions were supplied to the anolyte: 10 mL/L of a macronutrient solution containing 28 g/L NH<sub>4</sub>Cl, 10 g/L MgSO<sub>4</sub>·7H<sub>2</sub>O, and 0.57 g/L

CaCl<sub>2</sub>·2H<sub>2</sub>O, 2 mL/L of a micronutrient solution containing 2 g/L FeCl<sub>2</sub>·4H<sub>2</sub>O, 1 g/L CoCl<sub>2</sub>·6H<sub>2</sub>O, 0.5 g/L MnCl<sub>2</sub>·4H<sub>2</sub>O, 0.05 g/L ZnCl<sub>2</sub>, 0.05 g/L H<sub>3</sub>BO<sub>3</sub>, 0.04 g/L CuCl<sub>2</sub>·2H<sub>2</sub>O, 0.07 g/L (NH<sub>4</sub>)<sub>6</sub>Mo<sub>7</sub>O<sub>24</sub>·5H<sub>2</sub>O, 1 g/L NiCl<sub>2</sub>·6H<sub>2</sub>O, 0.16 g/L Na<sub>2</sub>SeO<sub>3</sub>·5H<sub>2</sub>O and 2 mL/L 37% HCl (adapted from (Van der Zee et al. 2001)), and 2 mL/L of a vitamin solution as described in (Ter Heijne et al., 2007).

Samples were taken from the anode each time that a measurement was performed and were analyzed for their acetate concentrations.

### 2.2.3 Measurements and data analysis

Current density  $I$  (A/m<sup>2</sup>) was calculated from the cell voltage  $E$  (V), the resistance  $R$  (Ω) and the projected electrode surface area  $A_{el}$  (m<sup>2</sup>) according to  $I = \frac{E}{R \cdot A_{el}}$ . Average current density, average anode potential, and their standard deviations were calculated over 24 hours from data obtained every 60 seconds. Polarization curves were obtained by dc-voltammetry, using the method chronoamperometry. The cell voltage was decreased stepwise and was kept at each voltage for 120 seconds in order to let the dc-current stabilize. The MFCs were measured in the range of 0.65 V – 0.30 V (cell voltage) in steps of 0.050 V, except for MFC with the uncoated titanium anode, which was measured in the range of 0.3 V – 0.1 V (cell voltage). The last data point at each voltage, after 120 seconds, was selected for data presentation. Anode potential was measured every 30 seconds during these measurements on a PC via the Fieldpoint module.

Impedance was measured at 22 frequencies between 40 – 0.003 Hz. The cell voltage at which the impedance measurement was performed was the cell voltage of the MFC when operated with the resistor, for both  $R=1000 \Omega$  and  $R=250 \Omega$ . As anode potential did not become stable at  $R=100 \Omega$ , impedance was measured at the same cell voltage as before with  $R=250 \Omega$ . Each MFC was pretreated for 300 seconds at this cell voltage before impedance measurement was started, so the MFC was stable at the start of the measurement.

The equivalent circuit to which the data were fitted consisted of a constant phase element (CPE) (He et al., 2007) and a charge transfer resistance ( $R_{ct}$ ) in parallel (representing the anode), placed in series with a solution resistance  $R_s$ . The impedance of the CPE was described by  $Z = \frac{1}{CPE^\alpha}$  where  $Z$  = magnitude of the impedance (Ω), and  $\alpha$  = roughness factor (-).

The equivalent circuit fitting was done by a program written in Mathcad. Four parameters were fitted: CPE,  $\alpha$ , charge transfer resistance, solution resistance. The capacitance was calculated

from the CPE and  $\alpha$  according to (Hsu and Mansfeld, 2001):  $C = CPE \cdot (\omega_{\max})^{(\alpha-1)}$  where  $C$  = capacitance (F), and  $\omega_{\max}$  = frequency at which the maximum  $R_{Im}$  is obtained (rad/s).

Acetate concentrations were determined using a Gas Chromatograph (GC). The GC (HP 5890 series II, Agilent Technologies, Amstelveen, the Netherlands) was equipped with an AT-Aquawax-DA column (Alltech) and a flame ionization detector (FID). Temperature was raised from 80 °C to 210°C, with 25°C/min. Nitrogen was used as carrier gas.

Biomass density could not be determined, because we performed consecutive runs in between which the MFCs could not be disassembled. We report the dependence of current on anode potential to show the microbial kinetics at different anode materials.

The use of  $Fe(III)[CN]_6^{3-}$  as an electron acceptor is convenient when studying the anode kinetics, however  $Fe(III)[CN]_6^{3-}$  is not suitable for practical application because it cannot be regenerated without external energy input. Cell voltage and power density are therefore not shown.

## 2.2.4 Mass transfer calculations

As non-porous electrodes are used, it may be safely assumed that the mass transfer is determined by the stagnant water layer attached to the electrode. This stagnant water layer is the result of the biofilm that holds water, and the hydrodynamic boundary layer. Biofilms observed so far in MFCs are thin, ranging from a monolayer (Bond and Lovley, 2003) to maximally about 40  $\mu m$  (Reguera et al., 2006). The thickness of the hydrodynamic boundary layer was calculated to be 155  $\mu m$  (see below), and therefore we assume that this hydrodynamic boundary layer, and not the biofilm, mainly determined the effect of mass transfer on the current density. The average mass transfer rate in the reactor for laminar flow can be calculated using (Hayes and Kolaczowski, 1994):

$$Sh = 3.66 \left( 1 + 0.095 \frac{D_T}{L} Pe \right)^{0.45}$$

$$Pe = \frac{D_T v}{D}$$

$$Sh = \frac{k \cdot D_T}{D}$$

$$\delta = \frac{D}{k}$$

where  $Sh$  = Sherwood number (-),  $D_T$  = hydraulic diameter (m) =  $\frac{2 \cdot W \cdot H}{W + H}$  (with  $W$  = width = 2.0 cm,  $H$  = height = 1.5 cm),  $L$  = channel length = 12 cm,  $Pe$  = Peclet number (-),  $v$  = flow velocity = 1.0 cm/s,  $D$  = diffusion coefficient for acetate =  $1.2 \times 10^{-9}$  m<sup>2</sup>/s (Wanner and Gujer 1986),  $k$  = mass transfer coefficient (m/s), and  $\delta$  = thickness of the hydrodynamic boundary layer (m).

The flow was calculated to be laminar using the Reynolds number:  $Re = \frac{D_T \cdot v \cdot \rho}{\mu} = 193$ ,

where  $\rho$  = density =  $1 \times 10^3$  kg/m<sup>3</sup>, and  $\mu$  = viscosity =  $8.9 \times 10^{-4}$  Pa.s.

The mass transfer coefficient was calculated to be  $k = 7.7 \times 10^{-6}$  m/s, and thus the thickness of the hydrodynamic boundary layer was 155  $\mu$ m.

When the substrate at the electrode surface is depleted, the maximum mass transfer rate is observed. Under these conditions a limiting current density, ( $I_l$ , A/m<sup>2</sup>) is observed, which can be calculated as:  $I_l = n \cdot F \cdot k \cdot c^*$  (Bard and Faulkner, 2001), where  $n$  = 8 (number of electrons per acetate),  $F$  = Faraday's constant (96485 C/mol), and  $c^*$  = bulk acetate concentration (mol/m<sup>3</sup>). The resulting limiting current density is for example 39 A/m<sup>2</sup> at an acetate concentration of  $6.5 \times 10^{-3}$  M.

### 2.2.5 Specific surface area (Atomic Force Microscopy)

The specific surface area of the electrode materials was determined with an Atomic Force Microscope (NanoScope IIIa, Veeco, Santa Barbara, California). To determine the specific surface area on relevant scales, we have studied the surfaces on the scale of the biofilm (20 x 20  $\mu$ m) and on the scale of a microorganism (2 x 2  $\mu$ m). The resolution used was between 512 x 256 and 512 x 512, depending on the roughness of the sample. The specific surface area was calculated as the actual surface area ( $\mu$ m<sup>2</sup>) divided by the projected surface area ( $\mu$ m<sup>2</sup>), and was thereafter normalized to the surface area of the flat graphite electrode.

## 2.3 Results and discussion

### 2.3.1 Overall performance of the bio-anodes

The average daily current densities with standard deviations of the four anodes in time are shown in Figure 2A.

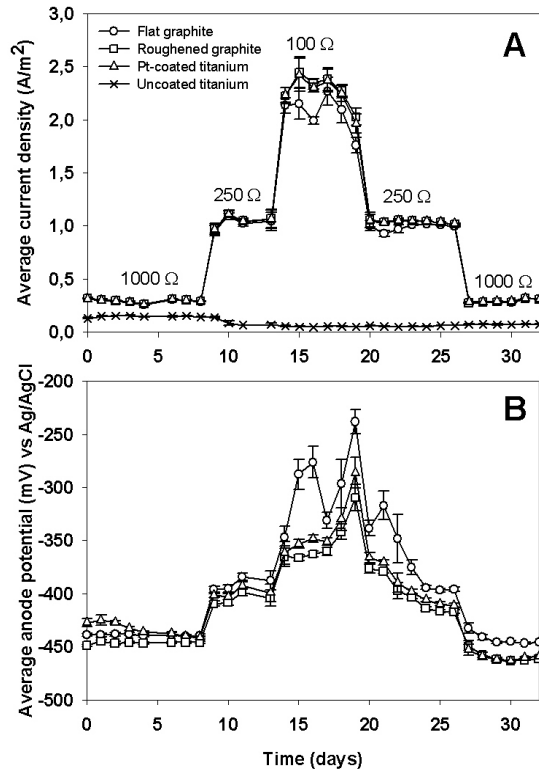


**Figure 2.** (A) Average daily current production (A/m<sup>2</sup>, normalized to the projected surface area) of the four anodes. (B) Average daily anode potential (mV) vs Ag/AgCl of the roughened graphite, Pt-coated titanium, and flat graphite electrode.

The average daily anode potential and the standard deviations of flat graphite, roughened graphite, and Pt-coated titanium are shown in Figure 2B. The anodes based on flat graphite, roughened graphite, and Pt-coated titanium operated steady at 1000 Ω (day 0-8) and at 250 Ω (day 9-13), however, they did not reach a stable potential and current when operated at 100 Ω (day 14-19). At this resistance, we observed high variations in the daily current density and anode potential, and the performance decreased considerably during the last two days of operation at this resistance.

The Pt-coated titanium, roughened graphite, and flat graphite anodes changed to steady operation again after the resistors were increased to 250 Ω (day 20-26), and to 1000 Ω (day 27-32), and the produced current was similar to the current at that same resistance before. The anode potential was similar to the anode potential at the same resistance before as well. The

uncoated titanium anode had the lowest current. This current did not increase as a result of the change in resistance.

Current production on uncoated titanium was far lower than on the other materials, and the anode potential was considerably higher ( $> -150$  mV vs Ag/AgCl at  $R=1000 \Omega$ ). This may be caused by anodic passivation, which is the formation of a thin metal oxide layer (Schmuki, 2002). These titanium oxides are formed when uncoated titanium is in contact with air and they significantly decrease the reaction rate at the electrode. Therefore, uncoated titanium is unsuitable as anode material.

The current density during operation at  $100 \Omega$  (Figure 2A) reached a limit between 2 and  $2.5 \text{ A/m}^2$  at which the anode potential and current density did not become stable. This limit and the instability might be caused by the locally low pH as a result of the accumulation of protons produced by the electrochemically active microorganisms. For each electron, they produce one proton, and when the diffusion of protons to the bulk solution is slow, this can result in a locally low pH, which inhibits the microorganisms. This hypothesis is supported by other research in which it was found that using a concentrated buffer solution, as well as using a buffer solution at high pH, considerably improved MFC performance (Cheng and Logan, 2007; Fan et al., 2007).

### 2.3.2 Bio-anode polarization curves (dc-voltammetry)

After operation at each resistance, polarization curves were made for the bio-anodes using chronoamperometry, allowing the current and anode potential to stabilize for 2 minutes for each data point. The result is shown in Figure 3A – 3E. The best performance – highest current densities in combination the lowest anode potentials – were found for the roughened graphite anode in all situations. After operation at a lower resistance ( $R=250 \Omega$ ), all anodes, except for the uncoated titanium anode, were able to maintain substantially higher current densities during the chronoamperometry measurement (Figure 3B) compared to before ( $R=1000 \Omega$ , Figure 3A). Figure 3C, which was made after the unstable operation at  $100 \Omega$ , shows that the performance of the anodes decreased compared to Figure 3B. During the second operation at  $250 \Omega$ , the anode potentials were stable, and the polarization curves showed higher current densities again (Figure 3D). These current densities however, were lower than obtained before at  $250 \Omega$ . After the second operation at  $1000 \Omega$ , the current densities showed a further increase (Figure 3E). The maximum current density decreased in the order roughened graphite  $>$  Pt-coated titanium  $>$  flat graphite in all situations.

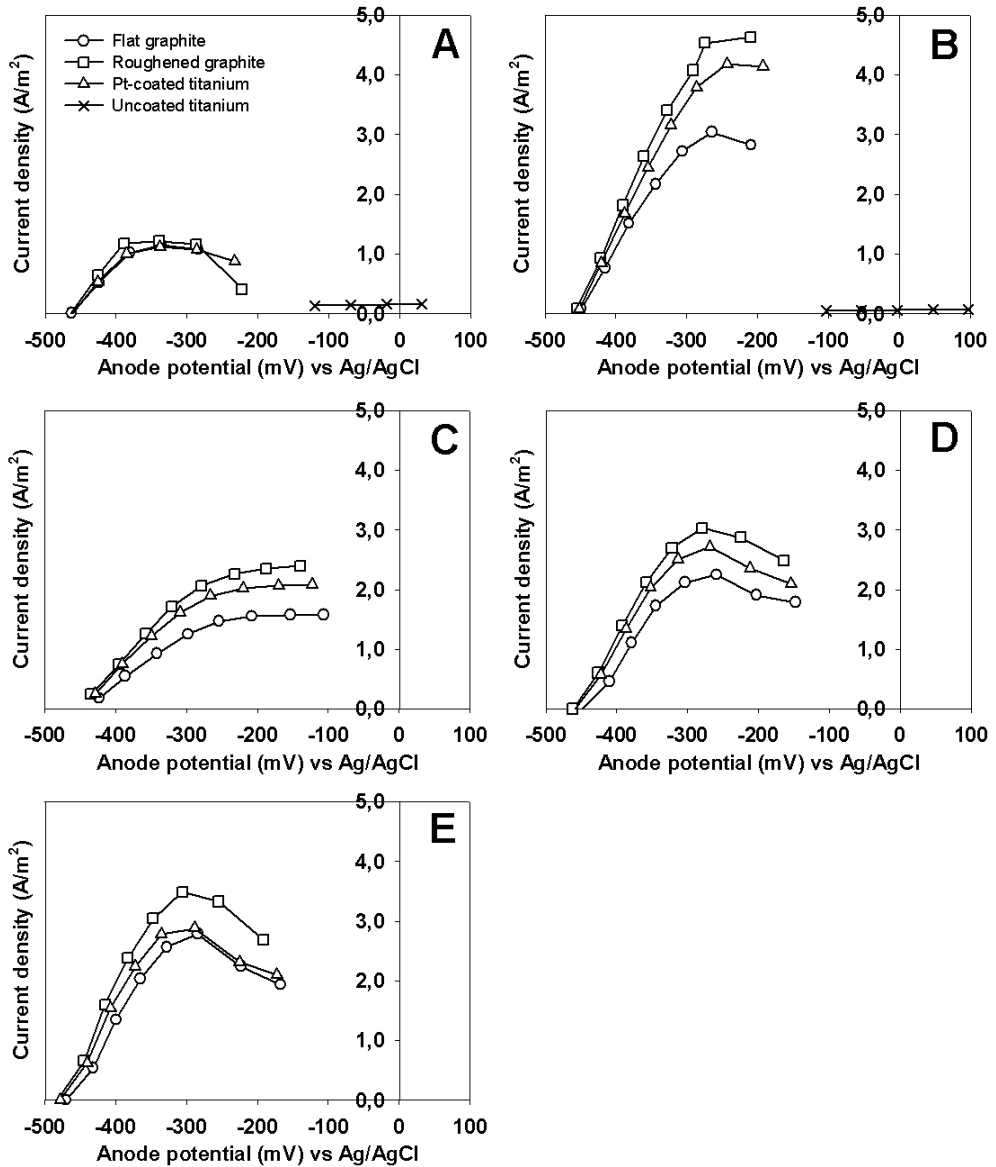


Figure 3A-E. Polarization curves after operation at A:  $1000 \Omega$  (1<sup>st</sup>), B:  $250 \Omega$  (1<sup>st</sup>), C:  $100 \Omega$ , D:  $250 \Omega$  (2<sup>nd</sup>), and E:  $1000 \Omega$  (2<sup>nd</sup>).

To determine the specific surface area of flat graphite, roughened graphite, and Pt-coated titanium on relevant scales, we have studied the surfaces on the scale of the biofilm ( $20 \times 20 \mu\text{m}$ ) and on the scale of a microorganism ( $2 \times 2 \mu\text{m}$ ). On the scale of the biofilm, the specific surface area normalized to flat graphite ( $1.1 \mu\text{m}^2/\mu\text{m}^2$ ) decreased in the order Pt-coated titanium (1.9) > roughened graphite (1.2) > Flat graphite (1.0). On the scale of a microorganism, the specific surface area normalized to flat graphite ( $1.1 \mu\text{m}^2/\mu\text{m}^2$ ) decreased in the same order: Pt-coated titanium (1.2) > roughened graphite (1.0) = flat graphite (1.0).

As the current density decreased in a different order (roughened graphite > Pt-coated titanium > flat graphite), the surface area is not the single variable explaining the differences in current density for the different materials. Other specific surface properties might have an effect on bacterial attachment and electron transfer and influence the current density in this way. One should also consider that mixed cultures as used in this research have variability by nature, making it more difficult to see the effect of surface area, which differed only a factor 2.

The higher current densities in Figure 3B as compared to Figure 3A show that operation at lower resistance improves MFC performance. A lower resistance results in an increased anode potential. At higher anode potentials, the electrochemically active microorganisms can gain more energy from the substrate, as the potential difference between the electron donor (acetate) and the electron acceptor (the anode) is larger. As a consequence, the microorganisms can theoretically gain more energy for growth and higher current can be produced.

### **2.3.3 Limiting current density was not caused by mass transfer of the substrate and reflects the maximum biomass activity**

A limiting current density was established in the polarization curves, which may indicate mass transfer limitations for the substrate or for the products. Mass transfer limitations for acetate however, were not likely for two reasons: (i) there was no relationship between the acetate concentration and the observed limiting current density ( $R^2 = -2.89$  for linear fit, which indicates that the average is a better representation than the linear fit), and (ii) the observed limiting current density was several times lower than the expected calculated limiting current density (see materials and methods), e.g.  $4.6 \text{ A/m}^2$  vs.  $39 \text{ A/m}^2$  at acetate concentration =  $6.5 \times 10^{-3} \text{ M}$ . The limiting current density was therefore not caused by mass transfer of the substrate and reflected the maximum biomass activity.

Accumulation of product (protons) can also be considered as a mass transfer limitation. Accumulation of products results in a lower overpotential. This mass transfer limitation can be overcome by increasing the overpotential, and does not inhibit or decrease the activity (current density) unless the product is toxic to the microorganisms. Because protons can be toxic to

microorganisms, mass transfer limitation of protons could be a reason for the occurrence of a limiting current density. Then however, the limiting current density in all polarization curves would be the same as the current density determines the rate of proton production. The limiting current was not the same, but different in all situations. So, mass transfer of protons as an explanation for the limiting current density cannot be ruled out for the polarization curve in Figure 3B which had the highest current density, but is unlikely in the other polarization curves.

We hypothesize that the decrease in current density at higher anode potentials could be caused by damage of enzymes. A higher anode potential might induce damage of the enzymes that are used for electron transfer, as enzymes have a maximum activity at a particular potential (Vincent and Armstrong, 2005). After operation at 100  $\Omega$  however, the polarization curves did show a limiting current, but no maximum (Figure 3C). At this resistance, the microorganisms were already accustomed to a higher anode potential during the week before the recording of the polarization curves. As a result, the enzymes for electron transfer might not have been damaged at these higher potentials.

### **2.3.4 Polarization curves showed high performance, but should be evaluated critically**

Most surprisingly, the current densities obtained in these polarization curves with a flat, non-porous electrode were of the same order of magnitude as the current densities normalized to the projected surface area of porous electrode materials in other studies like graphite felt and graphite cloth, with maximum current densities of e.g. 4.5 and 8 A/m<sup>2</sup> (Ter Heijne et al., 2007; Cheng and Logan, 2007). This implies that a large part of the surface area of these porous electrode materials was less active, as the same current density can be reached with non-porous electrodes.

Polarization curves are a powerful tool to rapidly evaluate MFC behavior and the development of activity of electrochemically active microorganisms in time (Logan et al., 2006; Aelterman et al., 2006). Although polarization curves are useful for rapid investigation of MFC behavior, the drawback of polarization curves is that they do not provide information about stable operation in MFCs, and MFC performance is easily overestimated. The maximum current density that was reached in the polarization curve (Figure 3C) could not be reached when operated for a longer time period (at lower resistances). Apparently, current densities as high as 4.6 A/m<sup>2</sup> can be reached on the roughened graphite anode, but due to a limitation in biomass activity it was not possible to sustain higher currents for a longer time period. Besides, large differences were seen in the polarization curves at different times and after operation at

different resistances, while the operational condition like temperature, pH, and sufficiently high acetate concentration, were similar in all experiments. The polarization curves that were made after the MFCs were operated for the second time at 250  $\Omega$  and 1000  $\Omega$  (Figure 3D and E), were very different from the polarization curves in Figure 3B (250  $\Omega$ , 1<sup>st</sup>) and A (1000  $\Omega$ , 1<sup>st</sup>), while the current density at these resistances during stable operation (Figure 2) was the same as before. The lack of stability of the anode potential at higher current densities, and the differences between polarization curves under seemingly similar conditions in this study show that polarization curves of MFCs should be evaluated critically, as was also noted in (Menicucci et al., 2006).

### 2.3.5 Impedance spectroscopy

The standard geometry of the MFCs enabled reproducible impedance measurements. Nyquist plots for the Pt-coated titanium at the end of each period are shown in Figure 4A.

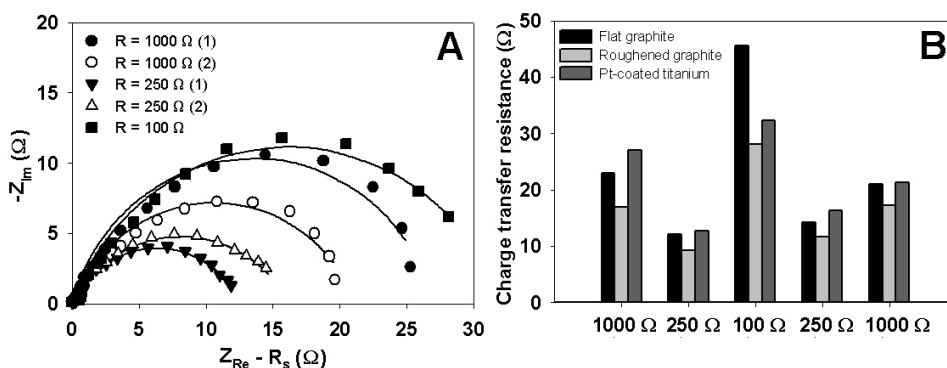


**Figure 4.** (A) Nyquist plots for the Pt-coated titanium anode, corrected for the solution resistance. Symbols represent the experimental data, lines represent the fit of these data to the equivalent circuit. (B) Charge transfer resistances as determined from the width of the semicircle in the Nyquist plot.

These Nyquist plots were corrected for the solution resistance to enable comparison. The solution resistances were all in the same range ( $12.6 \pm 1.7 \Omega$ ), which is in accordance with our expectations, as the same MFC configurations with the same electrolytes are used. The absence of a Warburg impedance in the Nyquist plots is another indication of the absence of mass transfer for acetate.

The charge transfer resistance for the anode materials, as determined from the width of the semicircle, was obtained by fitting with the equivalent circuit. The result is shown in Figure 4B, and supported the difference in performance of the bio-anodes that was found in the polarization curves. The charge transfer resistance for the uncoated titanium anode was  $1.8 \times 10^3 \Omega$  (data not shown), which was three orders of magnitude higher than for the other anodes. The roughened graphite anode had the best performance, which is supported by the lowest charge transfer resistance in all measurements. The charge transfer resistance decreased after operation at  $250 \Omega$  as compared to operation at  $1000 \Omega$ , which might be the result of increased biomass activity. The charge transfer resistance increased considerably after operation at  $100 \Omega$ , which is in accordance with the lower current density in the polarization curves (Figure 3B). The charge transfer resistance decreased again after operation at  $250 \Omega$ , which is in accordance with the higher current density in the polarization curves (Figure 3D). The differences in charge transfer resistance between the materials – like the differences in current density – could not be explained by the differences in specific surface area.

The capacitance, as calculated from the CPE, of the Pt-coated titanium anode was significantly higher ( $11.7 \pm 1.1 \text{ mF/cm}^2$ , average of the measurements at the 5 resistances) compared to the capacitance of the graphite anodes ( $0.72 \pm 0.22 \text{ mF/cm}^2$  for the roughened graphite anode, and  $0.23 \pm 0.14 \text{ mF/cm}^2$  for the flat graphite anode). A high capacitance corresponds with a rough electrode surface (He et al., 2006) and thus a high surface area, which is one of the reasons why Pt-coatings are used in fuel cells (Thompson, 2003). This higher capacitance however, makes the Pt-coated titanium anode less suited for impedance measurements than flat and roughened graphite, as low frequencies are needed to obtain a complete impedance picture. Impedance measurements at low frequencies have a practical drawback: they require a long measurement time, and it is more difficult to keep the MFC stable during the measurement.

## 2.4 Conclusions

With the new experimental setup used in this study, four different anode materials were compared in MFCs under the same conditions. Polarization curves and impedance spectroscopy showed that bio-anode performance normalized to the projected surface area

decreased in the order roughened graphite > Pt-coated titanium > flat graphite > uncoated titanium. Uncoated titanium was found to be unsuitable as anode material. For the other three materials, specific surface area was not the single variable explaining the differences in current density for the different materials. All polarization curves showed a clear limiting current. This limit could not be attributed to mass transfer of the substrate and reflected the maximum biomass activity. The high current densities that were recorded by dc-voltammetry however, could not be maintained in a stable way for a longer period. This shows that polarization curves of MFCs should be evaluated critically.

## Acknowledgements

We thank Vinnie de Wilde for technical assistance and design of the experimental set-up, Nienke Stein and Wim Borgonje at Wetsus for the MFC design, David Strik and Tom Sleutels for critically reading the manuscript, Mieke Kleijn and Herman van Leeuwen for discussing the results and for the help with the AFM, and Magneto Special Anodes BV for kindly supplying the titanium-based anode materials. This research was funded by SenterNovem, the Dutch governmental agency for sustainability and innovation from the Ministry of Economical Affairs; Besluit Energie Onderzoek Subsidie: Nieuw Energie Onderzoek (grant no: NEOT01015), and supported by Wetsus. Wetsus is funded by the city of Leeuwarden, the Province of Fryslân, the European Union European Regional Development Fund and by the EZ/KOMPAS program of the “Samenwerkingsverband Noord-Nederland”.

## 2.5 References

- Aelterman, P.; Rabaey, K.; Pham, H.T.; Boon, N.; Verstraete, W. 2006. Continuous electricity generation at high voltages and currents using stacked microbial fuel cells. *Environ. Sci. Technol.* 40, 3388-3394.
- Bard A.J.; Faulkner, L.R. 2001. *Electrochemical methods: fundamentals and applications*: 2nd ed., John Wiley & Sons, New York.
- Bond, D.R.; Lovley, D.R. 2003. Electricity production by *Geobacter sulfurreducens* attached to electrodes. *Appl. Environ. Microbiol.* 69, 1548-1555.
- Cheng, S.; Logan, B.E. 2007. Ammonia treatment of carbon cloth anodes to enhance power generation of microbial fuel cells. *Electrochem. Commun.* 9, 492-496.
- Fan, Y.; Hu, H.; Liu, H. 2007. Sustainable power generation in microbial fuel cells using bicarbonate buffer and proton transfer mechanisms. *Environ. Sci. Technol.* 41, 8154-8158.
- Hayes, R.E.; Kolaczowski, S.T. 1994. Mass and heat transfer effects in catalytic monolith reactors. *Chem. Engin. Sci.* 49, 3587-3599.
- He, Z.; Minteer, S.D.; Angenent, L.T. 2005. Electricity generation from artificial wastewater using an upflow microbial fuel cell. *Environ. Sci. Technol.* 39, 5262-5267.

- He, Z.; Shao, H.; Angenent L.T. 2007. Increased power production from a sediment microbial fuel cell with a rotating cathode. *Biosens. Bioelectron.* 22, 3252-3255.
- He, Z.; Wagner, N.; Minter, S.D.; Angenent, L.T. 2006. An upflow microbial fuel cell with an interior cathode: Assessment of the internal resistance by impedance spectroscopy. *Environ. Sci. Technol.* 40, 5212-5217.
- Hsu, C.H.; Mansfeld, F. 2001. Technical note: Concerning the conversion of the constant phase element parameter  $Y_0$  into a capacitance. *Corrosion.* 57, 747-748.
- Logan, B.E.; Hamelers, B.; Rozendal, R.; Schröder, U.; Keller, J.; Freguia, S.; Aelterman, P.; Verstraete, W.; Rabaey, K. 2006. Microbial fuel cells: Methodology and technology. *Environ. Sci. Technol.* 40, 5181-5192.
- Lovley, D.R. 2006. Bug juice: Harvesting electricity with microorganisms. *Nature Rev. Microbiol.* 4, 497-508.
- Menicucci, J.; Beyenal, H.; Marsili, E.; Veluchamy, R.A.; Demir, G.; Lewandowski Z. 2006. Procedure for determining maximum sustainable power generated by microbial fuel cells. *Environ. Sci. Technol.* 40, 1062-1068.
- Niessen, J.; Schröder, U.; Rosenbaum, M.; Scholz, F. 2004. Fluorinated polyanilines as superior materials for electrocatalytic anodes in bacterial fuel cells. *Electrochem. Commun.* 6, 571-575.
- Rabaey, K.; Clauwaert, P.; Aelterman, P.; Verstraete W. 2005. Tubular microbial fuel cells for efficient electricity generation. *Environ. Sci. Technol.* 39, 8077-8082.
- Reguera, G.; Nevin, K.P.; Nicoll, J.S.; Covalla, S.F.; Woodard, T.L.; Lovley, D.R. 2006. Biofilm and nanowire production leads to increased current in *Geobacter sulfurreducens* fuel cells. *Appl. Environ. Microbiol.* 72, 7345-7348.
- Rosenbaum, M.; Zhao, F.; Quaa, M.; Wulff, H.; Schröder, U.; Scholz, F. 2007. Evaluation of catalytic properties of tungsten carbide for the anode of microbial fuel cells. *Appl. Catal. B: Environ.* 74, 261-269.
- Schmuki, P. 2002. From Bacon to barriers: A review on the passivity of metals and alloys. *J. Solid State Electrochem.* 6, 145-164.
- Schröder, U. 2007. Anodic electron transfer mechanisms in microbial fuel cells and their energy efficiency. *Phys. Chem. Chem. Phys.* 9, 2619-2629.
- Schröder, U.; Nießen, J.; Scholz, F. 2003. A generation of microbial fuel cells with current outputs boosted by more than one order of magnitude. *Angew. Chem. Int. Ed.* 42, 2880-2883.
- Ter Heijne, A.; Hamelers, H.V.M.; Buisman, C.J.N. 2007. Microbial fuel cell operation with continuous biological ferrous iron oxidation of the catholyte. *Environ. Sci. Technol.* 41, 4130-4134.
- Ter Heijne, A.; Hamelers, H.V.M.; De Wilde, V.; Rozendal, R.A.; Buisman, C.J.N. 2006. A bipolar membrane combined with ferric iron reduction as an efficient cathode system in microbial fuel cells. *Environ. Sci. Technol.* 40, 5200-5205.
- Thompson, D. 2003, in: G. Hoogers (Ed.), Fuel cell technology handbook. CRC press.
- Van der Zee, F.P.; Bouwman, R.H.M.; Strik, D.P.B.T.B.; Lettinga, G.; Field, J.A. 2001. Application of redox mediators to accelerate the transformation of reactive Azo dyes in anaerobic bioreactors. *Biotechnol. Bioeng.* 75, 691-701.

- Vincent, K.A.; Armstrong, F.A. 2005. Investigating metalloenzyme reactions using electrochemical sweeps and steps: Fine control and measurements with reactants ranging from ions to gases. *Inorg. Chem.* 44, 798-809.
- Wanner, O.; Gujer, W. 1986. A multispecies biofilm model. *Biotechnol. Bioeng.* 28, 314-328.

## Chapter 3

# A bipolar membrane combined with ferric iron reduction as an efficient cathode system in microbial fuel cells

3

This chapter has been published as:

Ter Heijne, A.; Hamelers, H. V. M.; De Wilde, V.; Rozendal, R. A.; Buisman, C. J. N. 2006. A bipolar membrane combined with ferric iron reduction as an efficient cathode system in microbial fuel cells. *Environ. Sci. Technol.* 40, 5200-5205.

## Abstract

There is a need for alternative catalysts for oxygen reduction in the cathodic compartment of a microbial fuel cell (MFC). In this study, we show that a bipolar membrane combined with ferric iron reduction on a graphite electrode is an efficient cathode system in MFCs. A flat plate MFC with graphite felt electrodes, a volume of 1.2 L and a projected surface area of 290 cm<sup>2</sup> was operated in continuous mode. Ferric iron was reduced to ferrous iron in the cathodic compartment according to  $\text{Fe}^{3+} + \text{e}^- \rightarrow \text{Fe}^{2+}$  ( $E_0 = +0.77$  V vs NHE, normal hydrogen electrode). This reversible electron transfer reaction considerably reduced the cathode overpotential. The low catholyte pH required to keep ferric iron soluble was maintained by using a bipolar membrane instead of the commonly used cation exchange membrane. For the MFC with cathodic ferric iron reduction, the maximum power density was 0.86 W/m<sup>2</sup> at a current density of 4.5 A/m<sup>2</sup>. The Coulombic efficiency and energy recovery were 80-95% and 18-29% respectively.

### 3.1 Introduction

The microbial fuel cell (MFC) is a device in which microorganisms produce electricity from biodegradable material. In this way, chemical energy is converted directly into electrical energy (Rabaey and Verstraete, 2005; Bond and Lovley, 2003; Chaudhuri and Lovley, 2003). The MFC consists of two compartments: an anoxic compartment with an anode and an aerobic compartment with a cathode. At the anode, bacteria oxidize organic material to carbon dioxide, protons and electrons. Electrons are released to the anode and go through an electrical circuit to the cathode. There the electrons reduce oxygen, together with protons, to water. Protons migrate from anode to cathode through a cation exchange membrane, which separates both compartments. In the overall reaction, organic material and oxygen are converted into carbon dioxide, water and electricity.

Overall MFC performance is among others limited by the unfavorable reaction kinetics of oxygen reduction (Palmore and Kim, 1999; Zhao et al., 2006). To drive the oxygen reduction at the desired rate, a large part of the available energy is needed to establish the necessary overpotential. This problem has already been recognized earlier in the field of chemical fuel cells (Yeager, 1983; Taylor and Humffray, 1973).

Different approaches are currently explored to improve the performance of the cathode in MFCs. Aeration into the cathodic compartment and lowering the catholyte pH have been shown to increase cathode performance (Gil et al., 2003; Jang et al., 2004; Oh et al., 2004), but are insufficiently effective to take away the limitation. The use of hexacyanoferrate as an electron acceptor improves cathode performance considerably (Rabaey and Verstraete, 2005; Oh et al., 2004; Rabaey et al., 2003), but this compound is not suitable for application in practice because of its toxicity and its inability to be regenerated with oxygen (Rabaey et al., 2005a). The use of platinum as a catalyst on carbon electrodes clearly improves cathode performance (Jang et al., 2004; Oh et al., 2004). Air cathodes, covered with platinum, give good results because of the improved oxygen transfer (Liu and Logan, 2004).

Although platinum is a good catalyst, it is expensive and there is a need for alternatives (Zhao et al., 2005). One alternative is to replace platinum by chemical catalysts which are based on cheaper metals. Fe(II)- and Cobalt-based cathodes for example, show similar performance as compared to platinum (Zhao et al., 2005; Cheng et al., 2006). Besides chemical catalysts, biological catalysts combined with redox mediators, can also facilitate oxygen reduction. Biological catalysts are attractive as they are active at ambient temperatures and are renewable (Palmore and Kim, 1999). Biological catalysts can be applied in the form of enzymes (Palmore

and Kim, 1999; Topcagic and Minteer, 2006), or using microorganisms. Microorganisms have the additional benefit that they produce the desired enzymes in situ.

Bergel et al. (2005) found that a seawater biofilm on a stainless steel cathode increased cathode performance. They suggested that the biofilm directly reduced oxygen, although the mechanism was not elucidated. Rhoads et al. (2005) used biomineralized manganese oxides as cathodic reactants. Manganese dioxide ( $\text{MnO}_2$ ) was reduced to soluble  $\text{Mn}^{2+}$  at the cathode.  $\text{Mn}^{2+}$  was subsequently reoxidized with oxygen to manganese dioxide and deposited on the electrode by microorganisms. The redox couple  $\text{Mn}^{2+}/\text{MnO}_2$  thus acted as a mediator for electron transport from the electrode to the oxygen reducing ( $\text{Mn}^{2+}$ -oxidizing) microorganisms.

The objective of this study was to investigate the feasibility of using the redox couple  $\text{Fe}^{3+}/\text{Fe}^{2+}$  as a cathodic electron mediator for oxygen reduction. The redox couple  $\text{Fe}^{3+}/\text{Fe}^{2+}$  was selected for three reasons: (i) it is known for its fast reaction at carbon electrodes (Taylor and Humffray, 1973), (ii) it has a high standard potential (+0.77 V vs NHE for equal concentrations of  $\text{Fe}^{3+}$  and  $\text{Fe}^{2+}$  at low pH), and (iii) ferrous iron can be biologically oxidized to ferric iron with oxygen as the electron acceptor up to high potentials of +850 to +950 mV vs NHE (Rohwerder et al., 2003).

Earlier tests in our laboratory with ferric iron had indicated that a cation exchange membrane could not maintain the low catholyte pH required to keep ferric iron soluble. Cation exchange membranes transport other cations than protons as well, which can cause a pH rise in the cathodic compartment (Rozendal et al., 2006). This pH rise caused extensive iron precipitation that damaged the membrane. The focus of this study was to devise an MFC with sufficiently low catholyte pH (<2.5) to keep ferric iron soluble without external acid dosing. To achieve this, a bipolar membrane was used instead of the commonly used cation exchange membrane. A bipolar membrane has, to our knowledge, never been applied in MFCs before.

It consists of cation and anion exchange sections joined together in series (Simons and Khanarian, 1978; Hurwitz and Dibiani, 2001). A phenomenon that occurs in a bipolar membrane is water dissociation via electrodialysis. When applying an electric field, water dissociates into  $\text{H}^+$  and  $\text{OH}^-$  at the membrane junction, followed by proton migration through the cation exchange membrane (facing the cathode) and hydroxide migration through the anion exchange membrane (facing the anode). This study investigates the performance of the MFC with the bipolar membrane combined with ferric iron reduction on the graphite cathode. As ferrous iron oxidation has been studied extensively and has been shown to operate efficiently at a high rate (e.g. Ebrahimi et al. 2005; Boon et al., 1999; Mazuelos et al., 2000; Karamanev and Nikolov, 1988), the performance of the MFC was investigated without

regeneration of ferric iron. This enabled us to quantify ferric iron reduction and its effect on pH and to analyze the behavior of the membrane.

## 3.2 Materials and methods

### 3.2.1 Microbial fuel cell setup

The flat plate MFC, comparable to the one previously used by Min and Logan (2004), consisted of 6 plexiglas plates sized 28.0 x 28.0 cm bolted together (Figure 1). The four middle plates contained channels for solution transport. The membrane (fumasep FBM, FuMA-tech GmbH, St. Ingbert, Germany) was placed between the two middle plates (thickness and channel depth: 1.2 cm). Against these plates, the electrodes were placed. The electrodes were kept in position by the electrode supporting plates with a thickness of 1.5 cm and a channel depth of 1.2 cm. The two outer plates (thickness 1.5 cm) were massive and served as a physical support. Cathode and anode both had a channel volume of 0.62 L.

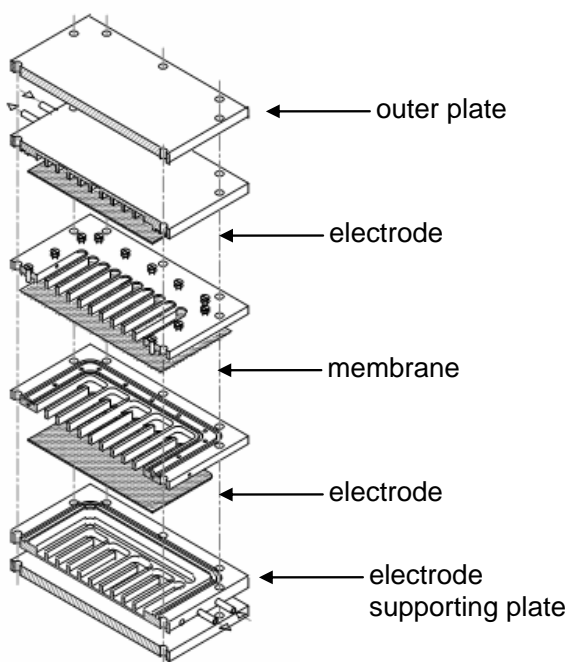


**Figure 1.** The flat plate microbial fuel cell

The electrodes consisted of graphite felt sized 19.0 cm x 19.0 cm (thickness: 3 mm – FMI Composites Ltd., Galashiels, Scotland), having – following Min et al. (2004) – an effective geometric channel surface of 290 cm<sup>2</sup>, which is 80% of the total surface area.

A gold wire was pressed on the electrode and served as current collector. The cathode and anode electrodes were connected via the gold wire to a resistor with a range of 0 - 100  $\Omega$ . The reference electrodes were Ag/AgCl, 3 M KCl electrodes (+205 mV vs NHE, ProSense QiS, Oosterhout, The Netherlands). The catholyte was recirculated continuously via an open bottle for passive oxygen supply. This was done to be able to compare the results from the Coulombic efficiency tests with other studies. The oxygen level was continuously measured. The oxygen concentration was always around 20%, the concentration in ambient air. The anolyte was recirculated at a rate of 10 L/h to prevent diffusion limitations for acetate, buffer and nutrients to the bacteria. Both anode and cathode potential were constantly logged, as well as catholyte pH, conductivity and temperature. Data were collected on a PC via a FieldPoint FP-AI-110 module. Anolyte pH was constantly monitored without logging. The program LabVIEW was used for data acquisition.

### 3.2.2 Microorganisms and medium

The anodic compartment was inoculated with effluent from another operating MFC run on acetate. The feeding to the anodic compartment contained a potassium acetate solution which was fed at a rate of 250 mL/d (HRT = 2.5 days), with varying acetate concentrations in the range of 8 to 40 mM, based on the expected current. Every 4 days, 1 mL of a macronutrient solution (consisting of 4.31 g/L NH<sub>4</sub>Cl, 5.39 g/L CaCl<sub>2</sub>·2H<sub>2</sub>O, 4.31 g/L MgSO<sub>4</sub>·7H<sub>2</sub>O and 54 mg/L FeCl<sub>3</sub>) and 10 mmol potassium phosphate buffer at pH = 7 was supplied to the anodic compartment (concentration = 10 mM).

### 3.2.3 Microbial fuel cell operation

The MFC was operated in a temperature-controlled room at T = 303 K. It was operated in continuous mode, except during start-up and when performing Coulombic efficiency tests.

The MFC was started in batch mode with a fumasep FKB cation exchange membrane and deionized water in the cathodic compartment. After stable operation in continuous mode, the cation exchange membrane was replaced by a fumasep FBM bipolar membrane. At this point, the power production was 22 mW/m<sup>2</sup>. The bipolar membrane was placed in the MFC with the cation exchange side facing the cathodic compartment and the anion exchange side facing the anodic compartment. The catholyte was first a 0.017 M ferric iron chloride (Fe(III)Cl<sub>3</sub>) solution. Thereafter, the catholyte was replaced with a 0.017 M ferric iron sulfate hydrate

(Fe(III)<sub>2</sub>(SO<sub>4</sub>)<sub>3</sub>.xH<sub>2</sub>O) solution and the MFC was operated with anolyte pH 7 and 6. For experiments with a longer duration, the catholyte was recirculated via a storage vessel, resulting in a total catholyte volume of around 17 liters.

The open circuit voltage (OCV) and open circuit potential (OCP) were measured by disconnecting the electrodes so that there was no current. Power density curves were generated by varying the circuit load of the resistor between 5 and 100 Ω. Coulombic efficiency was determined in batch mode by addition of potassium acetate after all acetate was removed from the anodic compartment. This was assumed to be the case after the cell voltage decreased below 5% of the maximum voltage, following Gil et al (2003).

### 3.2.4 Analyses

Anode and cathode potential were measured versus Ag/AgCl reference electrodes (+205 mV vs NHE). The voltage across the membrane was defined as the potential difference between the cathode reference electrode and the anode reference electrode. All potentials are reported versus Ag/AgCl reference electrodes.

Power density  $P$  (W/m<sup>2</sup>) and current density  $j$  (A/m<sup>2</sup>) were calculated from cell voltage  $E$  (V), circuit load  $R$  (Ω) and anode electrode surface area  $A$  (m<sup>2</sup>) according to:

$$P = \frac{E^2}{RA} \quad (1)$$

$$\text{and } j = \frac{E}{RA} \quad (2)$$

The internal resistance  $R_i$  (Ω) was calculated from the slope of the polarization curves (Liu et al. 2005a).

Coulombic efficiency  $\eta_C$  (%) was calculated from the charge in the produced current relative to the charge of the electrons present in the substrate:

$$\eta_C = \frac{\int_0^t I dt}{n F m_{Ac,in}} \cdot 100\% \quad (3)$$

where  $I$  = current (A),  $n$  = number of electrons involved per reaction ( $n = 8$ ),  $F$  = Faraday's constant (96,485 C/mol) and  $m_{Ac,in}$  = amount of acetate added (Bergel et al.).

Energy recovery  $\eta_E$  (%) was calculated from the measured cell voltage as compared to the maximum voltage from Gibb's free energy change  $\Delta G$  (kJ/mol) for the overall reaction, multiplied with the Coulombic efficiency:

$$\eta_E = \frac{E}{E_{\max}} \eta_C \text{ with } E_{\max} = \frac{-\Delta G}{nF} \quad (4)$$

The overall reaction in the MFC is  $\text{CH}_3\text{COO}^- + 2 \text{O}_2 \rightarrow 2 \text{HCO}_3^- + \text{H}^+$  with  $E_{\max} = 1.09 \text{ V}$ , standard conditions (Amend and Shock, 2001).

Total iron concentrations were measured using Hach Lange tests LCK 320.

A concept used in bipolar membrane studies is the water-splitting efficiency or the proton transport number  $t_w$  (Hurwitz and Dibiani, 2001). At 100% water splitting efficiency (proton transport number = 1) one mol of water is split into protons and hydroxides inside the membrane per mol of electrons traveling from anode to cathode, followed by migration into the adjacent solutions. The proton transport number is defined as the current carried by protons relative to the total current:

$$t_w = \frac{I_{\text{protons}}}{I_{\text{total}}} \quad (5)$$

where  $I_{\text{protons}}$  is the current carried by protons. The current carried by protons was calculated from the increase in proton concentration in time, multiplied with Faraday's constant.

## 3.3 Results

### 3.3.1 Power density and internal resistance

Power density curves are shown in Figure 2. The maximum power density was  $341 \text{ mW/m}^2$  ( $E = 0.39 \text{ V}$ ,  $R = 15 \Omega$ ) for the MFC with cathodic ferric iron reduction using ferric iron chloride. A similar result was obtained using ferric iron sulfate, which gave a maximum power density of  $298 \text{ mW/m}^2$  ( $E = 0.30 \text{ V}$ ,  $R = 10 \Omega$ ). The maximum power density increased to  $539 \text{ mW/m}^2$  ( $E = 0.40 \text{ V}$ ,  $R = 10 \Omega$ ) after lowering the anolyte pH to 6.

The internal resistance was  $10.3 \Omega$  for the MFC with the cathodic ferric iron reduction using ferric iron chloride and  $7.1 \Omega$  and  $8.4 \Omega$  using ferric iron sulfate with anolyte pH=7 and 6, respectively.

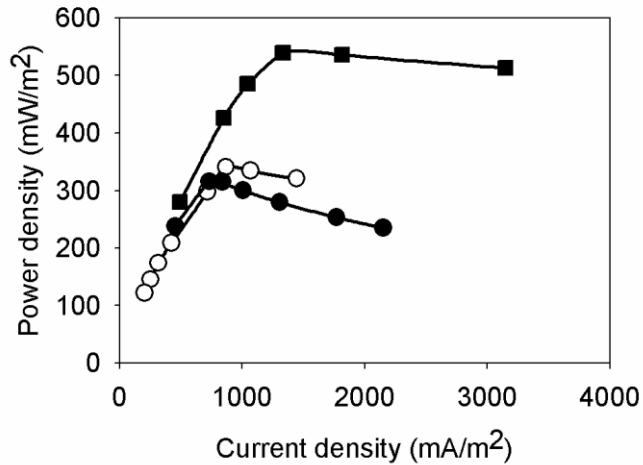


**Figure 2.** Power density curves for the MFC with cathodic ferric iron reduction using ferric iron chloride (○) and ferric iron sulfate with anolyte pH = 7 (●) and anolyte pH = 6 (■). Catholyte pH was between 2.0 and 2.5 in all experiments

### 3.3.2 Electrode potentials

The performance of the anode, cathode, cell and membrane were analyzed by E-j curves. The voltages and potentials in an open circuit ( $j = 0 \text{ A/m}^2$ ) indicate the maximum voltage or potential which is feasible under the existing experimental conditions. After connecting the resistor, thus allowing an electrical current through the system, it can be seen to what extent this maximum voltage or potential is reached.

For the MFC with cathodic ferric iron reduction using ferric iron sulfate, the anode and cathode potential as well as cell voltage and voltage across the membrane are shown in Figure 3. The OCV was  $679 \pm 5 \text{ mV}$  using ferric iron chloride and  $698 \pm 9 \text{ mV}$  using ferric iron sulfate. The open circuit cathode potential was  $+456 \pm 4 \text{ mV}$  using ferric iron chloride and  $+469 \pm 9 \text{ mV}$  using ferric iron sulfate. The cathode potential decreased slightly with increasing current density at a rate of  $0.04 \text{ mV}/(\text{mA/m}^2)$ . The anode potential showed similar behavior. Cell voltage decreased with increasing current density as the voltage loss across the membrane increased.

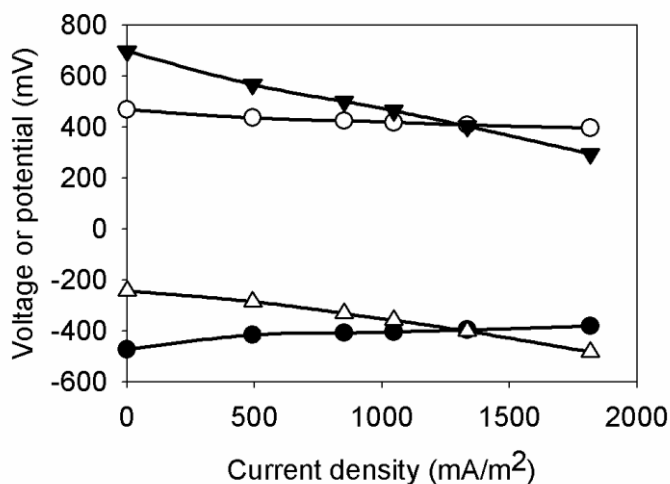


**Figure 3.** Anode potential (●), cathode potential (○), cell voltage (▼) and voltage across the membrane (Δ) as a function of current density (circuit load was varied between 5  $\Omega$  and 40  $\Omega$ ) for the MFC with cathodic ferric iron reduction using ferric iron sulfate. Analyte pH = 6. Anode and cathode showed low overpotential, whereas the voltage loss across the membrane increased with increasing current density.

### 3.3.3 Coulombic efficiency and energy recovery

Coulombic efficiency and energy recovery were determined at the circuit load at which the maximum power density was found.

The Coulombic efficiency for the MFC with cathodic ferric iron reduction using ferric iron chloride was 80% ( $j = 920$  mA/m<sup>2</sup>, addition of 1 mmol acetate). The energy recovery was 29%. The Coulombic efficiency for the MFC with cathodic ferric iron reduction using ferric iron sulfate was 85% ( $j = 1,028$  mA/m<sup>2</sup>, addition of 1 mmol acetate). The energy recovery was 21%. The Coulombic efficiency increased to 95% after lowering the circuit load to 5  $\Omega$  and addition of both 1 and 5 mmol acetate ( $j = 1,383$  mA/m<sup>2</sup> and  $j = 1,744$  mA/m<sup>2</sup> respectively) using ferric iron sulfate. The energy recovery was 18 and 23% respectively.

### 3.3.4 Continuous low load power production

The MFC with cathodic ferric iron reduction was operated for a period of almost 3 months at varying circuit loads, while the ferric iron solution was regularly refreshed. Finally, we investigated electricity production at constant low circuit load (1.5  $\Omega$ ) to confirm that not only instantaneous power was measured (Menicucci et al., 2006). During an operation period of over 50 h, power density increased from 0.5 to 0.86 W/m<sup>2</sup>, which

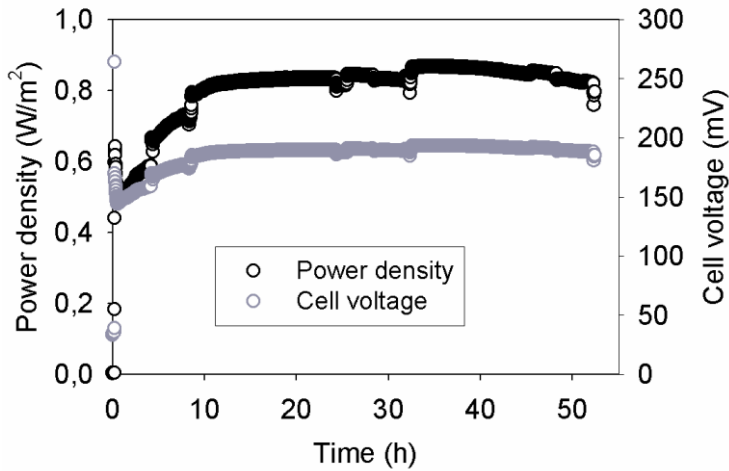


**Figure 4.** Stable power production and cell voltage at constant low circuit load ( $R=1.5 \Omega$ ) for the MFC with cathodic ferric iron reduction using ferric iron sulfate.

was the highest power density found in this study. This latter value corresponds to a volumetric power production of  $42 \text{ W/m}^3$ , normalized to the channel volume of the anodic compartment. Current density increased from  $3.4$  to  $4.5 \text{ A/m}^2$ . Cell voltage was stable at  $190 \text{ mV}$  (Figure 4).

The total iron concentration was measured at regular intervals during the experiment and was found to be always between  $16.3$  and  $16.4 \text{ mM}$ . This concentration was  $3.5\%$  lower than the expected concentration, but within accuracy of the measurement method and the purity of the iron sulfate.

## 3.4 Discussion

### 3.4.1 Bipolar membrane

The design for the MFC with cathodic ferric iron reduction and regeneration of ferric iron by the microorganism *Acidithiobacillus ferrooxidans* is shown in Figure 5. The low catholyte pH ( $<2.5$ ) required to keep ferric iron soluble was maintained by using a bipolar membrane. The bipolar membrane provides the cathodic compartment with protons and the anodic compartment with hydroxides as a result of water dissociation.

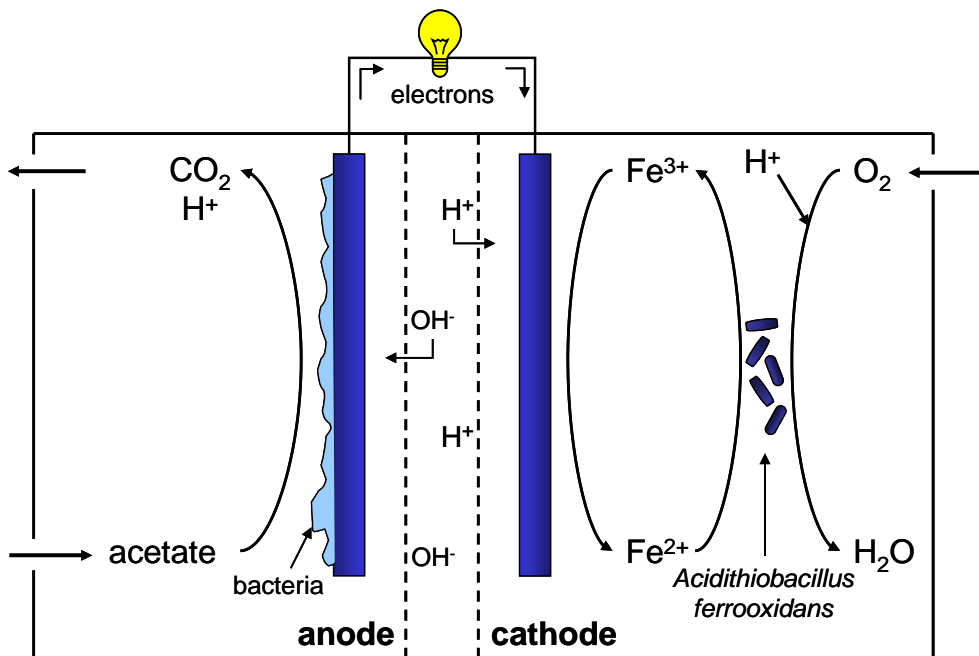


**Figure 5.** Design for the MFC with the iron-mediated cathode. Anodic and cathodic compartment are separated by a bipolar membrane with the cation exchange side facing the cathode and the anion exchange side facing the anode. The bipolar membrane maintains the low catholyte pH required to keep ferric iron soluble by means of water dissociation into H<sup>+</sup> and OH<sup>-</sup>. The redox couple Fe<sup>3+</sup>/Fe<sup>2+</sup> acts as a mediator for electron transport from the electrode to the oxygen reducing (ferrous iron oxidizing) microorganism *A. ferrooxidans*.

The low catholyte pH can be maintained in this way without the need of acid dosage. The bipolar membrane showed no detectable loss of iron. A cation exchange membrane, as normally used in an MFC, would fail in this respect as had been observed in earlier experiments with Nafion 117. These experiments show that the cathode performed well for only several hours. Catholyte pH increased rapidly, while anolyte pH decreased. Due to low solubility of ferric iron at pH > 2.5, ferric iron hydroxide precipitates were found inside the membrane as a result of ferric iron migration. The pH drop in the anodic compartment and the pH increase in the cathodic compartment were due to migration of protons and other cations through the cation exchange membrane. Not only protons but also other cations are likely to migrate through cation exchange membranes when present in higher concentrations (Rozendal et al., 2006).

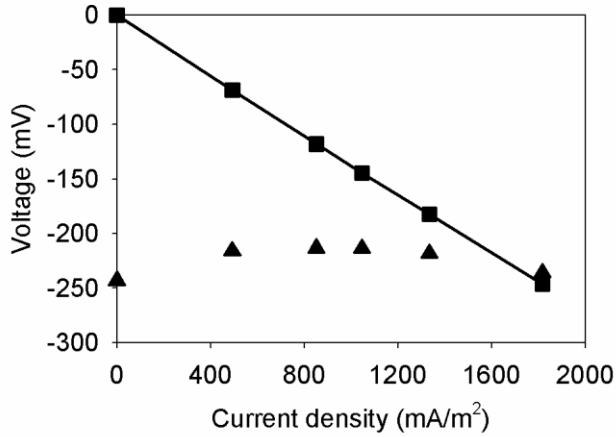


**Figure 6.** Voltage across the membrane (▲) corrected for the ohmic voltage drop (■) for the MFC with cathodic ferric iron reduction using ferric iron sulfate. The ohmic voltage drop increased with increasing current density, whereas the voltage across the membrane was between -200 and -250 mV, independent of current density. Ohmic losses limited MFC performance.

### 3.4.2 Voltage across the bipolar membrane

The voltage across the membrane was defined as the potential difference between the cathode reference electrode and the anode reference electrode. Ohmic losses can be expected as a result of the distance between the membrane and the electrodes. The measured voltage across the membrane thus consists of both ohmic losses and a true voltage across the membrane. The ohmic voltage drop  $\Delta V_{\Omega}$  (V) was calculated at both sides of the membrane, according to:

$$\Delta V_{\Omega} = \frac{dj}{\sigma} \quad (6)$$

where  $d$  = distance between membrane and reference electrode (cm),  $j$  = current density (A/cm<sup>2</sup>) and  $\sigma$  = conductivity (S/cm).

The measured voltage across the membrane was corrected for the ohmic voltage drop using  $d = 2.1$  cm,  $\sigma_{\text{anolyte}} = 2.5$  mS/cm and the logged value for  $\sigma_{\text{catholyte}}$ . The result is shown in Figure 6 for the MFC with cathodic ferric iron reduction using ferric iron sulfate and anolyte pH=6. The corrected (true) voltage across the membrane was between -200 and -250 mV.

A voltage drop across the bipolar membrane is required to start the water splitting reaction. This voltage drop was calculated to be 0.83 V for a 100% selective bipolar membrane for the generation of a one molar acid and base solution at 298 K (Hurwitz and Dibiani, 2001) using:

$$\Delta V = \frac{-2.3RT}{F} \Delta pH \quad (7)$$

The pH difference between the anodic and the cathodic compartment in our MFC was 3.5. According to eq (7), this results in a voltage drop of -0.21 V. The observed voltage across the membrane was thus sufficient to allow water splitting. The occurrence of water splitting was confirmed by the decrease in catholyte pH during ferric iron reduction. Bipolar membranes have never been characterized under the specific conditions in our MFC: low current densities, different anolyte and catholyte, low conductivity, and a small pH gradient across the membrane. Further research is necessary.

From our findings it turns out that that the ohmic losses make up a substantial part of the energy losses. MFC performance can be considerably improved by reducing the ohmic losses. This can be done by placing the electrodes and the membrane in close contact.

3

### 3.4.3 Ferric iron reduction

The measured cathode potential turned out to be proportional to the natural logarithm of the ratio  $[Fe^{3+}]/[Fe^{2+}]$ , as would be expected from the Nernst equation:

$$E_{cathode}(Fe^{2+}, Fe^{3+}) = E_{cathode}^0 + \frac{RT}{F} \ln \frac{[Fe^{3+}]}{[Fe^{2+}]} \text{ with } E_{cathode}^0 = 0.77 \text{ V vs NHE}$$

The measured cathode potential was corrected for the conductivity as the conductivity increased proportionally with increasing  $Fe^{2+}$  concentration. The ferric and ferrous iron concentrations at each point were calculated from the initial amount of ferric iron and the produced current. The measured cathode potential was found to be

$$E_{cathode} = 424 + 18.4 \ln \frac{[Fe^{3+}]}{[Fe^{2+}]} \quad (R^2 = 0.9953).$$

Analysis of other experimental data showed similar behavior. The slope, being 18.4 mV, is lower than the theoretical value of  $\frac{RT}{F} = 26.1$  mV. This could be an effect of diffusion limitation.

The formal (measured) potential is influenced by other substances in the solution and by the ionic strength of the solution (Bard and Faulkner, 2001). As a result, the measured  $E^0$  value (424 mV) can be lower than the theoretical value (565 mV vs Ag/AgCl).

### 3.4.4 Proton transport number

For the MFC with cathodic ferric iron reduction, a decrease in catholyte pH was observed. The increase in proton concentration was in the order of magnitude of 2 mM/h. Two

processes that would lead to a pH decrease in the cathodic compartment are (i) proton supply by the bipolar membrane as a result of water dissociation in the membrane and (ii) transport of alkalinity from the cathodic to the anodic compartment.

The water-splitting efficiency or proton transport number indicates the current carried by protons compared to the total current (Hurwitz and Dibiani, 2001). The proton production by the bipolar membrane was calculated from the pH drop in the cathodic compartment. Preliminary calculations showed a proton transport number of 0.6–0.7. This transport number however should be considered as an indication only, as the decrease in pH was small. This subject needs further investigation.

### 3.4.5 Perspectives for practical application

Ferric iron should be regenerated from ferrous iron to make the MFC with cathodic ferric iron reduction suitable for practical application. Chemical ferrous iron oxidation at low pH is very slow, as it is proportional to the squared  $\text{OH}^-$  concentration (Stumm and Morgan, 1981). Microorganisms such as *A. ferrooxidans* are capable of oxidizing ferrous iron to ferric iron at low pH, using oxygen as the terminal electron acceptor. Biological ferrous iron oxidation at low pH has been studied extensively and has been shown to operate efficiently at a high rate, e.g. (Ebrahimi et al., 2005; Karamanev and Nikolov, 1988). Ebrahimi et al. (2005) studied ferrous iron oxidation by the chemolithoautotrophic microorganisms *Acidithiobacillus ferrooxidans* and *Leptospirillum ferrooxidans*. In their biofilm airlift reactor, ferrous iron was reoxidized by *A. ferrooxidans* and *L. ferrooxidans* to ferric iron at a rate of  $145 \text{ mol Fe}^{2+}/\text{m}^3\text{h}$ . The optimal performance was obtained at  $100 \text{ mol Fe}^{2+}/\text{m}^3\text{h}$  with 98% conversion efficiency. If a similar setup is used for the MFC, assuming a current density of  $4.5 \text{ A}/\text{m}^2$  and a ferrous iron conversion rate of  $100 \text{ mol}/\text{m}^3\text{h}$  with 98% efficiency, the reactor size required to ensure complete regeneration of ferric iron would be 50 mL, which is only 4% of the reactor volume. The most suitable way in which ferric iron can be regenerated in this system will be investigated in further study.

The energetic efficiency of acetate conversion to electricity via combustion of methane gas after anaerobic treatment is up to 35% (Rabaey and Verstraete, 2005). To make the MFC a good alternative for conventional wastewater treatment techniques, its energy recovery should be comparable. The energy recovery in the MFC with cathodic ferric iron reduction was 18–29% at the maximum power density. In studies that used platinum-based cathodes with similar power densities, the energy recovery was 2–15% (Liu et al., 2005a; Liu et al., 2005b). For a continuous system, energy recovery was 2–26% as found by Rabaey et al. (2005b) with the use of hexacyanoferrate in the cathodic compartment.

The Coulombic efficiency in this study was considerably higher than that found in other studies: 80-95% in comparison to 40-75% at similar power densities (Rabaey et al., 2005b; Liu and Logan, 2004; Min and Logan, 2004; Liu et al., 2005a).

The MFC with a bipolar membrane combined with ferric iron reduction on a graphite cathode is shown to have a high Coulombic efficiency and energy recovery. Further research into the reactor design for ferric iron regeneration and into reduction of the internal resistance of the MFC is needed to further improve MFC performance.

## Acknowledgements

Part of this work was performed at Wetsus, Centre for Sustainable Water Technology. Wetsus is funded by the city of Leeuwarden, the Province of Fryslân, the European Union European Regional Development Fund and by the EZ/KOMPAS program of the “Samenwerkingsverband Noord-Nederland”

## 3.5 References

- Bergel, A.; Féron, D.; Mollica, A. 2005. Catalysis of oxygen reduction in PEM fuel cell by seawater biofilm. *Electrochem. Commun.* 7, 900-904.
- Bond, D. R.; Lovley, D. R. 2003. Electricity production by *Geobacter sulfurreducens* attached to electrodes. *Appl. Environ. Microbiol.* 69, 1548-1555.
- Boon, M.; Meeder, T. A.; Thöne, C.; Ras, C.; Heijnen, J. J. 1999. The ferrous iron oxidation kinetics of *Thiobacillus ferrooxidans* in continuous cultures. *Appl. Microbiol. Biotechnol.* 51, 820-826.
- Chaudhuri, S. K.; Lovley, D. R. 2003. Electricity generation by direct oxidation of glucose in mediatorless microbial fuel cells. *Nat. Biotechnol.* 21, 1229-1232.
- Cheng, S.; Liu, H.; Logan, B. E. 2006. Power densities using different cathode catalysts (Pt and CoTMPP) and polymer binders (Nafion and PTFE) in single chamber microbial fuel cells. *Environ. Sci. Technol.* 40, 364-369.
- Ebrahimi, S.; Morales, F. J. F.; Kleerebezem, R.; Heijnen, J. J.; van Loosdrecht, M. C. M. 2005. High-rate acidophilic ferrous iron oxidation in a biofilm airlift reactor and the role of the carrier material. *Biotechnol. Bioeng.* 90, 462-472.
- Gil, G. C.; Chang, I. S.; Kim, B. H.; Kim, M.; Jang, J. K.; Park, H. S.; Kim, H. J. 2003. Operational parameters affecting the performance of a mediator-less microbial fuel cell. *Biosens. Bioelectron.* 18, 327-334.
- Hurwitz, H. D.; Dibiani, R. 2001. Investigation of electrical properties of bipolar membranes at steady state and with transient methods. *Electrochim. Acta* 47, 759-773.
- Jang, J. K.; Pham, T. H.; Chang, I. S.; Kang, K. H.; Moon, H.; Cho, K. S.; Kim, B. H. 2004. Construction and operation of a novel mediator- and membrane-less microbial fuel cell. *Process Biochem.* 39, 1007-1012.

- Karamanev, D. G.; Nikolov, L. N. 1988. Influence of some physicochemical parameters on bacterial activity of biofilm: ferrous iron oxidation by *Thiobacillus ferrooxidans*. *Biotechnol. Bioeng.* 31, 295-299.
- Liu, H.; Logan, B. E. 2004. Electricity generation using an air-cathode single chamber microbial fuel cell in the presence and absence of a proton exchange membrane. *Environ. Sci. Technol.* 38, 4040-4046.
- Mazuelos, A.; Carranza, F.; Palencia, I.; Romero, R. 2000. High efficiency reactor for the biooxidation of ferrous iron. *Hydrometallurgy.* 58, 269-275.
- Oh, S.; Min, B.; Logan, B. E. 2004. Cathode performance as a factor in electricity generation in microbial fuel cells. *Environ. Sci. Technol.* 38, 4900-4904.
- Palmore, G. T. R.; Kim, H. H. 1999. Electro-enzymatic reduction of dioxygen to water in the cathode compartment of a biofuel cell. *J. Electroanal. Chem.* 464, 110-117.
- Rabaey, K.; Lissens, G.; Siciliano, S. D.; Verstraete, W. 2003. A microbial fuel cell capable of converting glucose to electricity at high rate and efficiency. *Biotechnol. Lett.* 25, 1531-1535.
- Rabaey, K.; Verstraete, W. 2005. Microbial fuel cells: novel biotechnology for energy generation. *Trends Biotechnol.* 23, 291-298.
- Rabaey, K.; Clauwaert, P.; Aelterman, P.; Verstraete, W. 2005a. Tubular microbial fuel cells for efficient electricity generation. *Environ. Sci. Technol.* 39, 8077-8082.
- Rabaey, K.; Ossieur, W.; Verhaege, M.; Verstraete, W. 2005b. Continuous microbial fuel cells convert carbohydrates to electricity. *Water Sci. Technol.* 52, 515-523.
- Rhoads, A.; Beyenal, H.; Lewandowski, Z. 2005. Microbial fuel cell using anaerobic respiration as an anodic reaction and biomineralized manganese as a cathodic reactant. *Environ. Sci. Technol.* 39, 4666-4671.
- Rohwerder, T.; Gehrke, T.; Kinzler, K.; Sand, W. 2003. Bioleaching review part A: Progress in bioleaching: fundamentals and mechanisms of bacterial metal sulfide oxidation. *Appl. Microbiol. Biotechnol.* 63, 239-248.
- Rozendal, R. A.; Hamelers, H. V. M.; Buisman, C. J. M. 2006. Effects of membrane cation transport on pH and microbial fuel cell performance. *Environ. Sci. Technol.* 40, 5206-5211.
- Simons, R.; Khanarian, G. 1978. Water dissociation in bipolar membranes: experiments and theory. *J. Membr. Biol.* 38, 11-30.
- Taylor, R. J.; Humffray, A. A. 1973. Electrochemical studies on glassy carbon electrodes. I. Electron transfer kinetics. *J. Electroanal. Chem.* 42, 347-354.
- Topcagic, S.; Minteer, S. D. 2006. Development of a membraneless ethanol/oxygen biofuel cell. *Electrochim. Acta*, 51, 2168-2172.
- Yeager, E. 1983. Electrocatalysts for O<sub>2</sub> reduction. *Electrochim. Acta.* 29, 1527.
- Zhao, F.; Harnisch, F.; Schröder, U.; Scholz, F.; Bogdanoff, P.; Herrmann, I. 2005. Application of pyrolysed iron(II) phthalocyanine and CoTMPP based oxygen reduction catalysts as cathode materials in microbial fuel cells. *Electrochem. Commun.* 7, 1405-1410.
- Zhao, F.; Harnisch, F.; Schröder, U.; Scholz, F.; Bogdanoff, P.; Herrmann, I. 2006. Challenges and constraints of using oxygen cathodes in microbial fuel cells. *Environ. Sci. Technol.* 40, 5193-5199.



## Chapter 4

# Microbial fuel cell operation with continuous biological ferrous iron oxidation of the catholyte

This chapter has been published as:

Ter Heijne, A.; Hamelers, H. V. M.; Buisman, C. J. N. 2007. Microbial fuel cell operation with continuous biological ferrous iron oxidation of the catholyte. *Environ. Sci. Technol.* 41, 4130-4134.

## Abstract

The oxygen reduction rate at the cathode is a limiting factor in microbial fuel cell (MFC) performance. In our previous study, we showed the performance of an MFC with ferric iron ( $\text{Fe}^{3+}$ ) reduction at the cathode. Instead of oxygen, ferric iron was reduced to ferrous iron ( $\text{Fe}^{2+}$ ) at the cathode with a bipolar membrane between the anode and the cathode compartment. This resulted in a higher cathode potential than usually obtained with oxygen on metal-based chemical catalysts in MFCs. In this study, we investigated the operation of the same MFC with ferric iron reduction at the cathode and simultaneous biological ferrous iron oxidation of the catholyte. We show that the immobilized microorganism *Acidithiobacillus ferrooxidans* is capable of oxidizing ferrous iron to ferric iron at a rate high enough to ensure an MFC power output of  $1.2 \text{ W/m}^2$  and a current of  $4.4 \text{ A/m}^2$ . This power output was 38% higher than in our previous study at a similar current density without ferrous iron oxidation. The bipolar membrane is shown to split water into 65 - 76% of the needed protons and hydroxides. The other part of the protons was supplied as  $\text{H}_2\text{SO}_4$  to the cathode compartment. The remaining charge was transported by  $\text{K}^+$  and  $\text{HSO}_4^-/\text{SO}_4^{2-}$  from the one compartment to the other. This resulted in increased salt concentrations in the cathode. The increased salt concentrations reduced the ohmic losses and enabled the improved MFC power output. Iron could be reversibly removed from the bipolar membrane by exchange with protons.

## 4.1 Introduction

The increasing threat of global warming by greenhouse gases requires further development of renewable energy sources. The microbial fuel cell (MFC) is a new energy technology in which microorganisms produce electricity directly from renewable biodegradable material (Chaudhuri and Lovley, 2003; Rabaey and Verstraete, 2005; Logan et al., 2006). The MFC consists of an anode and a cathode, separated by a membrane. At the anode, microorganisms convert organic material under anoxic conditions. These microorganisms use the electrode as the electron acceptor (Bond and Lovley, 2003). The electrons flow through an external circuit to the cathode, where oxygen is reduced to water. Oxygen is superior to other electron acceptors for its unlimited availability and its high redox potential (Zhao et al., 2006).

Oxygen reduction at the cathode, however, is kinetically limited, especially on carbon or graphite electrodes, and therefore needs a catalyst or electron mediator (Shukla et al., 2004). Platinum is a chemical catalyst that is often used in MFCs, but it has several disadvantages like its cost and its instability for oxygen reduction (Zhang et al., 2007). Biologically catalyzed cathodes have the advantage that of being cheaper and more renewable (He and Angenent, 2006).

In our previous study (Ter Heijne et al., 2006) we have investigated an alternative cathode reaction, namely the reduction of ferric iron ( $\text{Fe}^{3+}$ ) to ferrous iron ( $\text{Fe}^{2+}$ ) with a bipolar membrane between the anode and the cathode compartment. This bipolar membrane was needed to maintain the low catholyte pH (<2.5) required to keep ferric iron soluble, whereas the conventionally used cation exchange membrane failed to maintain the pH difference between the anolyte and the catholyte. A bipolar membrane consists of a cation and an anion exchange layer. At the junction, water is split into protons and hydroxides when a certain voltage is applied (Nagasubramanian et al., 1977). The protons migrate to the cathode, while the hydroxides move to the anode. The reduction of ferric iron results in a higher cathode potential than is obtained with oxygen on a metal-based catalyst in MFCs (Zhao et al., 2006; Cheng et al. 2006).

In this study, we investigate the performance of the MFC with a bipolar membrane and continuous ferrous iron oxidation of the catholyte by an acidophilic chemolithoautotrophic microorganism (Figure 1).

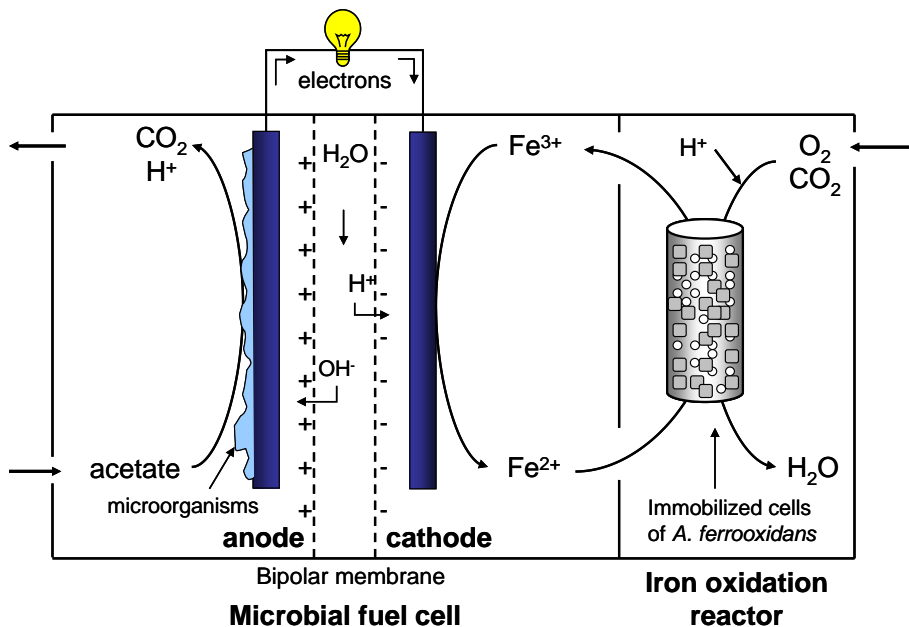
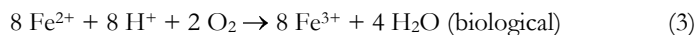
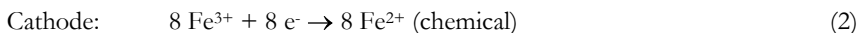
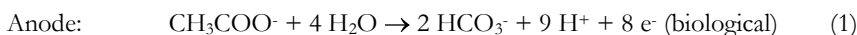


**Figure 1.** Microbial fuel cell with continuous ferrous iron oxidation.

We used the microorganism *Acidithiobacillus ferrooxidans*, which can be found in acid mine drainage and is a dominant organism in the process of ore bioleaching (Jensen and Webb, 1995). These microorganisms derive their energy from the oxidation of  $\text{Fe}^{2+}$ , using  $\text{CO}_2$  as a carbon source and  $\text{O}_2$  as the electron acceptor.

The following reactions occur in the MFC with continuous ferrous iron oxidation:



The oxidation of ferrous iron using oxygen as an electron acceptor yields only a relatively small amount of energy for microbial growth. The Gibb's free energy of iron oxidation has been estimated to be between -42 and -27 kJ/mol (Leduc and Ferroni, 1994; Rohwerder et al., 2003). The biomass yield of iron oxidizing microorganisms is consequently low: approximately 20 mol of ferrous iron is needed to produce 1 mole of biomass-C (Jensen and Webb, 1995; Leduc and Ferroni, 1994). The low energy consumption and low excess biomass production makes the couple ferric/ferrous iron an attractive electron mediator for oxygen reduction.

Our objective was to study the performance of the MFC with continuous ferrous iron oxidation. The MFC was operated with low iron concentrations in the catholyte, as these lower the chance of precipitation (Stumm and Morgan, 1981). At the same time, the initial ferrous iron oxidation rate should be sufficiently high for the investigation of MFC performance. Because of the low biomass yield of the iron oxidizing microorganisms, however, it takes time before a high conversion rate is obtained in a solution with low iron concentrations. The iron oxidizing microorganisms were therefore first grown on biomass support particles (BSPs) in a medium with a high ferrous iron concentration. Thereafter, we have placed this immobilized culture of *A. ferrooxidans* in a separate reactor and combined it with a ferric iron reducing cathode in an MFC.

In this study, we investigate the performance of the MFC with ferric iron reduction at the cathode and simultaneous biological ferrous iron oxidation.

## 4.2 Materials and methods

### 4.2.1 Microbial fuel cell setup

The flat plate MFC used for the experiments is described in more detail in (Ter Heijne et al., 2006). The effective projected surface area of both anode and cathode was 290 cm<sup>2</sup>, and each compartment had a liquid volume of 0.62 L. The electrodes were made of graphite felt (thickness: 3 mm, FMI Composites Ltd., Galashiels, Scotland). Both the cathode and the anode compartment contained reference electrodes (Ag/AgCl, 3 M KCl, +205 mV vs NHE, ProSense QiS, Oosterhout, The Netherlands). The anode and the cathode compartment were separated by a bipolar membrane (fumasep FBM, FuMa-tech GmbH, St. Ingbert, Germany) with the cation exchange side facing the cathode and the anion exchange side facing the anode. The anode and the cathode were connected via a resistor with a range of 0 – 50 Ω. Both anolyte and catholyte were recirculated at a rate of approximately 10 L/h (Figure 2).

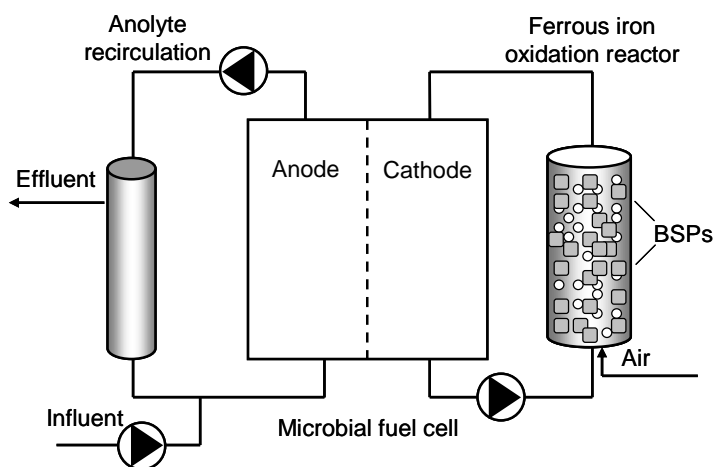


**Figure 2.** Process scheme of the MFC with continuous ferrous iron oxidation

## 4.2.2 Anode microorganisms and medium

The anode compartment was inoculated with effluent from another MFC running on acetate. The anode was continuously supplied with medium, containing potassium acetate and a 20-30 mM potassium phosphate buffer ( $\text{pH} = 7$ ) at a rate of 0.4 L/day. The acetate concentration was different for each current density and was at a level so that no acetate depletion occurred. Every fifth day, the anode was provided with macronutrients (10 mL of a solution containing 4.31 g/L  $\text{NH}_4\text{Cl}$ , 5.39 g/L  $\text{CaCl}_2 \cdot 2\text{H}_2\text{O}$  and 4.31 g/L  $\text{MgSO}_4 \cdot 4\text{H}_2\text{O}$ , micronutrients (1 mL of a solution containing 0.72 g/L  $\text{FeCl}_2 \cdot 4\text{H}_2\text{O}$ , 0.30 g/L  $\text{CoCl}_2 \cdot 6\text{H}_2\text{O}$ , 0.18 g/L  $\text{MnCl}_2 \cdot 4\text{H}_2\text{O}$ , 0.18 g/L  $\text{ZnCl}_2$ , 0.034 g/L  $\text{H}_3\text{BO}_3$ , 0.18 g/L  $\text{Na}_2\text{MoO}_4 \cdot 2\text{H}_2\text{O}$  and 0.50 g/L EDTA) and vitamins (1 mL of a solution containing 1 g/L pyridoxine.HCl, 0.5 g/L nicotinic acid, 0.25 g/L riboflavin, 0.25 g/L thiamine.HCl, 0.2 g/L biotin, 0.2 g/L folic acid and 0.01 g/L vitamin B12).

## 4.2.3 Ferrous iron oxidizing microorganisms and medium

*A. ferrooxidans* strain 583 (DSMZ, Braunschweig, Germany) was first grown in ferrous sulfate medium (33.3 g/L  $\text{FeSO}_4 \cdot 5\text{H}_2\text{O}$  and standard nutrients: 0.4 g/L  $(\text{NH}_4)_2\text{SO}_4$ , 0.4 g/L  $\text{KH}_2\text{PO}_4$  and 0.4 g/L  $\text{MgSO}_4$  in  $\text{H}_2\text{SO}_4$  at  $\text{pH}=2$ ) and thereafter immobilized on 1  $\text{cm}^3$  polyurethane foam biomass support particles (BSPs) each to ensure a high volumetric ferrous iron oxidation rate from the start of the experiments. The immobilization procedure was based on Nemati and Webb (1996). The first immobilization step consisted of inoculating 10% (v/v) of the culture into Erlenmeyer flasks containing 200 mL of ferrous sulfate medium and 25 BSPs each.

The flasks were incubated on a rotary shaker at 175 rpm at 30 °C. Before complete conversion of the ferrous iron, determined from the dark yellowish/brownish color of the solution, the medium was refreshed. After repeating this procedure 5 times, 75 BSPs were placed in the ferrous iron oxidation reactor together with 475 mL of medium. The ferrous iron oxidation reactor was operated first batch-wise with the same medium, but with a lower ferrous iron concentration equal to our previous study (0.95 g/L). The medium was recirculated and aerated with compressed air. Before all ferrous iron was converted, the medium was replaced. After this procedure was repeated 8 times, the ferrous iron oxidation reactor was connected to the MFC.

#### 4.2.4 Microbial fuel cell operation

The MFC was operated in a constant temperature chamber at 30 °C. The anode and the cathode potential were logged every 60 s on a PC via a FieldPoint FP-AI-110 module. Data were collected using LabVIEW.

The MFC was first characterized without ferrous iron oxidation with 0.95 g/L ferric iron (sulfate) at pH 2 as the catholyte by decreasing the external resistance from 50 to 5  $\Omega$ . Thereafter, the MFC was connected to the ferrous iron oxidation reactor containing BSPs with immobilized cells of *A. ferrooxidans*. The standard nutrients were supplied to the cathode compartment only at the beginning of the experiment. The total catholyte volume was kept at 1.35 L. The catholyte pH was controlled at 2.5 with 1.8 M H<sub>2</sub>SO<sub>4</sub>, and the amount of acid dosed was monitored. The current density of the MFC was increased stepwise by decreasing the external resistance from 20 to 2.1  $\Omega$ . The MFC was operated for at least 1 week at each current density. Four resistances were tested (run 1: 20  $\Omega$ ; run 2: 8.2  $\Omega$ ; run 3: 4.0  $\Omega$ ; and run 4: 2.1  $\Omega$ ), resulting in current densities similar to our previous study. Samples from the anode and cathode compartments were taken at least 5 times at each current density.

When the anolyte pH decreased below 6, it was manually adjusted to 6.6 with 2 M KOH.

The acetate concentration in the anode was measured regularly to ensure that no depletion of acetate occurred.

#### 4.2.4 Activity tests

To determine the activity of *A. ferrooxidans*, activity tests were performed at the end of each run. Three BSPs were randomly taken from the ferrous iron oxidation reactor, and each BSP was placed in an Erlenmeyer flask containing 25 mL of medium (0.95 g/L ferrous sulfate, and standard nutrients). The same was done with 1 mL of catholyte (n=3). Blanks with BSPs

without *A. ferrooxidans* in medium and blanks with medium alone were also tested ( $n=2$ ). Samples were taken twice within 10 h and analyzed for their ferric and total iron concentration according to the method described by Karamanev et al. (2002). The maximum activity was determined from the steepest part of the curves. After the activity test, the BSPs were placed back in the ferrous iron oxidation reactor.

#### 4.2.5 Analyses

Anode and cathode potential were measured versus their reference electrodes. The cell voltage was measured as the difference between anode and cathode. The difference between the cathode and the anode reference electrode was defined as the voltage across the membrane.

Current density  $j$  ( $A/m^2$ ) and power density  $P$  ( $W/m^2$ ) were calculated from the cell voltage  $E$  (V), the circuit load  $R$  ( $\Omega$ ), and the electrode surface area  $A_{el}$  ( $m^2$ ) according to:  $j = E / RA_{el}$  and  $P = E^2 / RA_{el}$ .

Ferric iron and total iron concentrations were measured according to (Karamanev et al. 2002).  $K^+$ , total S, total P and total Fe concentrations were measured using inductively coupled plasma – optical emission spectrometer (ICP-OES; Vista-MPX, Varian, Inc.).

The transport number  $t$  was calculated for  $H^+$ ,  $K^+$ , and S. This transport number indicates the charge carried by this species ( $Q^+$ ) as compared to the charge carried by the electrons in the electrical current ( $Q$ ). The equations for calculation of transport numbers for H,  $K^+$  and S and their derivation can be found in the appendix.

The bipolar membrane was stored in demineralized water after the MFC was stopped. For 24 h before elemental analysis, one sample of the membrane was stored in 1 M NaCl, and one sample was stored in 1 M HCl to test whether iron could be reversibly removed from the bipolar membrane. The membrane samples were washed with MilliQ water and then analyzed with energy dispersive X-ray spectrometry (EDX) to determine the element content of the outside layers (1 – 2  $\mu m$ ). For the EDX analysis, a JEOL JSM-6480LV scanning electron microscope (SEM) equipped with a NORAN System SIX model 300 X-ray microanalysis system (Thermo Electron Corporation) was used. Measurements were done at an acceleration voltage of 20 kV.

## 4.3 Results and discussion

### 4.3.1 The MFC with continuous ferrous iron oxidation showed a 38% higher power output than obtained in our previous study

The polarization curve of the MFC directly after ferric iron addition without ferrous iron oxidation showed power and current densities in the same range as in our previous study (Ter Heijne et al., 2006).

When connecting the MFC to the ferrous iron oxidation reactor, the circuit load was set at a fixed resistance ( $R = 20.2 \Omega$ ). This resulted in a current density of  $0.96 \pm 0.02 \text{ A/m}^2$ . After 1 week, the external resistance was decreased stepwise to yield  $2.0 \pm 0.05 \text{ A/m}^2$  ( $R = 8.2 \Omega$ ),  $3.0 \pm 0.95 \text{ A/m}^2$  ( $R = 4.0 \Omega$ ) and  $4.4 \pm 0.15 \text{ A/m}^2$  ( $R = 2.1 \Omega$ ). The MFC was operated at each current density for at least 7 days. The average values and standard deviations were calculated over the full period. Figure 3 shows the performance of the MFC with continuous ferrous iron oxidation.

The average power density increased to  $1.2 \text{ W/m}^2$  ( $55 \text{ W/m}^3$ ) at a current density of  $4.4 \text{ A/m}^2$ , which is 38% higher than the power density found in the previous study (Ter Heijne et al., 2006) at a similar current density. The cathode potential decreased upon increased current density, but was nearly constant during each run (run 1:  $0.448 \pm 0.004 \text{ V}$ ; run 2:  $0.396 \pm 0.005 \text{ V}$ ; run 3:  $0.372 \pm 0.007 \text{ V}$ ; and run 4:  $0.333 \pm 0.007 \text{ V}$ , all values vs. Ag/AgCl). This indicates a constant ratio of ferric/ferrous iron.

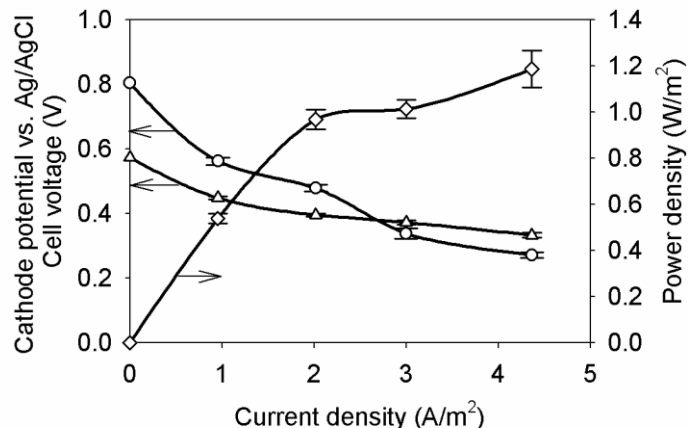


**Figure 3.** Performance of the MFC with continuous ferrous iron oxidation by *A. ferrooxidans*: Power density (◇), cell voltage (○) and cathode potential (△). Average values and standard deviations were calculated over a period of at least 7 days (except for open circuit conditions).

The decrease in cathode potential upon increased current was 1.6 times higher than in our previous study (Ter Heijne et al., 2006) in the current density range of  $0.96 - 2 \text{ A/m}^2$ . Part of the electrode might have been blocked by precipitates on the electrode and deposition of extracellular polymeric substances (EPS) produced by *A. ferrooxidans* on the electrode (Gehrke et al., 1998). A decreased surface area results in a higher current density at the electrode as compared to a situation where no precipitates were formed. As the cathode potential decreases with increasing current density, a lower cathode potential would occur in case part of the electrode is blocked.

In all runs, the ferrous iron concentration was below 6% of the total iron concentration, which indicates that the system's microbial ferrous iron oxidation capability was large enough for the MFC current in all runs. From this we can conclude that the ferrous iron oxidation reactor had an overcapacity. The activity tests showed that the microbial ferrous iron oxidation activity was mainly in the BSPs at the start of run 1: the fraction of the activity in the BSPs was  $0.95 \pm 0.03$  of the total activity, versus  $0.05 \pm 0.03$  in the catholyte. After run 4, the microbial ferrous iron oxidation activity in the catholyte turned out to be considerable as well: the fraction of the activity in the BSPs was  $0.62 \pm 0.06$  of the total activity, versus  $0.38 \pm 0.06$  in the catholyte. No ferric iron was found in the blanks of the activity tests, indicating the absence of chemical ferrous iron oxidation.

### 4.3.2 Ion transport through the bipolar membrane

Rozendal et al. (2006) showed that a cation exchange membrane in an MFC does not only transport protons, but also other cations are transported that are present in higher concentrations. We show that this bipolar membrane in an MFC, similarly, allows transport of both positively and negatively charged species other than protons and hydroxides. The migration of charged species through the membrane was analyzed by their transport numbers, indicating the charge carried by a species ( $Q^+$ ) as compared to the charge carried by electrons ( $Q^-$ ) in the electrical current. Electroneutrality requires that these charges should be equal. The proton transport number  $t_{\text{H}^+}$  is defined as the charge carried by protons relative to the total charge and is equal to the hydroxide transport number  $t_{\text{OH}^-}$ .

For each mole of electrons arriving at the cathode, 1 mole of ferric iron is reduced and 1 mole of protons is consumed by the microorganisms for ferrous iron oxidation (reactions (2) and (3); introduction). The catholyte pH would increase for a proton transport number lower than 1, as the protons produced by the water splitting reaction in the membrane would be less than the protons consumed by the ferrous iron oxidizing microorganisms. We indeed observed

a pH increase in the catholyte. The amount of acid ( $\text{H}_2\text{SO}_4$ ) dosed for pH control was used to calculate the proton transport number.

The dominant species present in the MFC, besides  $\text{H}^+$  and  $\text{OH}^-$  are  $\text{K}^+$ ,  $S_{\text{total}}$  ( $\text{SO}_4^{2-}/\text{HSO}_4^-$ ),  $\text{Fe}_{\text{total}}$  ( $\text{Fe}^{2+}/\text{Fe}^{3+}$ ), and  $\text{P}_{\text{total}}$  ( $\text{HPO}_4^{2-}/\text{H}_2\text{PO}_4^-$ ). Other positive ions, supplied to the anode compartment through the nutrient solutions, were present in concentrations less than 1% of the  $\text{K}^+$  concentration.  $\text{K}^+$  was therefore assumed to be responsible for the charge transport from the anode compartment to the cathode compartment. The direction of the current mainly determines the transport of these species: a positive charge migrates from the anode to the cathode compartment and/or a negative charge migrates from the cathode to the anode compartment (all contributing to  $Q^+$ ). We measured an increase in  $\text{K}^+$  concentration in the catholyte, from which the  $\text{K}^+$  transport number was calculated. With the dosage of  $\text{H}_2\text{SO}_4$  for pH control, S was added to the system as well. We measured an increase in S concentration in the catholyte, but this increase was lower than the increase we expected from the amount of acid dosed. Therefore, we concluded that S (in the form of  $\text{SO}_4^{2-}$  and  $\text{HSO}_4^-$ ) was transported from the cathode to the anode compartment. The concentrations of P and Fe in the catholyte were fairly constant, which is in accordance with the direction of the current. The calculated transport numbers for  $\text{H}^+$ ,  $\text{K}^+$ , and S for each run are shown in Table 1.

The proton transport number, varying between 0.65 in run 2 and 0.76 in run 3, is in the same range as found in our previous study (Ter Heijne et al., 2006): 0.6-0.7. This proton transport number not only had an effect on catholyte pH, but also on anolyte pH. Per mole of electrons (and protons) produced at the anode, only 0.65 – 0.76 mole hydroxide migrated from the membrane to the anode. Despite the buffer capacity in the influent, the anolyte pH decreased considerably especially at high current densities and a higher base dosage was required. There was a considerable transport of  $\text{K}^+$  from the anode to the cathode compartment ( $t_{\text{K}^+} = 0.15 - 0.31$ ).

**Table 1.** Transport numbers for  $\text{H}^+$ ,  $\text{K}^+$  and S (n.a. = not analyzed).

Average current density ( $\text{A}/\text{m}^2$ )	Transport number $\text{H}^+$	Transport number $\text{K}^+$	Transport number S
0.96	0.74	0.15	n.a.
2.0	0.65	0.31	0.08
3.0	0.76	0.17	0.13
4.4	0.71	0.19	0.08

The transport of species other than protons and hydroxides thus resulted in a pH increase in the catholyte and a pH decrease in the anolyte, and increased salt concentrations in the catholyte. The occurrence of salt ion transport through bipolar membranes has previously been studied in, for example, Elmoussaoui et al. (1994) and Wilhelm et al. (2001). The experimental setup and conditions however, were different from our MFC (high current densities, a six-compartment setup with several membranes, and high salt concentrations), and therefore no quantitative comparison can be made with these studies.

The bipolar membrane should have a water splitting effectiveness of >98% at a current density of 1000 A/m<sup>2</sup> according to the supplier FuMa-tech GmbH. A proton transport number below 1 can be a result of the relatively low current densities in an MFC as compared to industrial applications. Although no trend can be seen from Figure 3, with current densities considerably lower than 1000 A/m<sup>2</sup>, we expect that increased current densities could reduce the problem of pH changes in the catholyte and anolyte, and the problem of increasing salt concentrations in the catholyte.

### **4.3.3 Low iron concentrations in the catholyte still enabled a high power output, while high salt concentrations positively influenced power output**

Most iron was in the ferric form as observed by measurements and the stable cathode potential. After 2 weeks of operation, a sudden decrease in total iron concentration from 0.95 g/L to 0.5 g/L was observed. This concentration decrease occurred at the moment that pH = 2.5 was reached, the point where the pH control began. Iron is indeed subjected to precipitation at pH values around 2.5 (Stumm and Morgan, 1981). Furthermore, the decrease in iron concentration was not likely to be a result of iron migration through the membrane. On average, the iron concentration in the anolyte effluent was lower than or equal to the iron concentration in the micronutrient solution, and the transport of iron from the cathode to the anode compartment would be against the direction of the current. No decrease in MFC performance was found with a lower iron concentration down to 0.5 g/L. Low iron concentrations are beneficial, as these lower the chance of iron precipitation (Stumm and Morgan, 1981).

The power density of the MFC with continuous ferrous iron oxidation was found to be 38% higher than the power output of the same MFC in our previous study (Ter Heijne et al., 2006) at a similar current density. This increase in power density is a result of a higher cell voltage at the same current density. The higher cell voltage (0.271 V vs 0.186 V at  $j = 4.4 \text{ A/m}^2$  and  $4.5 \text{ A/m}^2$  respectively) could be explained by the higher salt concentrations in the catholyte

(conductivity up to 44 mS/cm vs 10 mS/cm) and the resulting decreased ohmic losses. The ohmic losses were calculated using the equation  $E_{ohmic} = \frac{dj}{\sigma}$  (Ter Heijne et al., 2006), where  $d$  = distance between membrane and electrode (cm),  $j$  = current density (A/cm<sup>2</sup>) and  $\sigma$  = conductivity (S/cm). The higher conductivity was calculated to contribute to decreased ohmic losses of 0.074 V, which is 86% of the difference in the cell voltage.

#### 4.3.4 Iron could be reversibly removed from the membrane by protons

Although no decrease in membrane performance was observed, we found that the membrane had an orange-brown color at the end of operation. Irreversible bounding of iron to the bipolar membrane could lead to decreased membrane and MFC performance. The outside layer of the bipolar membrane was exposed to the catholyte and was therefore expected to contain the highest iron concentrations. Therefore, the outside layers of the membrane samples were analyzed on the cation exchange side for their elements. For 24 h before analysis, one sample was stored in 1 M NaCl and one sample was stored in 1 M HCl to test whether iron could be reversibly removed from the membrane. A quantitative analysis of the spectrum identified 2.0% and 1.7% of the atoms as S for the cation exchange side of the samples stored in NaCl and HCl, respectively. These S groups represent the negatively charged sulfonate groups in the cation exchange side of the bipolar membrane. No iron was detected on the membrane stored in HCl (Figure 4A). Iron was detected on the cation exchange side of the membrane stored in NaCl (0.59 atom %) and occupied 30% of the S-groups (Figure 4B). The other S-groups were mainly occupied by Na<sup>+</sup> (69%) for the membrane stored in NaCl. The sample stored in demineralized water showed a similar spectrum to the one stored in NaCl, except that it contained K<sup>+</sup> instead of Na<sup>+</sup> (72% of the S-groups contained K<sup>+</sup> and 20% contained iron, data not shown). These findings show that iron can be reversibly removed from the membrane by exchange with protons.

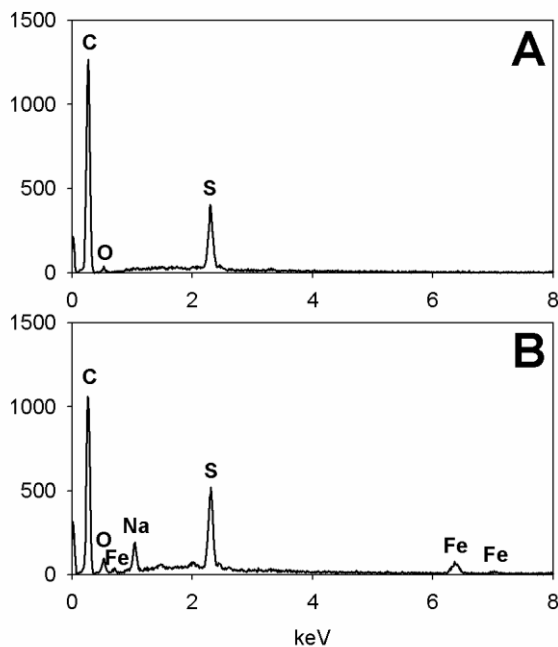


**Figure 4.** EDX spectrum for the cation exchange side of the bipolar membrane stored in 1 M HCl (A) and in 1 M NaCl (B)

### 4.3.5 Future perspectives

Continuous ferrous iron oxidation in the catholyte by *A. ferrooxidans* was successfully achieved. Ferrous iron was oxidized at a rate high enough to ensure an MFC power output of  $1.2 \text{ W/m}^2$  throughout more than a week. The ferrous iron oxidation reactor had an overcapacity, as less than 6% of the iron was found to be in the ferrous form during all runs. The MFC current density of  $4.4 \text{ A/m}^2$  requires a ferrous iron oxidation rate of  $13.4 \text{ g Fe}^{2+}/\text{L}/\text{day}$ , normalized to the liquid volume of the ferrous iron oxidation reactor. This is indeed considerably lower than the conversion rate in other research (e.g.,  $194 \text{ g/L}/\text{day}$  (Ebrahimi et al., 2005) and  $521 \text{ g/L}/\text{day}$  (Park et al., 2005)). It is therefore likely that a 10-fold higher current can still be achieved in the MFC with the same ferrous iron oxidation reactor size as used in our study ( $0.475 \text{ L}$  vs  $0.62 \text{ L}$  MFC cathode compartment).

For an MFC to be competitive with existing technologies, it should have a high power density as well as little or no use of chemicals and a low-cost, renewable catalyst for oxygen reduction. The power and current densities obtained in this study for the MFC with continuous ferrous iron oxidation are promising. To achieve higher power densities, a new

MFC design is required. A new reactor design with decreased ohmic losses and consequentially higher power and current densities could increase the proton transport number in the MFC, but further tests are necessary to verify this. As a result, relatively less acid and base will be needed. The performance of *A. ferrooxidans* and/or other iron oxidizing microorganisms in the catholyte of a newly designed MFC will be further studied. Thereafter, the MFC power output should be balanced with the power needed for aeration so that optimizing strategies can be investigated in more detail.

## Acknowledgements

We thank Janneke Tempel for her help with the SEM/EDX analyses and Nienke Stein and Vinnie de Wilde for their help with the experiments.

This work was supported by Wetsus. Wetsus is funded by the city of Leeuwarden, the Province of Fryslân, the European Union European Regional Development Fund and by the EZ/KOMPAS program of the “Samenwerkingsverband Noord-Nederland”.

## 4.4 References

- Bond, D. R.; Lovley, D. R. 2003. Electricity production by *Geobacter sulfurreducens* attached to electrodes. *Appl. Environ. Microbiol.* 69, 1548-1555.
- Chaudhuri, S. K.; Lovley, D. R. 2003. Electricity generation by direct oxidation of glucose in mediatorless microbial fuel cells. *Nat. Biotechnol.* 21, 1229-1232.
- Cheng, S.; Liu, H.; Logan, B. E. 2006. Power densities using different cathode catalysts (Pt and Co/TMPP) and polymer binders (Nafion and PTFE) in single chamber microbial fuel cells. *Environ. Sci. Technol.* 40, 364-369.
- Ebrahimi, S.; Morales, F. J. F.; Kleerebezem, R.; Heijnen, J. J.; van Loosdrecht, M. C. M. 2005. High-rate acidophilic ferrous iron oxidation in a biofilm airlift reactor and the role of the carrier material. *Biotechnol. Bioeng.* 90, 462-472.
- Elmoussaoui, R.; Pourcelly, G.; Macek, M.; Hurwitz, H. D.; Gavach, C. 1994. Co-ion leakage through bipolar membranes. Influence on I-V responses and water-splitting efficiency. *J. Membr. Sci.* 90, 283-292.
- Gehrke, T.; Telegdi, J.; Thierry, D.; Sand, W. 1998. Importance of extracellular polymeric substances from *Thiobacillus ferrooxidans* for bioleaching. *Appl. Environ. Microbiol.* 64, 2743-2747.
- He, Z.; Angenent, L. T. 2006. Application of bacterial biocathodes in microbial fuel cells. *Electroanalysis.* 18, 2009-2015.
- Jensen, A. B.; Webb, C. 1995. Ferrous sulfate oxidation using *Thiobacillus ferrooxidans* - A review. *Process Biochem.* 30, 225-236.
- Karamanev, D. G.; Nikolov, L. N.; Mamatarkova, V. 2002. Rapid simultaneous quantitative determination of ferric and ferrous ions in drainage waters and similar solutions. *Miner. Eng.* 15, 341-346.

- Leduc, L. G.; Ferroni, G. D. 1994. The chemolithotrophic bacterium *Thiobacillus ferrooxidans*. *FEMS Microbiol. Rev.* 14, 103-119.
- Logan, B. E.; Hamelers, B.; Rozendal, R.; Schröder, U.; Keller, J.; Freguia, S.; Aelterman, P.; Verstraete, W.; Rabaey, K. 2006. Microbial fuel cells: Methodology and technology. *Environ. Sci. Technol.* 40, 5181-5192.
- Nagasubramanian, K.; Chlanda, F. P.; Liu, K. J. 1977. Use of bipolar membranes for generation of acid and base - engineering and economic analysis. *J. Membr. Sci.* 2, 109-124.
- Nemati, M.; Webb, C. 1996. Effect of ferrous iron concentration on the catalytic activity of immobilized cells of *Thiobacillus ferrooxidans*. *Appl. Microbiol. Biotechnol.* 46, 250-255.
- Park, D.; Lee, D. S.; Park, J. M. 2005. Continuous biological ferrous iron oxidation in a submerged membrane bioreactor. *Water Sci. Technol.* 51, 59-68.
- Rabaey, K.; Verstraete, W. 2005. Microbial fuel cells: novel biotechnology for energy generation. *Trends Biotechnol.* 23, 291-298.
- Rohwerder, T.; Gehrke, T.; Kinzler, K.; Sand, W. 2003. Bioleaching review part A: Progress in bioleaching: Fundamentals and mechanisms of bacterial metal sulfide oxidation. *Appl. Microbiol. Biotechnol.* 63, 239-248.
- Rozendal, R. A.; Hamelers, H. V. M.; Buisman, C. J. N. 2006. Effects of membrane cation transport on pH and microbial fuel cell performance. *Environ. Sci. Technol.* 40, 5206-5211.
- Shukla, A. K.; Suresh, P.; Berchmans, S.; Rajendran, A. 2004. Biological fuel cells and their applications. *Curr. Sci.* 87, 455-468.
- Stumm, W.; Morgan, J. J. 1981. *Aquatic Chemistry: an introduction emphasizing chemical equilibria in natural waters*; 2nd ed.; John Wiley & Sons: New York.
- Ter Heijne, A.; Hamelers, H. V. M.; De Wilde, V.; Rozendal, R. A.; Buisman, C. J. N. 2006. A bipolar membrane combined with ferric iron reduction as an efficient cathode system in microbial fuel cells. *Environ. Sci. Technol.* 40, 5200-5205.
- Wilhelm, F. G.; Punt, I.; van der Vegt, N. F. A.; Wessling, M.; Strathmann, H. 2001. Optimisation strategies for the preparation of bipolar membranes with reduced salt ion leakage in acid-base electro dialysis. *J. Membr. Sci.* 182, 13-28.
- Zhang, J.; Sasaki, K.; Sutter, E.; Adzic, R. R. 2007. Stabilization of platinum oxygen-reduction electrocatalysts using gold clusters. *Science*. 315, 220-222.
- Zhao, F.; Harnisch, F.; Schröder, U.; Scholz, F.; Bogdanoff, P.; Herrmann, I. 2006. Challenges and constraints of using oxygen cathodes in microbial fuel cells. *Environ. Sci. Technol.* 40, 5193-5199.

## Appendix

Transport numbers ( $t$ ) for  $H^+$ ,  $K^+$  and  $S$  were calculated. Several phenomena were taken into account:

1) Equilibrium reactions for sulfuric acid



The first equilibrium  $H_2SO_4 \leftrightarrow H^+ + HSO_4^-$  is not relevant, as  $pK_a = -3$

The second equilibrium  $HSO_4^- \leftrightarrow H^+ + SO_4^{2-}$  is relevant, as  $pK_a = 1.92$  ( $T = 298$  K)

With a constant pH (controlled at 2.5), the ratio  $[SO_4^{2-}]/[HSO_4^-]$  is constant, and 79% of total S ( $[S_T]$  in M) is present as  $SO_4^{2-}$  ( $f_{SO_4^{2-}}[-] =$  fraction of S present as  $SO_4^{2-}$ ) while 21% of total S is present as  $HSO_4^-$  ( $f_{HSO_4^-}[-] =$  fraction of S present as  $HSO_4^-$ ). We can define:

$$[HSO_4^-] \text{ (in M)} = f_{HSO_4^-} \cdot [S_T] \text{ and } [SO_4^{2-}] \text{ (in M)} = f_{SO_4^{2-}} \cdot [S_T]$$

The subscripts 'end' and 'start' in the mass balances on the next page refer to the end and start concentrations respectively.  $V$  stands for volume (L)

2) Addition of H through  $H_2SO_4$

The pH was controlled at 2.5 by addition  $H_2SO_4$ . For every mole of  $H_2SO_4$  that is added for pH control, 2 moles of  $H^+$  are added to the system. The amount of  $H^+$  that is supplied to the system via  $H_2SO_4$  in the considered time period will be referred to as  $2\Delta S_T$ . After addition to the catholyte, part of this  $H^+$  ends up in  $HSO_4^-$  as a result of the dissociation equilibrium.

3) Addition of S through  $H_2SO_4$

The amount of S that is supplied to the system via  $H_2SO_4$  in the considered time period will be referred to as  $\Delta S_T$  [mol].

4) Total current in MFC

The charge transport through the electrical circuit is expressed as the current  $I$  integrated over time  $t$ , divided by Faraday's constant =  $\int_0^t I dt / F = C$  [mol]. The proton consumption by *A.*

*ferrooxidans* in the cathode is equal to  $C$ , because 1 mole of protons is consumed for every mol of electrons

5) Further assumptions

- $HSO_4^-$  and  $SO_4^{2-}$  have the same chance to migrate through the membrane

- No H<sub>2</sub>S diffuses through the membrane from the anode compartment to the cathode compartment, or all the S<sup>2-</sup> is readily oxidized in the cathode compartment
- No precipitation of sulfates occurs
- HCO<sub>3</sub><sup>-</sup> produced in the anode compartment does not diffuse through the membrane to the cathode compartment (against the direction of the current)

Mass balance for H<sup>+</sup> in cathode (in mol)

Total change in H (present as H<sup>+</sup> and HSO<sub>4</sub><sup>-</sup>) =

H<sub>added via H<sub>2</sub>SO<sub>4</sub></sub> - H<sub>consumed for ferrous iron oxidation</sub> + H<sub>supplied by the membrane</sub>

$$V([H^+]_{end} - [H^+]_{start}) + V([HSO_4^-]_{end} - [HSO_4^-]_{start}) = 2\Delta S_T - C + t_{H^+} C$$

$$V([H^+]_{end} - [H^+]_{start}) = 0 \text{ (pH=constant) and}$$

$$V([HSO_4^-]_{end} - [HSO_4^-]_{start}) = V f_{HSO_4^-} ([S_T]_{end} - [S_T]_{start})$$

Then:

$$t_{H^+} C = C - 2\Delta S_T + V f_{HSO_4^-} ([S_T]_{end} - [S_T]_{start})$$

$$t_{H^+} = 1 - \frac{2\Delta S_T}{C} + V \frac{f_{HSO_4^-} ([S_T]_{end} - [S_T]_{start})}{C}$$

Mass balance for K<sup>+</sup> in cathode (in moles)

Total change in K = K<sub>transported through membrane</sub>

$$V([K_T]_{end} - [K_T]_{start}) = t_{K^+} C$$

$$t_{K^+} = \frac{V([K_T]_{end} - [K_T]_{start})}{C}$$

Mass balance for S in cathode (in moles)

Total change in S = S<sub>added via H<sub>2</sub>SO<sub>4</sub></sub> - S<sub>transported through membrane</sub>

$$t_S = t_{S,HSO_4^-} + t_{S,SO_4^{2-}}$$

$$V([S_T]_{end} - [S_T]_{start}) = \Delta S_T - t_S C = \Delta S_T - (0.21 t_{S,HSO_4^-} C + 2 \cdot 0.79 t_{S,SO_4^{2-}} C)$$

$$t_S = \frac{\Delta S_T - V([S_T]_{end} - [S_T]_{start})}{1.79C}$$

## Chapter 5

# Cathode potential and mass transfer determine performance of oxygen reducing biocathodes in Microbial Fuel Cells

This chapter has been published as:

Ter Heijne, A.; Strik, D.P.B.T.B.; Hamelers, H. V. M.; Buisman, C. J. N. 2010. Cathode potential and mass transfer determine performance of oxygen reducing biocathodes in Microbial Fuel Cells. *Environ. Sci. Technol.* 44, 7151-7156.

## Abstract

The main limiting factor in Microbial Fuel Cell (MFC) power output is the cathode, because of the high overpotential for oxygen reduction. Oxygen reducing biocathodes can decrease this overpotential by the use of microorganisms as a catalyst. In this study, we investigated the factors limiting biocathode performance. Three biocathodes were started up at different cathode potentials and their performance and catalytic behaviour was tested by means of polarization curves and cyclic voltammetry. The biocathodes controlled at +0.05 V and +0.15 V vs Ag/AgCl produced current almost immediately after inoculation, while the biocathode controlled at +0.25 V vs Ag/AgCl produced no current until day 15. The biocathode controlled at +0.15 V vs Ag/AgCl reached the highest current density of 313 mA/m<sup>2</sup>. Cyclic voltammetry showed clear catalysis for all three biocathodes. The biocathodes were limited by both mass transfer of oxygen and by charge transfer. Mass transfer calculations show that the transfer of oxygen poses a serious limitation for the use of dissolved oxygen as an electron acceptor in MFCs.

## 5.1 Introduction

The Microbial Fuel Cell (MFC) is an emerging technology to produce electricity from biodegradable waste materials. An MFC consists of an anode and a cathode, usually separated by a membrane. At the anode, microorganisms oxidize biodegradable materials into CO<sub>2</sub>, protons and electrons. At the cathode, usually oxygen is reduced to water (Logan et al., 2006), but also many other reactions are possible (Hamelers et al., 2010).

MFC technology at this moment is not cost effective enough for practical application.

The main factor limiting MFC performance is the cathode. Oxygen has a high overpotential when uncatalyzed electrodes are used, but at the same time oxygen is the most practical electron acceptor because of its unlimited availability. Biological catalysts are an attractive alternative to chemical catalysts to decrease the overpotential for oxygen reduction, because of their low cost and sustainability (He et al., 2006). Until now, different biological catalysts have been tested for oxygen reduction, both in the form of enzymes (Schaetzle et al., 2009) and in the form of microorganisms. Microorganisms were shown to catalyze the oxygen reduction reaction via mediating compounds like manganese (Rhoads et al., 2005) and Fe<sup>2+</sup>/Fe<sup>3+</sup> (Ter Heijne et al., 2007), but also directly in seawater (Bergel et al., 2005) and freshwater (Clauwaert et al., 2007; Freguia et al., 2008; Freguia et al., 2010). These biocathodes show better performance than uncatalyzed materials, however, they are still limiting MFC performance. At this point, it has not been investigated what are the main factors limiting biocathode performance.

The objective of this study was to investigate the factors that are limiting biocathode performance. Performance of biocathodes is reflected in the combination of cathode potential and current density. Cathode potential regulates the energy that the microorganisms can gain from transferring the electrons from the electrode to oxygen, because it determines the energy level at which the electrons are released. Electrode potential can also have effects on microbial cell surface properties and enzyme activity (Liang et al., 2009) and therefore affects activity of the biofilm. The measured current reflects the rate of oxygen reduction. It is important to study cathode polarization curves, showing the relationship between current density and cathode potential, because the combination of cathode potential and current density determines the maximum power that can be gained from the cathodic part of the bioelectrochemical system.

In this study, three biocathodes were started up at three different cathode potentials. Performance of these biocathodes was investigated via polarization curves, and catalytic

behavior was analyzed using cyclic voltammetry. The biocathodes were studied on flat (2D) electrodes, enabling us to calculate mass transfer rates and limiting current density.

## 5.2 Materials and methods

### 5.2.1 Electrochemical cell setup

The experimental setup consisted of three electrochemical cells. The electrochemical cells contained two flow channels with a projected surface area of 22 cm<sup>2</sup> and a channel depth of 1.5 cm as described in (Ter Heijne et al., 2008). The flow channels were separated by a cation exchange membrane (Fumasep FTCEM-E, Fumatech, Braunschweig, Germany). The cathodes were rough graphite plates (AlO<sub>2</sub> blasted) (Müller & Rössner GmbH & Co, Troisdorf, Germany), while the anodes were flat graphite plates (Müller & Rössner GmbH & Co, Troisdorf, Germany).

### 5.2.2 Electrochemical cell operation

The catholyte was inoculated with nitrifying biomass from the wastewater treatment plant in Ede, the Netherlands. Nitrifying biomass was chosen because of the presence of autotrophic microorganisms. Each of the three cells was inoculated on day 1 with 100 mL nitrifying biomass. The catholyte had a total volume of 1 L and consisted of phosphate buffer (pH 7, 0.02 M), and macro- and micronutrients (10 mL/L and 1 mL/L) as described in (Ter Heijne et al., 2008). The anolyte also had a total volume of 1 L and was a 0.05 M potassium ferrocyanide solution in 0.02 M phosphate buffer at pH 7.

Biocathodes were started up at three different potentials: +0.05 V vs Ag/AgCl, +0.15 V vs Ag/AgCl, and +0.25 V vs Ag/AgCl with a multi-channel potentiostat (Bank Elektronik – Intelligent Controls GmbH, Pohlheim, Germany). To control cathode potential, a cell voltage was applied between anode and cathode, and this cell voltage was manually adjusted until the desired cathode potential was reached. This was checked every two or three days, and the deviation from the desired potential was <0.01 V during >95% of the experiment.

During all experiments, the catholyte was aerated with ambient air, resulting in an oxygen concentration of 6.5 mg/L. Oxygen concentration was measured with a hand-held oxygen meter (Hach Lange NV, Mechelen, Belgium). Catholyte pH was manually controlled at pH 7. A maximum deviation in pH of 0.5 was allowed; pH was adjusted back to 7.0 with NaOH or HCl. Anolyte and catholyte were recirculated at a rate of 12 L/h. Both anode and cathode compartments were equipped with Ag/AgCl, 3 M KCl reference electrodes (+0.205 V vs NHE). Potentials of anode and cathode were measured versus their reference electrodes and

collected every 60 seconds via a Fieldpoint FP-AI-110 module connected to a PC. All experiments were performed in a temperature controlled chamber at 30 °C.

### 5.2.3 Electrochemical (bio)cathode characterization

Before inoculation with nitrifying sludge, all electrodes were characterized for chemical oxygen reduction as an abiotic control, using the catholyte (medium with buffer and nutrients) as described above, aerated with ambient air. Polarization curves were recorded using a potentiostat (Iviumstat, IVIUM Technologies, Eindhoven, The Netherlands) using dc-voltammetry (chronoamperometry). Cathode potential was set at 9 levels decreasing from 0.3 V to -0.2 V vs Ag/AgCl in steps of 0.05 V. Each potential was set for 300 seconds to allow the current to stabilize. The last data point for each potential is shown in the polarization curve.

The polarization behavior of the biocathodes was regularly examined using dc-voltammetry (chronoamperometry). The circuit was opened and open circuit potential was measured after at least 600 seconds so that the potential had stabilized. After this, the measurement was started. The cathode potential was set at the open circuit cathode potential (cathode OCP) and decreased in steps of 0.05 V to the lowest value of 0 V vs Ag/AgCl. Each potential was set for 600 seconds to allow the current to stabilize. The last data point for each potential is shown in the polarization curve. It should be noted that the currents obtained during the polarization tests do not represent real steady-state currents, because only 300-600 s were given for each potential step. This time is too short to reach steady-state, but is valid for comparative tests.

The biocathodes were characterized using cyclic voltammetry to investigate catalytic behavior of the biocathodes. Besides, a cyclic voltammogram was recorded as an abiotic control (chemical oxygen reduction). Cyclic voltammograms were made in the range from cathode OCP down to 0 V vs Ag/AgCl and back to cathode OCP. For the abiotic control, a larger range was needed to produce a current, and the chosen range was from +0.25 V vs Ag/AgCl to -0.3 V vs Ag/AgCl. Scanrate was 1 mV/s and at least 2 cycles were performed. Second and third cycles always looked similar to the first, except for the current density measured at start which appeared different in the first cycle and the same in later cycles. Therefore the last cycle is shown. Cyclic voltammograms were first made under aerobic conditions, and then under nitrogen flushing, after flushing for at least 15 minutes.

Finally, the effect of flow rate and oxygen concentration on performance of biocathodes were studied. This experiment was done in the cell where cathode potential was originally controlled at +0.15 V vs Ag/AgCl. The cathode potential was controlled with the potentiostat at a fixed potential for 300 seconds to allow the current to stabilize. The last data point for each dataset is presented. Three different potentials were chosen: +0.2V, +0.28V, and +0.35 V

vs Ag/AgCl. Only potentials higher than +0.15 V vs Ag/AgCl were tested, because high cathode potential is desired when maximizing the performance of the MFC. First, the effect of flow rate on the current was tested by increasing the pump recirculation rate from 0 L/h up to 21 L/h in several steps. This resulted in a linear flow velocity between 0 and 2.4 cm/s as the flow diameter was 2.4 cm<sup>2</sup>. The effect of flow rate was tested at the three different cathode potentials. Finally, three different oxygen concentrations were tested at fixed cathode potential of +0.2 V vs Ag/AgCl and a fixed recirculation rate of 12 L/h. This was done by increasing the nitrogen supply, which resulted in oxygen concentrations of 7.3 mg/L, 4.7 mg/L, and 0.06 mg/L.

### 5.2.4 Analyses

Average current density and average cathode potential were calculated daily from the data obtained every 60 seconds.

Limiting current density (A/m<sup>2</sup>) was calculated as described in (12) by  $i_{lim} = n \cdot F \cdot k \cdot O_{2,b}$ , where n=4 (number of electrons per oxygen molecule), F=Faraday constant, k=mass transfer coefficient (m/s), and  $O_{2,b}$  = bulk oxygen concentration (mol/m<sup>3</sup>). The mass transfer coefficient is a function of both oxygen diffusion coefficient and linear flow velocity (Ter Heijne et al., 2008) as  $k = \frac{D}{\delta}$ , where D is the oxygen diffusion coefficient (assumed to be 2\*10<sup>-9</sup> m<sup>2</sup>/s (Piciooreanu et al., 1997)) and  $\delta$  = thickness of the boundary layer. This thickness of the boundary layer was calculated as a function of recirculation rate via the Peclet number (Ter Heijne et al., 2008). As shown in Williamson and McCarty (1976), there is an additional boundary layer attached to the biofilm that cannot be influenced by recirculation rate. As a result, we have an increase in boundary layer of 56  $\mu$ m (Williamson and McCarty, 1976).

## 5.3 Results and discussion

### 5.3.1 Start-up potential influenced start-up time of biocathodes

Three bioelectrochemical cells were started at three different potentials. The current density produced during the first 21 days is shown in Figure 1. Before inoculation, all cells produced negligible current, similar to or lower than the control experiments at the same potential.

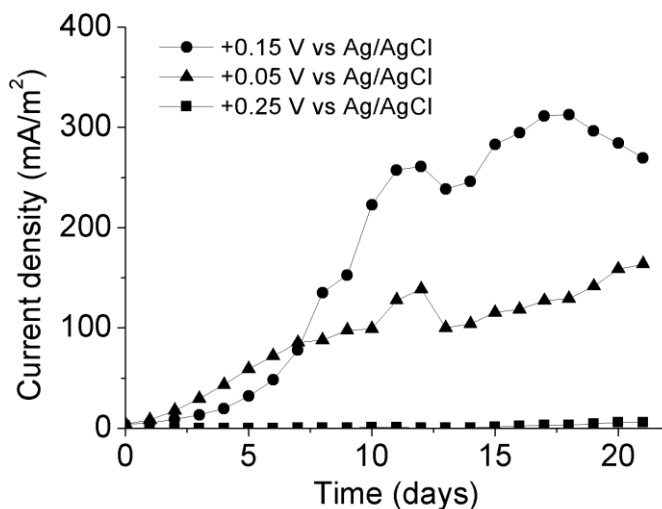


**Figure 1.** Current production of the three biocathodes controlled at different potentials. Highest current density was reached by the cathode controlled at +0.15 V vs Ag/AgCl, and the cathode controlled at +0.25 V vs Ag/AgCl did not produce any current until day 15.

The biocathodes controlled at +0.05 V and +0.15 V vs Ag/AgCl produced a current almost immediately after inoculation. The third biocathode produced no current until day 15. The biocathode controlled at +0.15 V vs Ag/AgCl reached the highest current density of 313 mA/m<sup>2</sup> on day 18. The biocathode controlled at +0.05 V vs Ag/AgCl reached a maximum current density of 164 mA/m<sup>2</sup> on day 21. The biocathode controlled at +0.25 V vs Ag/AgCl reached a maximum current density of 68 mA/m<sup>2</sup> on day 76.

All three biocathodes needed several weeks before maximum current was reached, ranging from 18 days to 76 days. Also other studies report start-up times in this range (Clauwaert et al., 2007; Freguia et al., 2008). while start-up times for bio-anodes are usually much shorter, ranging between 5-8 days before maximum current was produced (Aelterman et al., 2008; Cheng et al., 2007). Apparently, the microorganisms catalyzing oxygen reduction are slowly growing organisms, which makes us believe they are autotrophs, as they were not fed any organic carbon source after inoculation, and were grown from nitrifying sludge.

The cathode controlled at +0.25 V vs Ag/AgCl had the longest start-up time. This may be explained by the fact that cathode potential regulates the amount of energy to be gained by the cathodic microorganisms.

**Table 1.** Effect of control strategy on energy available for microorganisms and energy available for electricity production, expressed as  $\Delta G$  and voltage. For comparison, the energy available for microorganisms in aerobic wastewater treatment (activated sludge) is included.

Control strategy	$\Delta G$ available for cathodic microorganisms (kJ/mol e)	Potential available for cathodic microorganisms (V)	$\Delta G$ available for current production* (kJ/mol e)	Potential available for current production* (V)
MFC with $E_{\text{cat}} = +0.05$ V vs Ag/AgCl	-53	0.55	-52	0.54
MFC with $E_{\text{cat}} = +0.15$ V vs Ag/AgCl	-43	0.45	-62	0.64
MFC with $E_{\text{cat}} = +0.25$ V vs Ag/AgCl	-33	0.35	-72	0.74
Aerobic wastewater treatment in activated sludge using acetate as electron donor	-105	1.09	0	0

\* It is assumed that acetate is used as electron donor. Acetate oxidation at pH=7, 50 mM acetate, and 50 mM bicarbonate results in an anode potential of -0.494 V vs Ag/AgCl (2). Gibb's free energy ( $\Delta G$ ), expressed per mole of electrons, and potential (E) are related via  $E = -\Delta G/nF$ , where n is 1.

Oxygen reduction theoretically occurs at a potential of +0.60 V vs Ag/AgCl at pH=7 and  $pO_2=0.2$  bar (Hamelers et al., 2010). This potential is the maximum cathode potential at which oxygen reduction can occur. The difference between this thermodynamic potential and the controlled cathode potential represents the maximum potential to be gained by the cathodic microorganisms. When cathode potential is controlled at +0.25 V vs Ag/AgCl, maximally 0.35 V is to be gained by the microorganisms, while at a cathode potential of +0.05 V vs Ag/AgCl, 0.55 V is to be gained by the microorganisms (Table 1).

At the same time, cathode potential regulates the potential to be gained when applied in an MFC. So, when cathode is controlled at a higher potential, less energy is to be gained by the microorganisms, which may result in slower growth and longer start-up time. The potential available for electricity production however, is higher at higher cathode potential. From Table 1, it becomes clear that in aerobic wastewater treatment, at least twice as much energy is available to the microorganisms compared to the biocathodes, however, no electricity can be gained.

Besides differences in start-up time, there were also differences in the current produced at the different potentials. The biocathode controlled at +0.15 V vs Ag/AgCl had the highest current, while the biocathode with the highest overpotential, the one controlled at +0.05 V vs Ag/AgCl had considerably lower current. We hypothesize that this lower current may be caused by possible production of H<sub>2</sub>O<sub>2</sub> at the electrode. The thermodynamic potential at which H<sub>2</sub>O<sub>2</sub> is produced is +0.269 V vs NHE at pH=7 and pO<sub>2</sub>=0.2 bar (Hamelers et al., 2010), which corresponds to a cathode potential of +0.064 V vs Ag/AgCl. Only at potentials lower than this thermodynamic potential, H<sub>2</sub>O<sub>2</sub> can be formed. So, the biocathode controlled at +0.05 V vs A/gAgCl may have been negatively affected by H<sub>2</sub>O<sub>2</sub> and therefore produced a lower current. No H<sub>2</sub>O<sub>2</sub> measurements have been done in this study, however, these would be useful to study if H<sub>2</sub>O<sub>2</sub> negatively affects biocathode performance.

### 5.3.2 Biocathode performance increased with time

Performance of the biocathodes during and after start-up was analyzed with time by polarization curves. The result for each cell is shown in Figure 2A-C, where the first two biocathodes were studied from day 0 to day 23, and the third biocathode was studied from day 0 to day 76. Performance of all three biocathodes improved with time: the maximum current density that is reached in the polarization curves increases with time, and also cathode potential increases with time at the same current density. The increase in performance with time was most pronounced for the cell with the biocathode controlled at +0.15 V vs Ag/AgCl, and less pronounced for the cell with the biocathode controlled at +0.25 V vs Ag/AgCl, when considering the same time frame from 0 until 23 days. This supports the observed differences in start-up time. The biocathode controlled at +0.25 V vs Ag/AgCl was tested and characterized during a longer time period, which resulted in a similar polarization curve as the biocathode at +0.05 V vs Ag/AgCl, only after 76 days instead of 23 days. Especially the polarization curve for the biocathodes controlled at +0.15 V vs Ag/AgCl shows a limiting current: below a cathode potential of +0.2 V vs Ag/AgCl, a further decrease in potential does not result in an increase in current density. This may indicate that maximum activity of the biofilm is reached, or that mass transfer of oxygen is limiting biocathode performance.

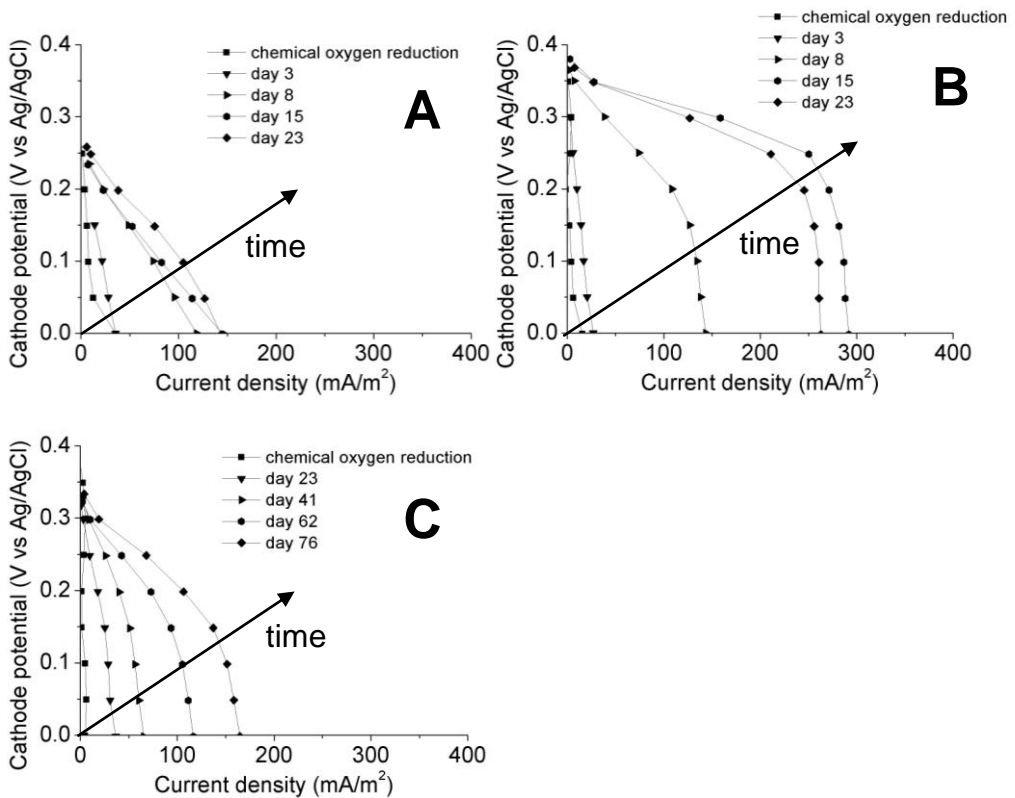


**Figure 2.** Development of the biocathodes can be seen in the polarization curves of the three cathodes. The three cells show an increase in performance with time, showing activity of the biofilm. The cathodes were controlled at (A) +0.05 V vs Ag/AgCl, (B) +0.15 V vs Ag/AgCl, and (C) +0.25 V vs Ag/AgCl. Note that Figure A and B show the development from day 0 to day 23, while Figure C shows the development from day 0 to day 76.

### 5.3.3 Cyclic voltammetry showed catalytic behavior for oxygen reduction

At the end of the experiment, the catalytic behavior of the biocathodes was tested using cyclic voltammetry. The biocathodes were tested under aerobic and anaerobic conditions. The result for the biocathode controlled at +0.15 V vs Ag/AgCl is shown in Figure 3. It can be seen that the maximum current density of 295 mA/m<sup>2</sup> was reached at a cathode potential of +0.2 V vs Ag/AgCl. At lower cathode potential, this current density was constant. Under constant nitrogen flushing, the current density was considerably decreased to 45 mA/m<sup>2</sup>, indicating that

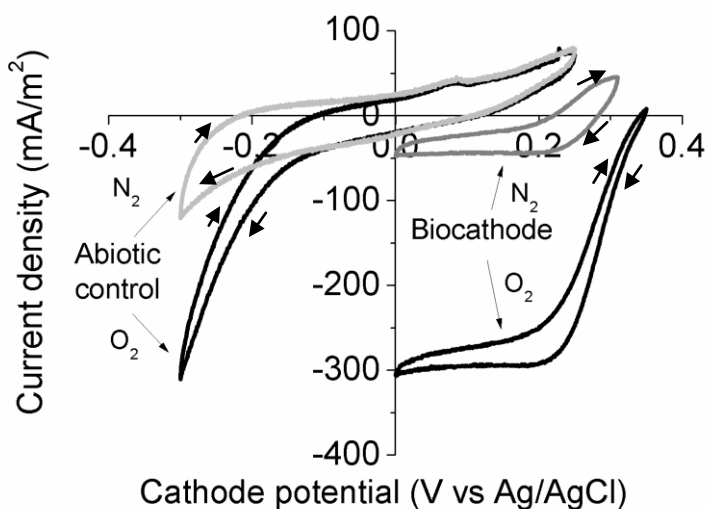


**Figure 3.** Biocathode controlled at +0.15 V vs Ag/AgCl shows catalytic behavior for oxygen reduction, at an oxygen concentration of 6.5 mg/L (O<sub>2</sub>) and <0.1 mg/L (N<sub>2</sub>). The abiotic control produced a current only below a cathode potential of +0.1 V vs Ag/AgCl at an oxygen concentration of 7.5 mg/L (O<sub>2</sub>) and 0.2 mg/L (N<sub>2</sub>).

indeed oxygen reduction is the reaction that is catalyzed. When comparing these results with the cyclic voltammograms obtained for chemical oxygen reduction, it can be seen that indeed the oxygen reduction reaction is catalyzed by the microorganisms: the abiotic control does not produce a current before the cathode potential decreased below +0.1 V vs Ag/AgCl, while the biocathode produced 295 mA/m<sup>2</sup> at this same potential. Under constant nitrogen flushing, current production decreased as a result of low oxygen concentration.

The other two biocathodes showed similar catalytic behaviour to the biocathode controlled at +0.15 V vs Ag/AgCl, the main difference being a lower maximum current density for both cells compared to the biocathode controlled at +0.15 V vs Ag/AgCl. The solution alone was also tested for catalytic behaviour by means of cyclic voltammetry. No catalytic behavior was found, and there was no distinct difference between anaerobic and aerobic cyclic voltammetry scans of the solution, meaning that the catalytic activity was caused by the biofilm on the electrode.

### 5.3.4 Biocathodes were both mass transfer and charge transfer limited

To investigate the limiting factors in biocathode performance, the current density of the biocathode was studied at different oxygen concentrations, different recirculation rates, and different potentials. This experiment was done in the cell where cathode potential was originally controlled at +0.15 V vs Ag/AgCl. Current was limited by mass transfer of oxygen, as a decrease in oxygen concentration from 100% to 65% to 0.8% resulted in a decrease in current density of 241 to 194 to 15 mA/m<sup>2</sup>. This mass transfer effect was further studied by changing the recirculation rate, hereby changing oxygen transfer.

Figure 4 shows the current density at different recirculation rates when cathode potential was controlled at +0.2 V, +0.28 V, and +0.35 V vs Ag/AgCl. Two effects can be seen here: current density increases with increasing recirculation rate, and with decreasing cathode potential. This shows that the biocathode was both limited by mass transfer of oxygen and by potential (charge transfer of the electrons from the electrode to oxygen). When cathode potential is lower, current density increases because the driving force increases, and charge transfer increases. The limitations in charge and mass transfer can also be seen in the cyclic voltammogram (Figure 3). In Figure 3, we can see that for the biocathode controlled at +0.15 V vs Ag/AgCl, the performance at 0.28 V and 0.35 V vs Ag/AgCl is limited. This limited performance may be caused by the fact that these potentials are too positive for the active catalytic enzymatic component that interacts with the electrode. At potentials lower than +0.2 V vs Ag/AgCl, oxygen mass transfer becomes limiting, while at the other two potentials charge transfer is more dominant (Figure 4).

Increase in current density or decrease in flow velocity may lead to local pH increase at the electrode, resulting in higher cathode overpotential (Jeremiassé et al., 2009). It was shown by Jeremiassé et al. (2009) that cathode overpotential did not change at current densities up to 2 A/m<sup>2</sup> when using a buffer of 20 mM, which indicates that proton supply from bulk to the electrode was sufficient to keep constant pH at the electrode surface. It is therefore likely that under the circumstances in our biocathode with the same buffer concentration and a lower current density, proton transport was sufficiently high, and thus mass transfer can be attributed to oxygen only and not to protons.

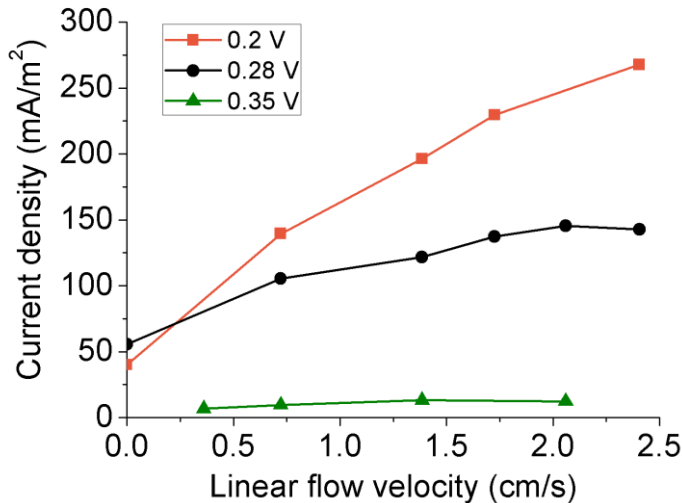


**Figure 4.** Increasing recirculation rate and decreasing cathode potential result in an increase in current density. This means that both mass transfer and charge transfer are limiting biocathode performance.

Limiting current density was calculated to investigate if mass transfer limitations could be expected. The calculations were based on the assumption that the boundary layer is composed of a stagnant layer attached to the biofilm, that cannot be influenced by flow rate, and a diffusion layer that can be influenced by flow rate. These calculations do not take into account oxygen diffusion inside the biofilm itself. Furthermore, it is assumed that all oxygen at the electrode surface is consumed. This limiting current density was calculated to be 848 mA/m<sup>2</sup> at a recirculation rate of 21 L/h (linear flow velocity of 2.4 cm/s, resulting in  $k=1.6 \cdot 10^{-5}$  m/s and a total boundary layer thickness of 182  $\mu\text{m}$ ). This is a factor 3 higher than the measured current density. This difference can be explained by several factors: (i) charge transfer is limited by cathode potential, (ii) slower effective diffusion of oxygen in the biofilm compared to the theoretical diffusion coefficient in water, as the biofilm was not taken into account in the calculation, and (iii) coverage and activity of biofilm was not at its maximum, i.e., in the calculations it is assumed that the full electrode is covered and that biofilm activity is not limited by factors other than potential and oxygen. It is clear that mass transfer of oxygen strongly affects biocathode performance as the increase in recirculation rate results in an increase in current density. More insight in the contribution of mass and charge transfer to biocathode performance may be gained by the use of electrochemical methods like Electrochemical Impedance Spectroscopy (EIS), which will be the subject of further study.

### 5.3.5 Implications

The maximum current density produced by the best performing biocathode was 313 mA/m<sup>2</sup> at a cathode potential of +0.15 V vs Ag/AgCl. Bio-anodes tested on the same flat electrodes reached a maximum current density of 4,630 mA/m<sup>2</sup> (Ter Heijne et al., 2008). So, the current density of the best performing biocathode was still a factor 15 lower than bio-anodes on the same rough graphite electrode. Our results show, that biocathodes are already close to reach the limit of mass transfer of oxygen. In this respect, the rate of oxygen transfer can be well compared to other nitrifying biofilms. The oxygen transfer rate of the biocathode  $r_{O_2}$  (g O<sub>2</sub>/m<sup>2</sup>.d) can be calculated according to  $r_{O_2} = \frac{i \cdot 24 \cdot 3600 \cdot M_{O_2}}{n \cdot F}$ , where  $i$ =current density (A/m<sup>2</sup>),  $M_{O_2} = 32$  g/mol,  $n$ =number of electrons involved (=4 in case of oxygen), and  $F$ =Faraday constant (C/mol). The maximum current density of 313 mA/m<sup>2</sup> gives an oxygen transfer rate of 2.2 g O<sub>2</sub>/m<sup>2</sup>.d. This rate is comparable to the oxygen transfer rate for autotrophic microorganisms during nitrification, for example 1.0 g O<sub>2</sub>/m<sup>2</sup>.d in a biological rotating contactor (Metcalf&Eddy, 2003), or 5.1 g O<sub>2</sub>/m<sup>2</sup>.d in a trickling filter (Siegrist and Gujer, 1987).

Oxygen diffusion from bulk to the microorganisms takes place through three adjacent layers: the diffusion layer facing the bulk solution, the stagnant water layer attached to the biofilm, and the biofilm itself. By increasing the linear flow rate, only the thickness of the layer facing the bulk solution can be decreased and in this way, oxygen transfer through this layer can be improved. Besides, air cathodes with a biofilm, to which a thin water layer is attached, may be developed for better oxygen transfer. Oxygen diffusion inside the biofilm and the stagnant water layer however, cannot be influenced by flow rate. To improve oxygen transfer into the biofilm, several directions are possible: use of pure oxygen (Dekker et al., 2009), pressurized air (Fornero et al., 2008), or photosynthetic microorganisms that can create oxygen concentrations up to 20 mg/L (Strik et al., 2010). Care should be taken, however, with too high oxygen concentrations, as these may be toxic to the microorganisms. Furthermore, increased thickness of the biofilm leads to improved oxygen transfer in homogeneous nitrifying biofilms (Siegrist and Gujer, 1987), possibly because of a lower biofilm density and easier diffusion of oxygen as a result. This may be a direction for improvement of oxygen transfer in biocathodes as well. Another direction to increase volumetric productivity is the use of 3D electrodes with a high specific surface area, like graphite felt or carbon granules (Logan et al., 2007; Sleutels et al., 2010). When the flow is well-directed through the porous electrode (Sleutels et al., 2010), this can also further increase the volumetric current production of biocathodes.

Oxygen mass transfer was, besides cathode potential, the main factor limiting biocathode performance, while oxygen transfer rates were reached that were comparable to the rates in other nitrifying biofilms. As discussed above, several directions can be followed to improve oxygen mass transfer. When mass transfer and volumetric current production of biocathodes are further improved, there is great potential for biocathodes to increase electricity production in MFCs.

## Acknowledgements

The exploratory pre-research by Mark van den Ham, the help of Olivier Schaetzle with Cyclic Voltammetry and mass transfer investigations, and the critical comments of Tom Sleutels are kindly acknowledged. Part of this work was funded by SenterNovem, the Dutch governmental agency for sustainability and innovation from the Ministry of Economical Affairs; Besluit Energie Onderzoek Subsidie: Nieuw Energie Onderzoek (grant no: NEOT01015) and Lange Termijn (grant no: EOSLT06020). This work was performed in the TTIW-cooperation framework of Wetsus, Centre of Excellence for Sustainable Water Technology ([www.wetsus.nl](http://www.wetsus.nl)). Wetsus is funded by the Dutch Ministry of Economic Affairs, the European Union European Regional Development Fund, the Province of Fryslân, the city of Leeuwarden and by the EZ-KOMPAS Program of the “Samenwerkingsverband Noord-Nederland”. The authors like to thank the participants of the research theme “Bio-energy” for the fruitful discussions and their financial support.

## 5.4 References

- Aelerman, P.; Freguia, S.; Keller, J.; Verstraete, W.; Rabaey, K. 2008. The anode potential regulates bacterial activity in microbial fuel cells. *Appl. Microbiol. Biotechnol.* 78, 409-418
- Bergel, A.; Feron, D.; Mollica, A. 2005. Catalysis of oxygen reduction in PEM fuel cell by seawater biofilm. *Electrochem. Comm.* 7, 900-904.
- Cheng, S.; Logan, B.E. 2007. Ammonia treatment of carbon cloth anodes to enhance power generation of microbial fuel cells. *Electrochem. Comm.* 9, 492-496
- Clauwaert, P.; Van Der Ha, D.; Boon, N.; Verbeken, K.; Verhaege, M.; Rabaey, K.; Verstraete, W. 2007. Open air biocathode enables effective electricity generation with microbial fuel cells. *Environ. Sci. Technol.* 41, 7564-7569.
- Dekker, A.; Ter Heijne, A.; Saakes, M.; Hamelers, H. V. M.; Buisman, C. J. N. 2009. Analysis and improvement of a scaled-up and stacked microbial fuel cell. *Environ. Sci. Technol.* 43, 9038-9042.
- Fornero, J. J.; Rosenbaum, M.; Cotta, M. A.; Angenent, L. T. 2008. Microbial fuel cell performance with a pressurized cathode chamber. *Environ. Sci. Technol.* 42, 8578-8584.
- Freguia, S.; Rabaey, K.; Yuan, Z.; Keller, J. 2008. Sequential anode-cathode configuration improves cathodic oxygen reduction and effluent quality of microbial fuel cells. *Water Res.* 42, 1387-1396.

- Freguia, S.; Tsujimura, S.; Kano, K. 2010. Electron transfer pathways in microbial oxygen biocathodes. *Electrochim. Acta*, 55, 813-818.
- Hamelers, H.V.M.; Ter Heijne, A.; Sleutels, T.H.J.A.; Jeremiasse, A.W.; Strik, D.P.B.T.B.; Buisman, C.J.N. 2010. New applications and performance of bioelectrochemical systems. *Appl. Microbiol. Biotechnol.* 85, 1673-1685.
- He, Z.; Angenent, L. T. 2006. Application of bacterial biocathodes in microbial fuel cells. *Electroanalysis*. 18, 2009-2015.
- Jeremiasse, A.W.; Hamelers, H.V.M.; Kleijn, J.M.; Buisman, C.J.N. 2009. Use of biocompatible buffers to reduce the concentration overpotential for hydrogen evolution. *Environ. Sci. Technol.* 43, 6882-6887.
- Liang, P.; Fan, M.; Cao, X.; Huang, X. 2009. Evaluation of applied cathode potential to enhance biocathode in microbial fuel cells. *J. Chem. Technol. Biotechnol.* 84, 794-799.
- Logan, B. E.; Hamelers, B.; Rozendal, R.; Schröder, U.; Keller, J.; Freguia, S.; Aelterman, P.; Verstraete, W.; Rabaey, K. 2006. Microbial fuel cells: Methodology and technology. *Environ. Sci. Technol.* 40, 5181-5192.
- Logan, B.; Cheng, S.; Watson, V.; Estadt, G. 2007. Graphite fiber brush anodes for increased power production in air-cathode microbial fuel cells. *Environ. Sci. Technol.* 41, 3341-3346.
- Metcalf & Eddy, Inc; Tchobanoglous, G.; Burton, F.L.; Stensel, H.D. 2003. *Wastewater treatment and reuse*; McGraw-Hill: New York.
- Picioareanu, C.; Van Loosdrecht, M. C. M.; Heijnen, J. J. 1997. Modelling the effect of oxygen concentration on nitrite accumulation in a biofilm airlift suspension reactor. *Water Sci. Technol.* 36, 147-156.
- Rhoads, A.; Beyenal, H.; Lewandowski, Z. 2005. Microbial fuel cell using anaerobic respiration as an anodic reaction and biomineralized manganese as a cathodic reactant. *Environ. Sci. Technol.* 39, 4666-4671.
- Schaetzle, O.; Barrière, F.; Schröder, U. 2009. An improved microbial fuel cell with laccase as the oxygen reduction catalyst. *Energy Environ. Sci.* 2, 96-99.
- Siegrist, H.; Gujer, W. 1987. Demonstration of mass transfer and pH effects in a nitrifying biofilm. *Water Res.* 21, 1481-1487.
- Sleutels, T. H. J. A.; Lodder, R.; Hamelers, H. V. M.; Buisman, C. J. N. 2010. Improved performance of porous bio-anodes in microbial electrolysis cells by enhanced mass and charge transport. *Int. J. Hydrogen Energy.* 34, 9655-9661.
- Strik, D. P. B. T. B.; Hamelers, H. V. M.; Buisman, C. J. N. 2010. Solar energy powered microbial fuel cell with a reversible bioelectrode. *Environ. Sci. Technol.* 44, 532-537.
- Ter Heijne, A.; Hamelers, H. V. M.; Buisman, C. J. N. 2007. Microbial fuel cell operation with continuous biological ferrous iron oxidation of the catholyte. *Environ. Sci. Technol.* 41, 4130-4134.
- Ter Heijne, A.; Hamelers, H. V. M.; Saakes, M.; Buisman, C. J. N. 2008. Performance of non-porous graphite and titanium-based anodes in microbial fuel cells. *Electrochim. Acta.* 53, 5697-5703.
- Williamson, K.; McCarty, P. L. 1976. A model of substrate utilization by bacterial films. *J. Water Pollut. Control Fed.* 48, 9-24.

## Chapter 6

# Copper recovery combined with electricity production in a Microbial Fuel Cell

This chapter has been published as:

Ter Heijne, A.; Liu, F.; Van der Weijden, R.; Weijma, J.; Buisman, C. J. N.; Hamelers, H. V. M. 2010. Copper recovery combined with electricity production in a microbial fuel cell. *Environ. Sci. Technol.* 44, 4376-4381.

## Abstract

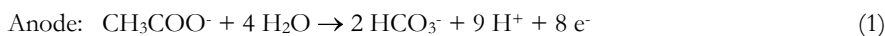
A metallurgical Microbial Fuel Cell (MFC) is an attractive alternative for recovery of copper from copper containing waste streams, as the metal is recovered in its metallic form at the cathode, while the energy for metal reduction can be obtained from oxidation of organic materials at the anode with possible additional production of electricity. We studied the recovery of copper in an MFC using a bipolar membrane as a pH separator. Under anaerobic conditions, the maximum power density was  $0.43 \text{ W/m}^2$  at a current density of  $1.7 \text{ A/m}^2$ . In the presence of oxygen, MFC performance improved considerably to a maximum power density of  $0.80 \text{ W/m}^2$  at a current density of  $3.2 \text{ A/m}^2$ . Pure copper crystals were formed on the cathode, and no  $\text{CuO}$  or  $\text{Cu}_2\text{O}$  was detected. Removal efficiencies of  $>99.88\%$  were obtained. The cathodic recovery of copper compared to the produced electricity was  $84\%$  (anaerobic) and  $43\%$  (aerobic). The metallurgy MFC with the  $\text{Cu}^{2+}$  reducing cathode further enlarges the application range of MFCs.

## 6.1 Introduction

Microbial Fuel Cells (MFCs) are a novel technology to convert biodegradable materials directly into electricity (Logan et al., 2006). During the last years, applications of Microbial Fuel Cells expanded from wastewater purification combined with electricity production to production of added-value components in the cathode, like H<sub>2</sub> and H<sub>2</sub>O<sub>2</sub> (Hamelers et al., 2010).

A new potential application of MFCs is the removal and recovery of metals from mining and metallurgical wastewaters and leachates. Depending on the origin of these streams, they contain heavy metals such as copper, nickel, cobalt and zinc (Johanson and Hallberg, 2005; Johnson, 2000; Heikkinen et al., 2009). The mining and metallurgical industries are main contributors of anthropogenic copper emissions to the environment (Flemming and Trevors, 1989). At low concentrations, copper is a micronutrient and is essential to virtually all plants and animals. At higher concentrations, copper can become toxic to all life forms, although toxicity levels vary widely. Due to its effects on plants, copper is a serious threat to agriculture (Flemming and Trevors, 1989). Therefore, it is important that copper is removed from waste streams. Current methods for copper removal are, amongst others, cementation (Hor and Mohamed, 2003) co-precipitation with calcium carbonate (Khosravi and Alamdari, 2009), and adsorption (Alkan et al., 2008; Kazemipour et al., 2008). In addition to removal, treatment of these waste streams should preferably result in the recovery of copper for (re-)use in industry.

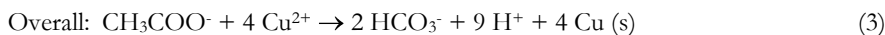
To achieve this combination of copper removal and recovery, we propose the metallurgical MFC. In the metallurgical MFC, oxidation of organic material is coupled to reduction of copper, according to:



$$E_{\text{an}} = -0.289 \text{ V vs NHE} \quad (\text{pH} = 7, [\text{CH}_3\text{COO}^-] \text{ and } [\text{HCO}_3^-] = 0.05 \text{ M})$$



$$E_{\text{cat}} = +0.286 \text{ V vs NHE} \quad ([\text{Cu}^{2+}] = 1 \text{g/L})$$



$$E_{\text{cell}} = 0.575 \text{ V}$$

The overall process is shown in Figure 1.

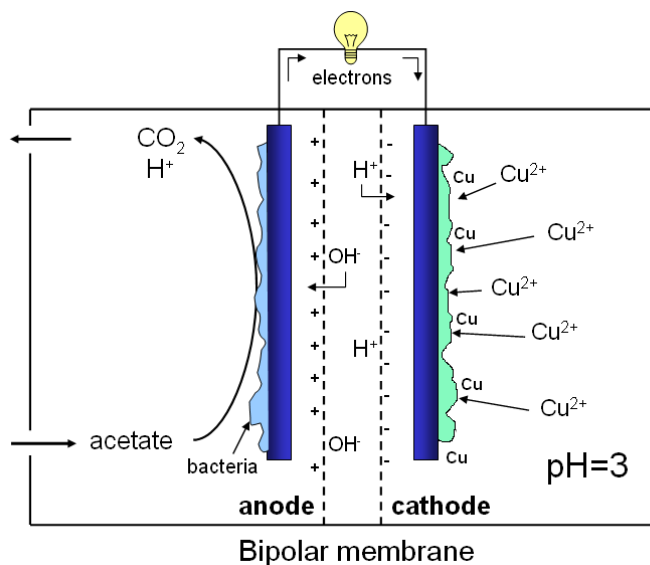


**Figure 1.** Principle of the MFC with copper reduction and a bipolar membrane as a pH separator

At the anode, organic material is oxidized to  $\text{CO}_2$ , protons and electrons. At the cathode,  $\text{Cu}^{2+}$  is reduced to Cu. This principle is applied for a typical acidic (pH 3) waste stream containing considerable amounts of copper (1 g/L). Such a low pH is necessary for the performance of the metal reducing cathode, as at a  $\text{pH} > \sim 4.5$ ,  $\text{Cu}^{2+}$  may precipitate as CuO or  $\text{Cu}_2\text{O}$  and may not be available for reduction. Besides, no pH adjustment of the copper containing waste stream is necessary when the cathode is operated at low pH. A bio-anode however, can not be operated at such a low pH, and is preferably operated at near neutral pH to achieve higher current densities. A barrier is thus needed between the anode and cathode to keep the pH difference intact. This barrier prevents the pH in the catholyte to increase and the anolyte pH to drop.

For this purpose, a bipolar membrane was used, which has been shown to be an effective pH separator in previous studies (Ter Heijne et al., 2006; Ter Heijne et al., 2007), although part of the energy was lost for maintaining the pH difference. The bipolar membrane produces acid and base via the water splitting reaction that occurs between the anion exchange layer and the cation exchange layer (Figure 1). Protons migrate through the cation exchange layer to the cathode compartment, while hydroxyl ions migrate through the anion exchange layer to the anode compartment. In this way, the pH difference between both compartments can be maintained.

Application of MFCs in metal removal has until now only been studied for the reduction of Cr(VI) to Cr(III) at the cathode for detoxification purposes (Wang et al., 2009; Li et al., 2009), but Cr(III) reuse is not feasible. In addition to its potential as environmental remediation technology, MFCs could also be used to produce metals from low grade ores in hydrometallurgical processes (Dreisinger, 2009).

By applying biodegradable organic compounds in a metallurgical MFC, electricity is produced, copper is recovered on electrodes, and acid is generated. This has several advantages compared to the currently applied methods for copper recovery, like electrowinning (Jergensen, 1999) and precipitation with sulfide, which is produced via sulphate reduction (Bijmans et al., 2009). Compared to electrochemical processes, electricity is produced instead of used. Compared to sulphate reduction, the metallurgical MFC is more efficient both in organic carbon and energy use. Only two moles of electrons are needed to recover one mole of copper, instead of the eight moles of electrons that are needed to reduce the sulphate to sulfide (Bijmans et al., 2009). Therefore, the metallurgical MFC is four times as efficient in organic carbon use. Besides, electricity is produced, elemental copper is produced instead of copper sulfide, and the sulfuric acid remains available, which can be used for the bioleaching operation.

MFC performance was studied through batch performance, polarization curves, and copper removal with ICP. Oxygen is the preferred electron acceptor in MFCs because of its availability and high redox potential. Presence of oxygen could affect MFC performance, also in case of  $\text{Cu}^{2+}$  reduction, and therefore, the process was studied under both anaerobic and aerobic conditions. The recovered copper product was examined using scanning electron microscopy and X-ray powder diffraction. We show that MFCs can recover pure copper with an efficiency of >99.88% with simultaneous electricity production.

## 6.2 Materials and methods

### 6.2.1 Research setup

The electrochemical cell used in this study has been previously described in (Ter Heijne et al., 2008). The setup contained two flow channels sized 10cm x 2cm x 1.5cm (w x h x d), which were separated by a bipolar membrane (Fumasep FBM, Fumatech, Germany). The membrane and electrode surface area was 22 cm<sup>2</sup>. The anode was a rough (sandpapered) graphite plate (Müller&Rössner GmbH, Troisdorf, Germany), while the cathode was a piece of graphite foil, 1.0 g/cc density, 99% purity (Coidan Graphite Products Ltd, York, UK), pressed on a mixed metal oxide coated titanium plate that functioned as a current collector (Magneto

Special Anodes BV, Schiedam, The Netherlands). Anode and cathode potentials were measured versus reference electrodes (Ag/AgCl, 3M KCl, ProSense QiS, Oosterhout, The Netherlands). The potential of these reference electrodes was regularly checked versus a Standard Calomel Electrode (SCE, +0.241 V vs NHE) and showed a negligible drift (<2 mV).

### 6.2.2 Start-up and operation

The anode was inoculated with a mixed culture anolyte from operating MFCs running on acetate. Anode medium was continuously fed to the system at a rate of 12 mL h<sup>-1</sup>. The anode medium consisted of acetate (20 mM), phosphate buffer (pH 7, 20 mM), and nutrients and vitamins as described in (Ter Heijne et al., 2008). The actual acetate concentration in the MFC during the whole experiment was measured with Gas Chromatography and was always higher than 5 mM. The catholyte was prepared with copper chloride dihydrate (analytical grade) obtained from Merck (Darmstadt, Germany). The pH was lowered to 3 by addition of HCl. Both anode and cathode compartments had a flow rate of ~10 L h<sup>-1</sup>. The total catholyte volume was 800 mL. Anolyte was controlled at pH=7, while catholyte was controlled at pH=3. All experiments were performed in a temperature controlled chamber at 30 °C.

The cathode was operated in batch and continuously recirculated over a recirculation bottle. The total catholyte volume was 800 mL. Copper reduction in the cathode was first tested under anaerobic conditions (catholyte recirculation bottle was continuously flushed with nitrogen gas), and secondly under aerobic conditions (catholyte recirculation bottle was open to air). The bio-anode was started up with a catholyte consisting of 20 mM phosphate buffer at pH=7, via a recirculation bottle which was open to air.

Anode and cathode were connected via a resistance of 1000 Ω which was stepwise decreased. The MFC was considered to be started up when current density was stable at a value higher than 0.3 A/m<sup>2</sup> for at least 10 hours, and the anode potential was lower than -0.5 V vs Ag/AgCl. When these criteria were met, the catholyte was replaced with Cu<sup>2+</sup> solution (1 g/L) at pH=3 under anaerobic conditions. Resistance was decreased stepwise in the first 24 hours from 100 to 50, 30, 15, 10 and finally 4.7 Ω for the anaerobic experiment. During the remainder of the experiment, resistance was kept constant at 4.7 Ω. At the end of the experiment, the MFC was opened and directly re-assembled with the same bio-anode and a new bipolar membrane and a new cathode graphite paper. Cu<sup>2+</sup> solution was added directly under aerobic conditions. The resistance was decreased stepwise in the first 20 hours from 50 to 20, 10, and finally 5.0 Ω. During the remainder of the experiment, resistance was kept constant at 5.0 Ω.

### 6.2.3 Analyses

Polarization curves were recorded using dc-voltammetry (chronoamperometry). For the  $\text{CuCl}_2$  cathode, cell voltage was decreased in 17 steps from open circuit voltage (OCV) down to 0 V. For the blank (oxygen reduction at  $\text{pH}=7$ ), cell voltage was decreased in 10 steps from 0.4 to 0 V. At each voltage, current was stabilized for at least 15 minutes. The last data point is shown in the polarization curve.

Samples of anolyte and catholyte were analyzed once or twice every day for their copper concentration. It was assumed that all copper in solution was present as  $\text{Cu}^{2+}$ , and copper was determined with an Inductively Coupled Plasma – Optical Emission Spectrometer (ICP-OES; Vista-MPX, Varian, Inc.).

When all copper was depleted, the MFC was opened and the graphite paper with visible precipitation was washed with demineralized water and air-dried. The morphology of precipitates on the electrode were examined with SEM and crystal structure with XRPD. Measurements with the Scanning Electron Microscope (SEM, NORAN System SIX model 300 X-ray microanalysis system, Thermo Electron Corporation) were done at an acceleration voltage of 10 kV. X-ray powder diffraction (XRPD) patterns were recorded in a Bragg-Brentano geometry in a Bruker D5005 diffractometer equipped with Huber incident-beam monochromator and Braun PSD detector. Data collection was carried out at room temperature using monochromatic  $\text{Cu K}\alpha 1$  radiation ( $\lambda = 0.154056 \text{ nm}$ ) in the  $2\theta$  region between  $5^\circ$  and  $90^\circ$ , step size 0.038 degrees  $2\theta$ . Both samples were measured under identical conditions. The samples of about 20 milligrams were deposited on a Si <510> wafer and were rotated during measurement. Data evaluation was done with the Bruker program EVA.

Cathodic efficiency  $\eta_{\text{cat}}$ , the amount of copper reduced compared to the current produced,

$$\text{was calculated as } \eta_{\text{Cat}} = \frac{([\text{Cu}^{2+}]_0 - [\text{Cu}^{2+}]_t) \cdot V}{\int_0^t I \cdot dt} \cdot 2F \text{ where } [\text{Cu}^{2+}]_t = \text{Cu}^{2+}$$

concentration at time t (mol/L),  $[\text{Cu}^{2+}]_0 = \text{Cu}^{2+}$  concentration at time 0 (mol/L), V = catholyte volume (L), I = current (A), and F=Faraday constant (96485 C/mol).

## 6.3 Results and discussion

### 6.3.1 Anaerobic cathodic copper reduction resulted in high MFC performance

The first run was performed under anaerobic conditions with the catholyte consisting of 1 g/L of  $\text{Cu}^{2+}$  as  $\text{CuCl}_2$  at pH 3. The catholyte was continuously flushed with nitrogen gas to maintain anaerobic conditions. Current density increased instantaneously from 0.34  $\text{A/m}^2$  (MFC at the end of start-up period with oxygen reduction) to 1.5  $\text{A/m}^2$  at a cell voltage of 0.31 V. At a resistance of 4.7  $\Omega$ , a current density of 4.5  $\text{A/m}^2$  was found. In the course of time, as copper concentration decreased, current density decreased to  $<0.1 \text{ A/m}^2$  after 7 days. The second run was performed in the same MFC but now the catholyte was open to air, resulting in an oxygen concentration of 6.5 mg/L. After addition of copper chloride, current density increased to a maximum of 6.2  $\text{A/m}^2$  at a resistance of 5.0  $\Omega$ . Similarly to the anaerobic experiment, in course of time, cell voltage and current density decreased, to  $<0.7 \text{ A/m}^2$  after 8 days.

A polarization curve was made under anaerobic and aerobic conditions when  $\text{Cu}^{2+}$  concentration was 0.93 g/L and 0.94 g/L and was compared to the blank experiment with oxygen reduction at pH 3 (Figure 2A).

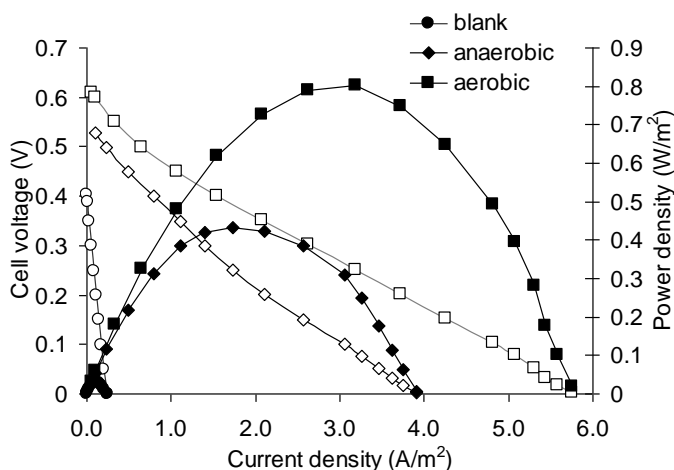


**Figure 2A.** Polarization curves for copper reduction under aerobic conditions showed a maximum power density (closed symbols) of 0.80  $\text{W/m}^2$ . This was almost two-fold higher than the power density for copper reduction under anaerobic conditions, and more than 30-fold higher than the power produced in the blank experiment with oxygen reduction at pH 3. Open symbols represent cell voltage.

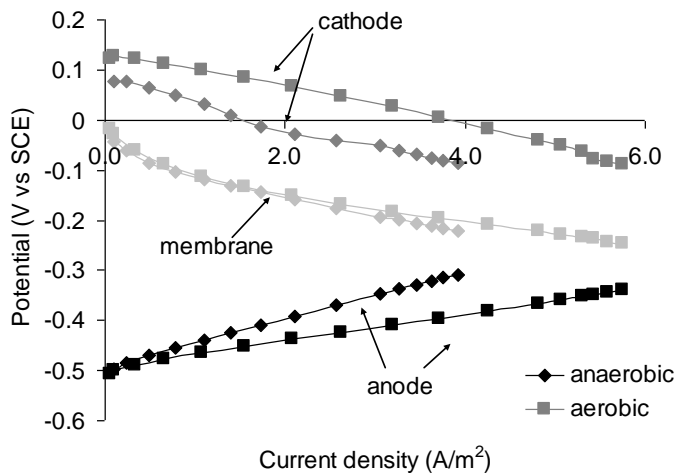


**Figure 2B.** Analysis of the potentials in both polarization curves shows that under aerobic conditions, cathode potential was higher than under anaerobic conditions. Combined with an improvement in anode performance (lower anode potential at same current density), overall MFC performance clearly improved.

Under anaerobic conditions, the maximum power density was  $0.43 \text{ W/m}^2$  at a current density of  $1.7 \text{ A/m}^2$ . Under aerobic conditions, the maximum power density was almost two-fold higher:  $0.80 \text{ W/m}^2$  at a current density of  $3.2 \text{ A/m}^2$ . A further increase in oxygen concentration to  $7.5 \text{ mg/L}$  had no influence on MFC performance meaning that oxygen transfer was not limiting MFC performance. Performance of the MFC with copper in the catholyte was considerably higher than in the blank experiment without copper, where the maximum power density was a factor 35 lower compared to aerobic copper reduction:  $0.023 \text{ W/m}^2$  at a current density of  $0.12 \text{ A/m}^2$ .

### 6.3.2 Aerobic copper reduction resulted in improved performance

The power density of the MFC with  $\text{Cu}^{2+}$  reduction was improved by almost a factor two under aerobic conditions compared to anaerobic conditions. Figure 2B shows the anode and cathode potentials and the voltage across the membrane in both the anaerobic and the aerobic situation. From Figure 2B it can be seen that under aerobic conditions, cathode potential was between  $0.05$  and  $0.1 \text{ V}$  higher than under anaerobic conditions. In combination with better anode performance (lower anode potential at the same current density), the overall MFC performance was twice as high under aerobic conditions as under anaerobic conditions. The presence of oxygen in the catholyte apparently leads to combined reduction of oxygen and

copper, resulting in higher performance. The performance of the anode may have been better because the aerobic experiment was performed as the second run, and therefore the anode microorganisms had been accustomed for a longer time to produce electricity.

Visual inspection of the membrane after disassembling the MFC showed no precipitates on the membrane after both the anaerobic and the aerobic experiment. No copper was detected in the anolyte, indicating that there was no copper leakage through the bipolar membrane from cathode to anode.

### 6.3.3 Pure copper crystals were formed on the cathode

XRPD measurements showed that pure copper crystals were formed on the cathode for both the anaerobic and aerobic experiment. No trace of other copper crystals ( $\text{CuO}$ ,  $\text{Cu}_2\text{O}$ ) were detected with XRPD.

The SEM pictures (Figure 3) suggest that copper grows from units with a rounded or more octahedral habit that eventually connect to form a dense layer (Figure 3A and 3B).

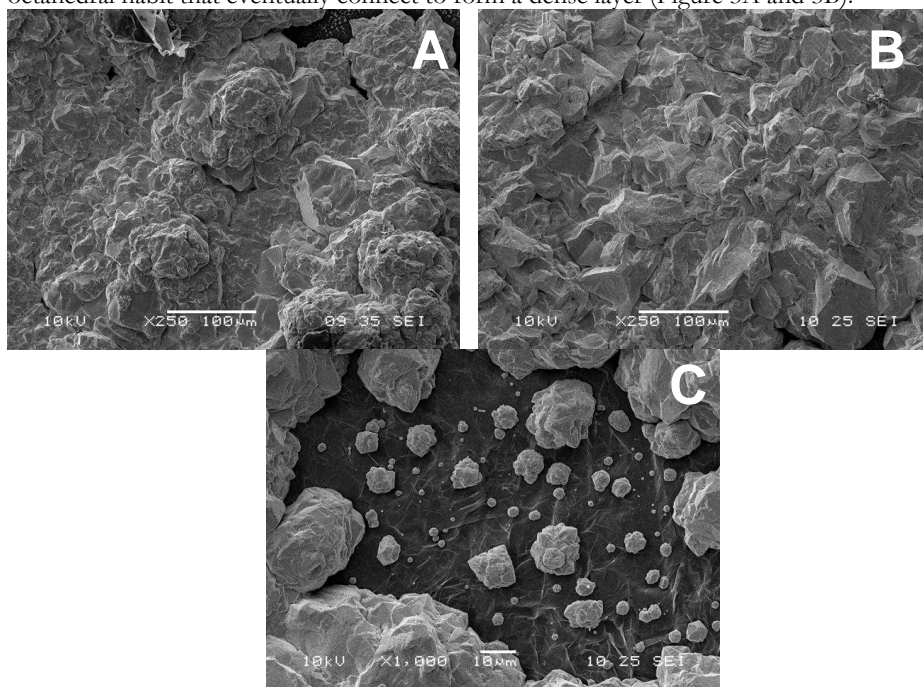


**Figure 3** (A) Copper deposited under anaerobic conditions on graphite electrode. (B) Copper deposited under aerobic conditions on graphite electrode (C) Growth of copper on graphite electrode imperfections (picture taken under aerobic conditions).

These units seem to be rather evenly spread over the cathode surface. Under both anaerobic and aerobic conditions, the copper growth units appear to be dominant close to the light gray lines in the background (Figure 3C). This means that copper growth starts at the edges where graphite surface elevation changes. The copper deposited under aerobic conditions displays more octahedral habit features and a less cauliflower-like overall structure than does the copper precipitated under anaerobic conditions (Figure 3A and 3B). This may be attributed to a somewhat slower growth of copper under aerobic conditions (8 days vs 7 days under anaerobic conditions), which leads to larger and more pronounced crystal faces. The denseness of the copper product allowed for strips of copper to be peeled off the electrode for recovery.

### 6.3.4 MFC performance decreased with decreasing copper concentration

The polarization curves were made at  $\text{Cu}^{2+}$  concentrations of 0.93 g/L (aerobic), and 0.94 g/L (anaerobic). As the copper concentration decreased with time as a result of the reduction reaction, the cathode potential decreased with time as well. This resulted in a decrease in MFC cell voltage and current density.

The effect of  $\text{Cu}^{2+}$  concentration on MFC performance was further investigated.  $\text{Cu}^{2+}$  concentrations with time for both the anaerobic and the aerobic experiment are shown in Figure 4A.

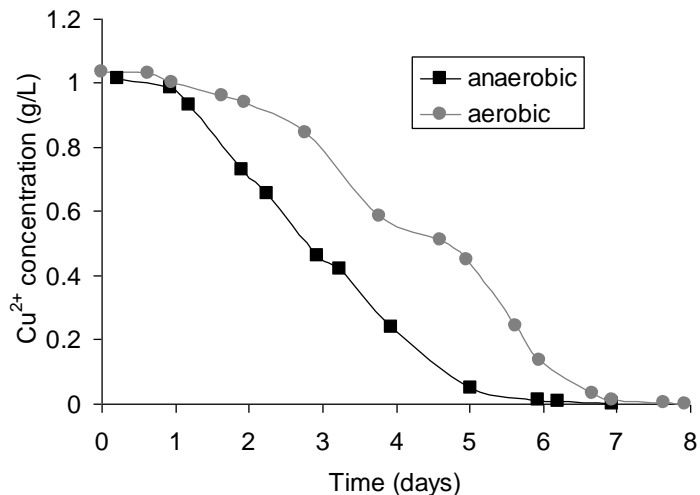


**Figure 4A.**  $\text{Cu}^{2+}$  concentration decreased with time for both the anaerobic and the aerobic experiment.

In both experiments, a slower decrease in copper concentration was observed during the first 2 days, when current density was still low as the result of the high resistance used. After this, a constant resistance of  $4.7 \Omega$  (anaerobic) and  $5.0 \Omega$  (aerobic) was used, and copper concentration decreased quite linearly until low copper concentrations were reached. The last measured copper concentration was  $1.2 \text{ mg/L}$  for the anaerobic experiment, and  $0.5 \text{ mg/L}$  for the aerobic experiment. As no copper was detected in the anolyte, and no precipitates were visible in other parts of the system, it can be assumed that all copper was precipitated on the cathode. The maximum copper removal efficiency was calculated to be 99.88% in the anaerobic experiment, and 99.95% in the aerobic experiment.

The effect of copper concentration on current density at constant resistance of  $4.7 \Omega$  (anaerobic) and  $5.0 \Omega$  (aerobic) is shown in Figure 4B.

A decrease in copper concentration resulted in a decrease in cathode potential. As a result, cell voltage and current density decreased as well. At copper concentrations below  $0.2 \text{ g/L}$ , we see a steep drop in current density in both experiments. Thus, when high current densities are required, a copper concentration above this level is required. The current densities in the aerobic experiment were higher than in the anaerobic experiment.

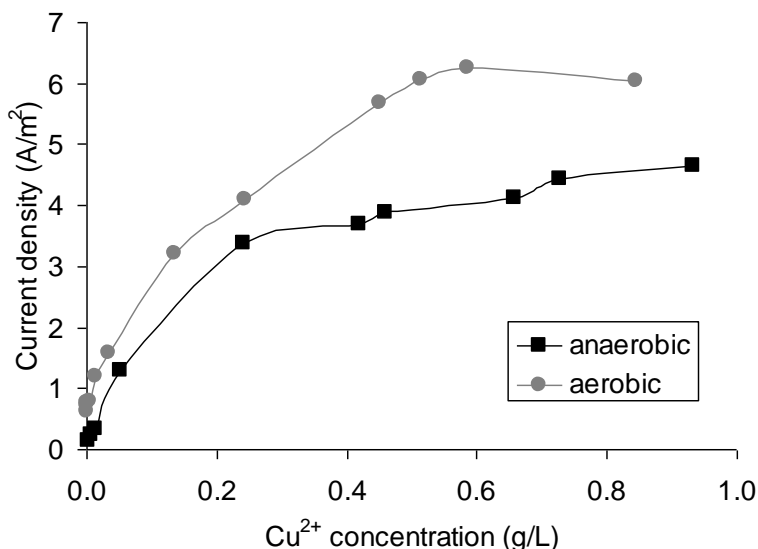


**Figure 4B.**  $\text{Cu}^{2+}$  concentration at a constant resistance had a pronounced effect on the produced current density. Especially at low  $\text{Cu}^{2+}$  concentrations ( $<0.2 \text{ g/L}$ ), current density decreased.

Also when all copper was removed, we still measured a current density of  $0.7 \text{ A/m}^2$ , compared to  $0.1 \text{ A/m}^2$  in the anaerobic experiment. The presence of oxygen in the system may produce a background current as a result of oxygen reduction. The combination of oxygen reduction and copper reduction resulted in higher current densities.

Cathodic efficiency was calculated from the decrease in copper concentration and the produced current. In the anaerobic experiment, the cathodic efficiency was 84%. This means, that more electrons were recorded as current than electrons were consumed for copper reduction. Apparently, there was another electron sink present in the catholyte. Even though the catholyte was continuously flushed with nitrogen gas, there may have been some trace concentrations of oxygen in the system, which could take up part of the electrons. The cathodic efficiency of the aerobic experiment was significantly lower: 43%. This lower efficiency under aerobic conditions compared to anaerobic conditions further indicates that besides copper, also oxygen was reduced at the cathode.

Open circuit cathode potential was  $+0.08 \text{ V}$  vs SCE at a copper concentration of  $0.93 \text{ g/L}$ , corresponding to a value of  $+0.321 \text{ V}$  vs NHE. At open circuit, no losses occur at the electrode and the measured potential should be equal to the theoretical potential. The theoretical potential of the reaction  $\text{Cu}^{2+} + 2 \text{e}^- \rightarrow \text{Cu}$  is  $+0.34 \text{ V}$  vs NHE. A copper concentration of  $0.93 \text{ g/L}$  would then result in a cathode potential of  $+0.285 \text{ V}$  vs NHE. So, the measured open circuit potential was somewhat higher than the theoretical cathode potential. This may be an indication of some oxygen present even though the catholyte was continuously flushed with nitrogen gas. Under aerobic conditions, open circuit cathode potential was even higher:  $+0.12 \text{ V}$  vs SCE ( $+0.361 \text{ V}$  vs NHE). As the open circuit potential for oxygen reduction at  $\text{pH}=3$  is and  $\text{pO}_2=0.2 \text{ bar}$  is  $+1.04 \text{ V}$  vs NHE, oxygen is a more preferred electron acceptor. The higher measured open circuit cathode potential may thus be the result of a mixed potential of both copper and oxygen reduction.

### 6.3.5 Implications

A high removal efficiency of 99.88% combined with high energy production makes this new process of interest for copper recovery. The obtained power densities are comparable to results achieved with other well-performing cathode systems using oxygen (Ter Heijne et al., 2007; Cheng et al., 2006; Freguía et al., 2008). This is surprising, considering that the standard potential of  $\text{Cu}^{2+}/\text{Cu}$  is considerably lower than that of oxygen reduction:  $+0.286 \text{ V}$  vs NHE for  $\text{Cu}^{2+}$  reduction compared to  $+0.805 \text{ V}$  vs NHE for oxygen reduction. Besides, the use of the bipolar membrane leads to an additional potential loss. Despite these drawbacks, the system achieved a cell voltage of  $0.25 \text{ V}$  at the maximum power density under aerobic

conditions, which corresponds to a voltage efficiency of 43% using the maximum cell voltage based on the thermodynamic cathode potential for copper ( $E_{\text{cell}}=0.585$  V), or 23% using the maximum cell voltage based on the thermodynamic cathode potential for oxygen reduction ( $E_{\text{cell}}=1.09$  V).

The high performance of the MFC with  $\text{Cu}^{2+}$  reducing cathode could be a result from a number of factors: (i) mass transfer of  $\text{Cu}^{2+}$  is faster as copper has high solubility at acidic conditions (we used 16 mM), while mass transfer limitations of oxygen occur as a result of low oxygen solubility of only 0.20 mM when catholyte was saturated with air. We see that only below 0.2 g/L of  $\text{Cu}^{2+}$  (Figure 4B) that there is a limitation that might be attributed to mass transfer limitations, (ii) the oxygen reduction reaction has a high overpotential, while the overpotential for  $\text{Cu}^{2+}$  reduction is much lower, and (iii) copper might function as a catalyst for the oxygen reduction reaction. Considering the low cathodic efficiency under aerobic conditions, the increased current under aerobic conditions was clearly a result of additional oxygen reduction. This additional current was however much higher than expected from the performance of the blank experiment.

Expressing the cathode overpotential in terms of the current at which cathode potential was zero, we find for the blank, anaerobic, and aerobic experiment a current density of 0, 1.5, and 3.8 A/m<sup>2</sup>. This difference between the current produced by the anaerobic and aerobic  $\text{Cu}^{2+}$  reduction reaction cannot be explained by the catalytic activity of the carbon cathode for oxygen reduction, as the blank produced no current at a cathode potential of 0 V vs SCE. This would be an indication that copper is somehow involved as a catalyst.

This new metallurgical MFC combines electricity production with copper recovery. As the metallurgical MFC is still in early stage of development, it cannot be directly compared to the current recovery methods like electrowinning (Jergensen, 1999) and precipitation with sulfides (Bijmans et al., 2009), however, some main points of attention will be addressed here to position the metallurgical MFC within the field of copper recovery.

First, compared to electrowinning, the metallurgical MFC has the advantage of electricity production instead of electricity consumption, and the high removal efficiency leading to final copper concentrations <1.2 mg/L. It should be noted however, that electrowinning occurs at current densities of several orders of magnitudes higher than reported in this study, and it should be investigated to what extent the energy losses in the metallurgical MFC increase when operating at similar current densities as electrowinning.

Secondly, an organic source is needed to provide the anodic microorganisms with the necessary energy. These organics are not always available on sites where mining and metallurgical streams and leachates, or waste streams from industry are present. So, application

of the metallurgical MFC is limited to locations where both organics and copper streams can be found in proximity.

Thirdly, the metallurgical MFC has a high carbon efficiency compared to precipitation with sulfides, because only 2 electrons are needed for copper reduction instead of 8 electrons for sulphate reduction. The key parameter to determine carbon efficiency in the metallurgical MFC is the Coulombic efficiency, which indicates how many electrons from the organic carbon source end up as electric current. Previous studies have shown that Coulombic efficiencies up to 95-100% have been achieved (Ter Heijne et al., 2006; Aelterman et al., 2008). Besides Coulombic efficiency, also cathodic efficiency is important in this respect, because the product of both determines which part of the electrons present in the organic source end up in the final copper product. In this study, we reached a maximum cathodic efficiency of 84% in the anaerobic experiment. Combined with a Coulombic efficiency of 95%, 80% of the electrons in the carbon source end up in copper. At 100% efficiency, the organic carbon use in the metallurgical MFC is 0.25 kg COD/kg Cu, and 80% efficiency thus results in an organic carbon use of 0.31 kg COD/kg Cu. This makes the metallurgical MFC more than 3 times as efficient as sulphate reduction, where at 100% efficiency, 0.99 kg COD/kg Cu is needed. In case of copper recovery in the metallurgical MFC, it would be an advantage if the system can be operated anaerobically, because this results in increased (cathodic) efficiency.

Fourthly, another option for the use of MFCs for copper recovery would be to use the 'green' electricity produced in the MFC to supply power for electrowinning. The metallurgical MFC then has the advantage that the reactions take place in only one system, which reduces the overall energy losses.

Besides a technology for copper recovery,  $\text{Cu}^{2+}$  reduction as a cathodic reaction is thus an interesting option to consider for the improvement of MFC performance, as we have shown that it can compete with oxygen reduction as an efficient cathode option. In this case, further study of the catalytic behavior of copper for oxygen reduction is important. Of course, application is limited to situations where  $\text{Cu}^{2+}$  solutions are available. As we have shown that the formed copper is pure and can thus be reused, while electricity is produced, this makes the metallurgy MFC an attractive option for copper recovery. The  $\text{Cu}^{2+}$  reducing cathode thus enlarges the application range of MFCs even further and illustrates once more the flexibility of MFC applications.

## Acknowledgments

We would like to thank Astrid Paulitsch at Wetsus for the SEM analysis. Ruud Hendriks at the Department of Materials Science and Engineering of the Delft University of Technology is acknowledged for the X-ray analysis. Wetsus is funded by the Dutch Ministry of Economic Affairs, the city of Leeuwarden, the Province of Fryslân, the European Union European Regional Development Fund and by the EZ/KOMPAS program of the “Samenwerkingsverband Noord-Nederland”.

## 6.4 References

- Aelterman, P.; Freguia, S.; Keller, J.; Verstraete, W.; Rabaey, K. 2008. The anode potential regulates bacterial activity in microbial fuel cells. *Appl. Microbiol. Biotechnol.* 78, 409-418.
- Alkan, M.; Kalay, B.; Doğan, M.; Demirbaş, O. 2008. Removal of copper ions from aqueous solutions by kaolinite and batch design. *J. Hazard. Mater.* 153, 867-876.
- Bijmans, M. F. M.; Dopson, M.; Peeters, T. W. T.; Lens, P. N. L.; Buisman, C. J. N. 2009. Sulfate reduction at pH 5 in a high-rate membrane bioreactor: Reactor performance and microbial community analyses. *J. Microbiol. Biotechnol.* 19, 698-708.
- Cheng, S.; Liu, H.; Logan, B. E. 2006. Increased performance of single-chamber microbial fuel cells using an improved cathode structure. *Electrochem. Commun.* 8, 489-494.
- Dreisinger, D. 2009. Copper leaching from primary sulfides: Options for biological and chemical extraction of copper. *Hydrometallurgy.* 83, 10-20.
- Flemming, C. A.; Trevors, J. T. 1989. Copper toxicity and chemistry in the environment: A review. *Water Air Soil Pollut.* 44, 143-158.
- Freguia, S.; Rabaey, K.; Yuan, Z.; Keller, J. 2008. Sequential anode-cathode configuration improves cathodic oxygen reduction and effluent quality of microbial fuel cells. *Water Res.* 42, 1387-1396.
- Hamelers, H.V.M.; Ter Heijne, A.; Sleutels, T.H.J.A.; Jeremiasse, A.W.; Strik, D.P.B.T.B.; Buisman, C.J.N. 2010. New applications and performance of bioelectrochemical systems. *Appl. Microbiol. Biotechnol.* 85, 1673-1685.
- Heikkinen, P.M.; Räisänen, M.L.; Johnson, R.H. 2009. Geochemical characterisation of seepage and drainage water quality from two sulphide mine tailings impoundments: Acid mine drainage versus neutral mine drainage. *Mine Water Environ.* 28, 30-49.
- Hor, Y. P.; Mohamed, N. 2003. Removal and recovery of copper via a galvanic cementation system part I: Single-pass reactor. *J. Appl. Electrochem.* 33, 279-285.
- Jergensen, G.V., Ed. 1999. *Copper Leaching, Solvent Extraction & Electrowinning Technology*; Society for Mining, Metallurgy, and Exploration, Inc: Littleton.
- Johnson, D.B. 2000. Biological removal of sulfurous compounds from inorganic wastewaters. In: *Environmental Technologies to Treat Sulfur Pollution: Principles and Engineering*; Lens, P., Hulshoff Pol, L., Eds. IWA Publishing: London.

- Johnson, D.B.; Hallberg K.B. 2005. Acid mine drainage remediation options: a review. *Sci. Total Environ.* 338, 3-14
- Kazemipour, M.; Ansari, M.; Tajrobehkar, S.; Majdzadeh, M.; Kermani, H. R. 2008. Removal of lead, cadmium, zinc, and copper from industrial wastewater by carbon developed from walnut, hazelnut, almond, pistachio shell, and apricot stone. *J. Hazard. Mater.* 150, 322-327.
- Khosravi, J.; Alamdari, A. 2009. Copper removal from oil-field brine by coprecipitation. *J. Hazard. Mater.* 166, 695-700.
- Li, Y.; Lu, A.; Ding, H.; Jin, S.; Yan, Y.; Wang, C.; Zen, C.; Wang, X. 2009. Cr(VI) reduction at rutile-catalyzed cathode in microbial fuel cells. *Electrochem. Commun.* 11, 1496-1499.
- Logan, B. E.; Hamelers, B.; Rozendal, R.; Schröder, U.; Keller, J.; Freguia, S.; Aelterman, P.; Verstraete, W.; Rabaey, K. 2006. Microbial fuel cells: Methodology and technology. *Environ. Sci. Technol.* 40, 5181-5192.
- Ter Heijne, A. ; Hamelers, H.V.M. ; De Wilde, V.; Rozendal, R.A.; Buisman, C.J.N. 2006. A bipolar membrane combined with ferric iron reduction as an efficient cathode system in microbial fuel cells. *Environ. Sci. Technol.* 40, 5200-5205.
- Ter Heijne, A.; Hamelers, H.V.M.; Buisman, C.J.N. 2007. Microbial fuel cell operation with continuous biological ferrous iron oxidation of the catholyte. *Environ. Sci. Technol.* 41, 4130-4134.
- Ter Heijne, A.; Hamelers, H.V.M.; Saakes, M.; Buisman, C.J.N. 2008. Performance of non-porous graphite and titanium-based anodes in microbial fuel cells. *Electrochim. Acta.* 53, 5697-5703.
- Wang, G.; Huang, L.; Zhang, Y. 2008. Cathodic reduction of hexavalent chromium [Cr(VI)] coupled with electricity generation in microbial fuel cells. *Biotechnol. Lett.* 30, 1959-1966.



## Chapter 7

# Improvement of the cathode of a scaled-up Microbial Fuel Cell

This chapter has been submitted:

Ter Heijne, A.; Liu, F.; Van Rijnsoever, L.S.; Saakes, M.; Hamelers, H. V. M.; Buisman, C. J. N. 2010. Improvement of the cathode of a scaled-up Microbial Fuel Cell.

## Abstract

Scale-up studies of MFCs are required before practical application comes into sight. We studied an MFC, which consisted of a single cell with a surface area of  $0.5 \text{ m}^2$  and a total volume of 5 L. Ferric iron ( $\text{Fe}^{3+}$ ) was used as the electron acceptor to improve cathode performance. MFC performance continuously increased in time as a combined effect of growth of the electrochemically active microorganisms at the bio-anode, stepwise increase in iron concentration from 1 g/L to 6 g/L, and increased activity of the iron oxidizers to regenerate the ferric iron. Finally, a power density of  $2.0 \text{ W/m}^2$  ( $200 \text{ W/m}^3$ ) was obtained at a current density of  $4.2 \text{ A/m}^2$ . Analysis of internal resistances showed that the anode resistance decreased from 109 to  $7 \text{ m}\Omega\cdot\text{m}^2$  in the course of the experiment, while cathode resistance decreased from 939 to  $85 \text{ m}\Omega\cdot\text{m}^2$ . The cathode was still the main limiting factor, as it contributed to 58% of the total internal resistance. For practical application of MFCs, further study on cathodes, stacking, and scaling up is needed.

## 7.1 Introduction

Wastewaters are being recognized as a renewable energy source in the form of biodegradable organic matter. Extracting energy from wastewaters is a valuable contribution to the production of renewable energy and the reduction of greenhouse gas emissions. Microbial Fuel Cells (MFCs), using microorganisms as the catalyst, are regarded as a promising technology for the production of electricity from wastewater (Logan et al., 2006).

Advantage of the MFC compared to current technologies like anaerobic digestion, is the potentially high energy efficiency, as electricity is produced directly without an energy inefficient combustion step. Unlike anaerobic digestion however, the feasibility of MFC technology has not been proven on a commercial scale yet (Rozendal et al., 2008). This has both economic and technological reasons. From an economic point of view, MFC installations at this point require higher capital costs. From a technological and energetic point of view, the maximum power production is limited by ohmic losses in the solution and electrochemical losses at the electrodes, and bacterial metabolic losses (Logan et al., 2006; Rozendal et al., 2008; Hamelers et al., 2010). Essential measures to overcome losses in the MFC are to maintain short internal distances to reduce the ohmic resistance, and to choose highly conductive electrodes (Clauwaert et al., 2008), and to improve the cathode as the oxygen reduction reaction requires high overpotentials.

Small-scale MFCs with volumes ranging between 10 mL and 1 L and projected surface areas between 1 cm<sup>2</sup> and 400 cm<sup>2</sup> have been tested worldwide for many years now. However, larger-scale MFC research has been lagging behind. The first successful attempt for scaling-up the MFC was published by Dekker et al. (2009). It was shown that a scaled-up system consisting of four stacked cells and with a total volume of 20 L, achieved 144 W/m<sup>3</sup>. The major bottlenecks were cathode performance, cell reversal, and flow characteristics.

We continued the study on scaling up MFCs to gain more insight in its operation. Our approach was to replace oxygen as the electron acceptor by ferric iron (Fe<sup>3+</sup>) to improve cathode performance (Ter Heijne et al., 2006; 2007), and to operate the MFC under improved flow characteristics compared to previous study. We operated a single scaled-up cell instead of four cells, so that scaling up could be studied without the effect of cell reversal. In this setup, the MFC was operated during 37 days, and performance was analyzed by development of current and power production with time and by polarization curves.

## 7.2 Materials and methods

### 7.2.1 Reactor configuration

The scaled-up MFC was previously described in Dekker et al. (2009). The two electrodes were made of two layers of titanium mesh coated with platinum and iridium (330 mm × 1500 mm) on a flat plate, resulting in a projected surface area of 0.5 m<sup>2</sup>. The Pt-Ir coating was used to reduce the internal resistance and overpotentials of the cell (Dekker et al., 2009). Ferric iron was used as electron acceptor at the cathode, combined with biological ferrous iron oxidation (Ter Heijne et al., 2007) to regenerate the ferric iron. In order to maintain the low catholyte pH required to keep ferric iron soluble, a bipolar membrane (Fumasep FBM, Fumatech, Germany) was used to separate anolyte and catholyte.

The thickness of the anode and cathode compartment was 5 mm, which led to a total cell volume of 5 L and a volumetric surface area of 100 m<sup>2</sup>/m<sup>3</sup>. The flow in both anode and cathode side was directed from three inlets on the bottom to three outlets on the top. This was done to improve the flow characteristics compared to previous study, where an S shape flow path from the inlet at the bottom to the outlet at the top was used (Dekker et al., 2009). Both anode and cathode compartment contained Ag/AgCl reference electrodes connected to the top of the cell (PreSense QiS, Oosterhout, the Netherlands). The potential of these reference electrodes were regularly checked versus an SCE reference electrode (+0.241 V vs NHE). The potentials of anodes and cathodes were converted and expressed vs. SCE throughout.

### 7.2.2 Start-up and operation

Sludge from an anaerobic digester was used to inoculate the anode. Acetate was used as a carbon and energy source in a nutrient solution containing 10 mM macro-nutrients, 1 mM micro-nutrients, 1 mM vitamins and 20 mM phosphate buffer as previously described (Dekker et al. 2009). Acetate concentration in the medium was calculated from the produced current, and the resulting minimum acetate concentration in the MFC was 20 mM so that no acetate depletion would occur. This synthetic medium was continuously fed into the anode recirculation vessel with a feeding rate of 54 mL/h. The system was operated at 30 °C in a constant temperature chamber.

Both anolyte and catholyte were recirculated at a flow rate of 70 L/h. The anode recirculation vessel had a volume of 1 L, whereas the cathode recirculation vessel had a volume of 30 L. The anolyte was controlled at pH 7 with 3 M KOH, and the catholyte was controlled at pH 1.6 with 1.8 M H<sub>2</sub>SO<sub>4</sub>. The catholyte consisted of ferric iron sulfate solution (1 g/L), and was inoculated with biomass support particles (BSPs) containing ferrous iron oxidizing

bacteria. Before inoculation, these iron oxidizers were grown from Rio Tinto sludge following the procedure described in (Ter Heijne et al., 2007): the biomass support particles were placed in a  $\text{Fe}^{2+}$  containing medium (3.3 g/L  $\text{Fe}^{2+}$ ), and incubated on a rotary shaker at 175 RPM. After several replacements of the medium, the BSPs were placed in the recirculation vessel of the cathode. The standard nutrients for the iron oxidizers (0.4 g/L  $(\text{NH}_4)_2\text{SO}_4$ , 0.4 g/L  $\text{KH}_2\text{PO}_4$  and 0.4 g/L  $\text{MgSO}_4$ ) were supplied to the cathode compartment only at the beginning of the experiment. Air was continuously sparged in the cathode recirculation vessel through four porous Teflon cylinders.

The strategy for MFC operation was the following. The first 7 days were used for start-up, until anode potential became stable at a value of -0.47 V vs SCE. During these 7 days, the external resistance was decreased from 50  $\Omega$  to 2  $\Omega$  in several steps. From day 7 on, the cell voltage of the MFC was potentiostatically controlled in a 2-electrode setup using a HP 96-20 potentiostat (Bank Elektronik – Intelligent Controls GmbH, Pohlheim, Germany). The operating mode was changed from using an external resistance (load) to potentiostatic control to enable an increase in current density. At this point, the load was 2  $\Omega$ . In scaled-up systems, a low external resistance is needed to produce considerable current and power, because of the large size of the electrode: an increase in electrode size results in a decrease in internal resistance of the electrode. At a certain point however, the external resistance cannot be further decreased without creating large inaccuracies in determining the current. These inaccuracies are caused by the fact that the resistance of the electrodes, wires, and contacts together is unknown and can reach several tenths of ohms or even reach several ohms. The actual resistance is then the sum of the external resistance and the resistances of electrode, wires, and contacts. Thus, the actual resistance is higher than the value of the external resistance alone. When the measured cell voltage is converted into current by using the value of the load, the current density is thus largely overestimated. To enable accurate estimation of the current and to enable further improvement of MFC performance, the control strategy was thus changed from operation with an external resistance to potentiostatic control.

From day 7-12, the current density was increased by decreasing the controlled cell voltage from 0.575 V to 0.47 V. From day 12-37, MFC performance was further improved by increasing the iron concentration in the catholyte in 5 steps from 1 g/L to measured concentrations of 2 g/L, 3 g/L, 5 g/L, 5.5 g/L, and 6 g/L. This was done at constant controlled cell voltage of 0.475 V until day 28, where cell voltage was decreased to 0.45 V until the end of the experiment.

### 7.2.3 Measurements and analyses

During the experiment, cell voltage, electrode potentials, and the voltage across the membrane (potential difference between the reference electrodes) were collected every 60 seconds via a Fieldpoint data acquisition system, connected to a PC. Current density and power density were normalized to the projected surface area of 0.5 m<sup>2</sup> or to the total cell volume of 5 L.

Anolyte and catholyte were sampled every two or three days and analyzed for their iron concentration. The ratio of ferrous and ferric iron was measured using Dr. Lange test LCK 320 (Hach Lange GmbH, Düsseldorf, Germany).

Acetate concentrations were measured with gas chromatography as described in (Ter Heijne et al., 2008)

Polarization curves were recorded using dc-voltammetry with the HP 96-20 potentiostat. For this, cell voltage was decreased stepwise from open circuit voltage down to 0 V in steps of 0.025 to 0.1 V. At each voltage, current was stabilized for at least 10 minutes.

The volumetric resistance was calculated from the anode and cathode overpotentials (V) divided by the current density (A/m<sup>2</sup>). Anode overpotential was calculated as the measured anode potential minus the thermodynamic anode potential of -0.535 V vs SCE (at 20 mM acetate, 50 mM bicarbonate, pH=7). Cathode overpotential was calculated as the thermodynamic cathode potential of +0.581 V vs SCE (at Fe<sup>3+</sup>/Fe<sup>2+</sup>=90%) minus the measured cathode potential. Resistances were expressed in  $\Omega\text{m}^2$ , and can be converted into volumetric resistance ( $\Omega\text{m}^3$ ) by dividing by the specific surface area of 100 m<sup>2</sup>/m<sup>3</sup>.

## 7

## 7.3 Results and discussion

### 7.3.1 MFC performance in time

The performance of the scaled-up MFC during the 37 days of operation is shown in Figure 1. Figure 1A shows the cell voltage, potentials of anode and cathode, and the membrane potential as a function of time. Figure 1B shows the related development in current density and power density. Anode potential became stable at -0.47 V vs SCE after 7 days. At this point, current density was 0.36 A/m<sup>2</sup>. During the rest of the experiment, the bio-anode was able to maintain a low and stable anode potential around -0.5 V vs SCE. This anode potential stayed stable, while current density continuously increased, which means that the performance of the bio-anode improved with time.

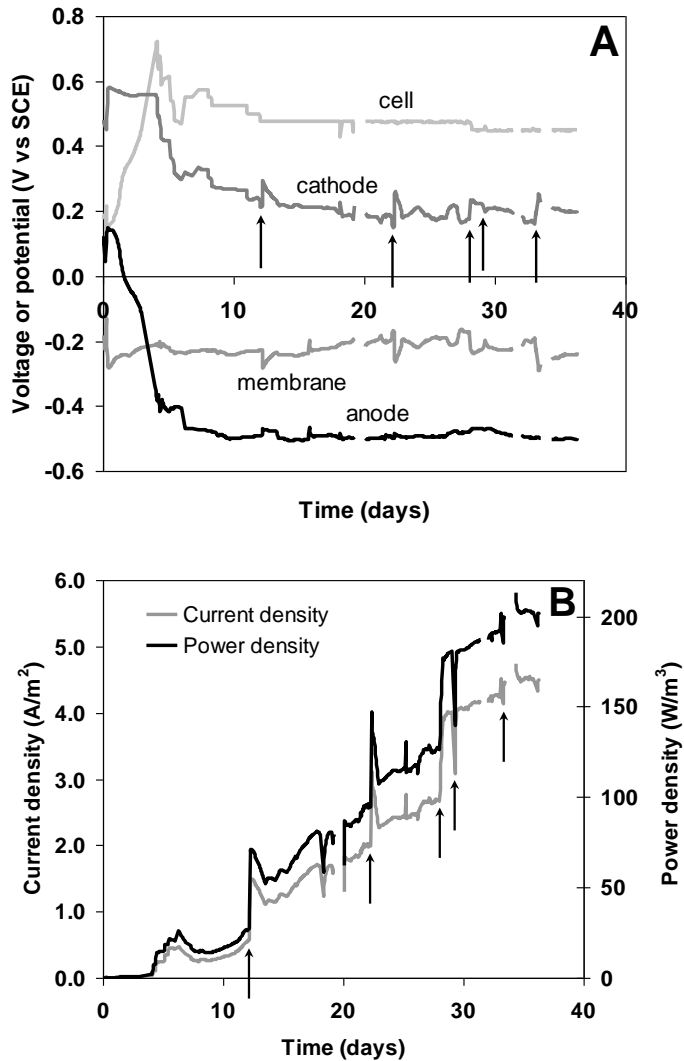


**Figure 1.** Performance of the MFC using acetate as electron donor and ferric iron ( $\text{Fe}^{3+}$ ) was reduced at the cathode. Anode and cathode were separated by a bipolar membrane. Anolyte pH was 7, while catholyte pH was 1.6. The MFC was operated for 37 days, and its performance is shown in terms of cell voltage, cathode potential, anode potential, and voltage across the membrane (A), and in terms of current and power density (B). Additions of iron to the catholyte are indicated with arrows.

Not only the bio-anode performance improved, also the cathode performance improved in time. During the whole experiment, we observed an increase in current and power density, while additional sudden increases in current density were found when the iron concentration was increased, as indicated by arrows in Figure 1. This jump in current density after each addition of iron, means that the iron concentration was one of the factors limiting MFC performance. The continuous increase in current density in time is probably a combined effect of the growth and development of the bio-anode with time, higher iron concentrations, and increased activity of the iron oxidizers with time, resulting in more available  $\text{Fe}^{3+}$ , which is favorable for the reduction reaction. While the first three additions of iron were done in the form of  $\text{Fe}^{3+}$ , the last two additions of iron were done in the form of  $\text{Fe}^{2+}$  (sulphate). Whereas addition of  $\text{Fe}^{3+}$  resulted in a positive peak in current density, the addition of  $\text{Fe}^{2+}$  resulted first in a decrease in current density, but as soon as the iron oxidizers had oxidized the added  $\text{Fe}^{2+}$  into  $\text{Fe}^{3+}$ , current density started increasing. The voltage across the membrane stayed constant throughout the experiment, although current density increased. This is in accordance with previous findings (Ter Heijne et al., 2006) and can be explained by the fact that the voltage loss over the bipolar membrane is a function of the pH difference between both compartments, and this pH difference was constant throughout the experiment.

During the last 5 days of the experiment, at an iron concentration of 6 g/L, the maximum power density of 2.0 W/m<sup>2</sup> was found, corresponding with 200 W/m<sup>3</sup>, at a current density of 4.2 A/m<sup>2</sup>, while cell voltage was controlled at 0.475 V.

### 7.3.2 Polarization curves

The increasing performance of the scaled-up MFC with time is also reflected in the polarization curves, which were recorded on day 18, 29, and 34 (Figure 2A and B). On day 18, the iron concentration in the catholyte was 1.7 g/L. The maximum power density was 40 W/m<sup>3</sup> at a current density of 1.3 A/m<sup>2</sup>. On day 29, after the third increase in iron concentration, the maximum power density in the polarization test reached 157 W/m<sup>3</sup> at a current density of 2.1 A/m<sup>2</sup> and an iron concentration was 5.2 g/L. On day 34, the iron concentration was 5.7 g/L, and this resulted in a maximum power density of 185 W/m<sup>3</sup> at a current density of 4.6 A/m<sup>2</sup>. Whereas the anode overpotential was stable with increasing current density, reflecting the ability of the bio-anode to adapt to higher current densities without additional energy losses, both the cathode and the membrane showed considerable overpotentials. With time, performance of the cathode improved as a result of the higher  $\text{Fe}^{3+}$  concentration.

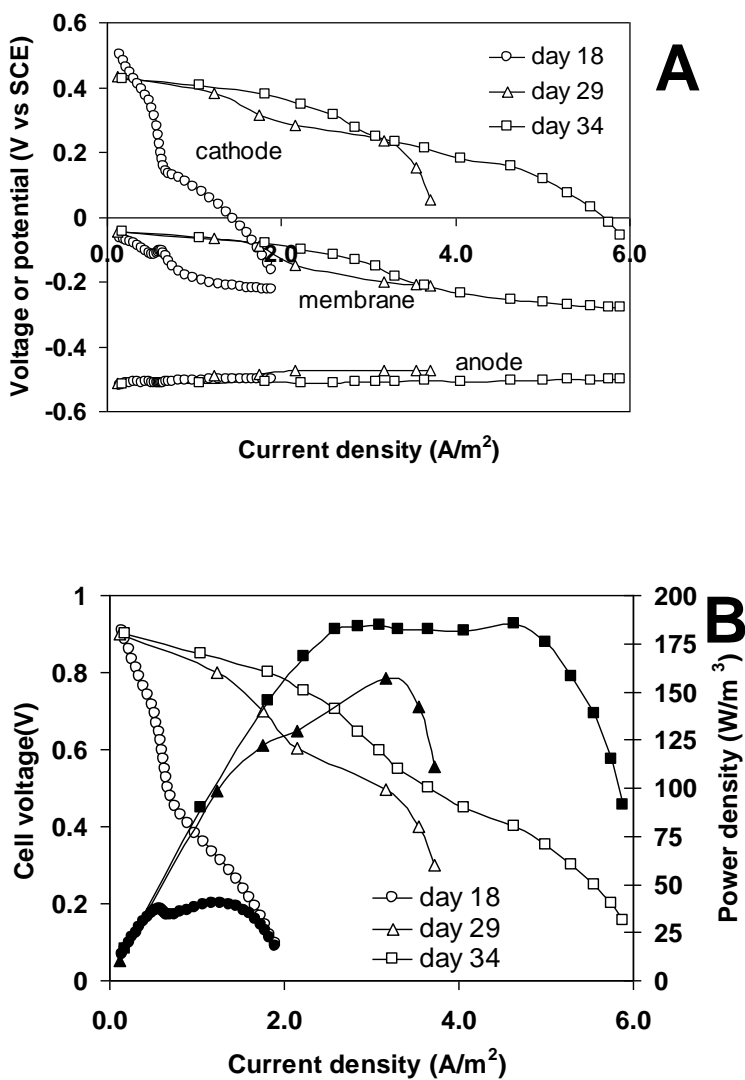


**Figure 2.** Polarization curves of scaled-up MFC with time, for anode, cathode, and membrane (A) and cell voltage (open symbols) and power density (closed symbols) (B).

The maximum power density in the polarization curves was lower than the power produced during stable operation. This seems to be caused by the time chosen for each step of the polarization curve. We used a time of 10 minutes for each potential step. This was not enough for the current to stabilize, as cell voltage and current density still gradually increased after 10

minutes. Therefore, MFC performance was underestimated in the polarization curve. This may be a result of the large electrodes used in this study compared to other studies, that may need longer time to reach equilibrium. In smaller systems, on the other hand, usually performance is overestimated when recording polarization curves (Menicucci et al., 2006; Ter Heijne et al., 2008). Still, polarization curves provide essential information on the response of electrode potentials and cell voltage to a change in current density. For characterization of MFCs, it is therefore important to combine results of long-term operation with polarization curves.

### 7.3.3 Iron concentration decreased with time

The iron concentrations in the catholyte are shown in Figure 3. Overall, most iron was in the form of  $\text{Fe}^{3+}$ , and thus the biological ferrous iron oxidation rate was high enough to sustain the produced current. In the first half of the experiment, the ratio  $\text{Fe}^{3+}/\text{Fe}^{2+}$  was always  $>90\%$ , while the ratio slightly decreased in the second half of the experiment, with ratios between  $80\%$  and  $90\%$ . The lower ratio  $\text{Fe}^{3+}/\text{Fe}^{2+}$  during the second half of the experiments may be caused by (i) the higher current density, for which a higher oxidation rate of  $\text{Fe}^{2+}$  is needed, and this may lead to limitations in oxygen transfer,

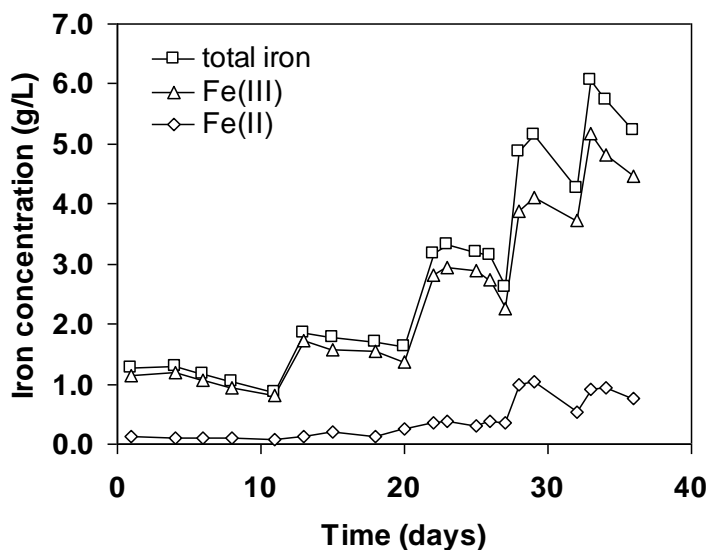


**Figure 3.** Iron concentration in the catholyte, at pH=1.6. The ratio  $\text{Fe}^{3+}/\text{Fe}^{2+}$  was always  $>80\%$ , showing enough capacity of the iron oxidizing microorganisms.

or (ii) limited activity of the iron oxidizers as a result of higher  $\text{Fe}^{2+}$  concentrations, which can have an inhibitory effect on growth and oxidizing capacity at concentrations in the range of 2 to 5.6 g/L (Nemati, 1998).

After each addition of iron, the iron concentration did not stay constant but decreased with time. It is unlikely that iron diffused through the membrane to the anolyte, as samples of the anolyte showed no iron, as also observed in previous study (Ter Heijne et al., 2007). Precipitation of iron seems the most reasonable explanation for the decrease in iron concentration, as it was observed on the cathode when disassembling the MFC. Inspection of these precipitates under the microscope showed that they consisted of yellow/orange rod-shaped microorganisms in combination with salt structures. These yellow precipitates were probably a combination of the iron oxidizers with iron salts. The risk of iron precipitation is an important point of attention for further development of scaled-up systems using  $\text{Fe}^{3+}$ .

### 7.3.4 Analysis of internal resistances

When looking at the performance of the MFC during the operation time in Figure 1A, on first sight it seems that no considerable changes occur; all potentials are more or less constant and the highest peaks correspond with a potential change of about 0.1 V. Only when combining the potentials in Figure 1A with the current density in Figure 1B, it can be seen that big changes occur with time. The reason that this change is not seen in Figure 1A is partly a result of the potentiostatic operation mode, where the cell voltage is kept constant. In this way, there is not much room for the potentials to change; instead, current density changes. To visualize the changes in performance, it is useful to express the energy losses in the system in terms of their internal resistances or resistance (in  $\Omega\text{m}^2$  or  $\Omega\text{m}^3$ ). This resistance is calculated as the overpotential (difference between theoretical potential and measured potential) divided by current density. In this way, the effect of current density is taken into account, and it makes comparison with other systems with different electrode sizes possible (Clauwaert et al., 2008; Sleutels et al., 2009).

The three parts of the MFC where we measured the energy losses were anode, cathode, and membrane. The resistance for anode and cathode at each iron concentration was averaged during the most stable 24 hours (Figure 4).

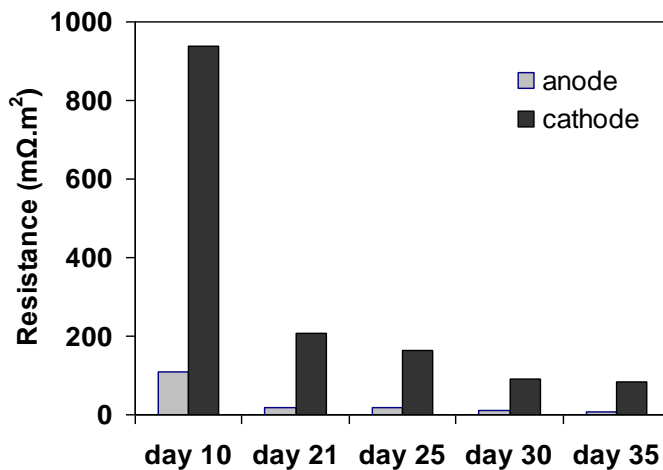


**Figure 4.** Resistance of anode and cathode throughout the operation period. Total resistance decreased a factor 10, while cathode resistance was considerably higher than anode resistance.

As the voltage loss over the membrane was independent of current density, its resistance is not shown. Anode resistance decreased from 109 to 7 mΩ.m<sup>2</sup> in the course of the experiment, reflecting the increase in activity of the electro-active biofilm. Cathode resistance decreased from 939 to 85 mΩ.m<sup>2</sup> as a result of the increase in Fe<sup>3+</sup> concentration. So, both anode and cathode resistance decreased almost a factor 10 within the operating period, resulting in the increase in MFC performance with time. Total cell resistance (anode, cathode, and membrane) decreased from 1,756 mΩ.m<sup>2</sup> in the beginning of the experiment to 146 mΩ.m<sup>2</sup> in the final stage of the experiment. At maximum performance, the cathode contributed to 58% of the total resistance, which shows that the cathode was still the main factor limiting MFC performance. At the same time, the membrane contributed to 37% of the total internal resistance.

### 7.3.5 Outlook

The obtained power density of 200 W/m<sup>3</sup> (2.0 W/m<sup>2</sup>) is a next achievement in scaling-up MFCs. It is a factor 1.4 higher than the 140 W/m<sup>3</sup> previously obtained in the same scaled-up MFC (Dekker et al., 2009), and illustrates again that it is possible to reach power densities similar to those obtained in lab experiments. While the anode had a low resistance of 7.5 mΩ.m<sup>2</sup> (0.075 mΩ.m<sup>3</sup>), the cathode resistance was 84 mΩ.m<sup>2</sup> (0.84 mΩ.m<sup>3</sup>) and made up 58% of the total resistance caused by anode, cathode and membrane together. The replacement of

oxygen reduction by ferric iron reduction resulted in a decrease in cathode resistance from (on average)  $1.3 \text{ m}\Omega\cdot\text{m}^3$  (Dekker et al., 2009) to  $0.85 \text{ m}\Omega\cdot\text{m}^3$ . This demonstrates the superior performance of ferric iron reduction compared to oxygen reduction, even when oxygen reduction takes place on a Pt-coated electrode at pH 4, with pure oxygen.

An important parameter to consider besides power density, and resistances, is the energy efficiency. The energy efficiency reflects which part of the energy in the carbon source is converted into electrical energy, and is the product of Coulombic efficiency and voltage efficiency. The Coulombic efficiency was determined between day 20 and 30 and was found to be 65%. The theoretical maximum cell voltage of acetate oxidation in combination with iron reduction, assuming that 90% of the iron is present in the form of  $\text{Fe}^{3+}$ , is 1.12 V. The applied cell voltage of 0.475 V then results in a voltage efficiency of 43%. This combination of coulombic efficiency and voltage efficiency results in an energy efficiency of 28%. In the polarization curve on day 34, voltage efficiency was considerably higher. This polarization curve (Figure 2B) showed a maximum power density of  $180 \text{ W}/\text{m}^3$ , at a current density of  $2.6 \text{ A}/\text{m}^2$ . At this point, the cell voltage was 0.7 V, resulting in a voltage efficiency of 63%. Combined with a coulombic efficiency of 65%, this results in an energy efficiency of 41%.

In terms of power production and energy efficiency, it is interesting to compare the MFC with anaerobic digestion, the only other technology in which similar wet organic waste streams are converted into electricity. For comparison, we assume that all COD in the anaerobic digester is present in the form of acetate. The energy content of the acetate can be calculated similarly to the MFC: with oxygen as the final electron acceptor (in combustion), the Gibb's free energy is  $-844 \text{ kJ}/\text{mol}$ . The energy content of the formed  $\text{CH}_4$  can then be calculated from the reaction  $\text{CH}_4 + 2 \text{ O}_2 \rightarrow \text{CO}_2 + 2 \text{ H}_2\text{O}$ , and is  $-810 \text{ kJ}/\text{mol}$ . This means, that of the energy in acetate,  $34 \text{ kJ}/\text{mol}$  is lost in the conversion to  $\text{CH}_4$ . This corresponds with an energy loss of roughly 5%. Furthermore, if we assume that 5% of the energy in acetate is incorporated in biomass (Van Lier et al., 2008), so that the efficiency of conversion of acetate into methane is 90%, and an average combustion efficiency of  $\text{CH}_4$  of 33% (Weiland et al., 2006), we find an overall energy efficiency of acetate into electricity of 30%. The power that can be produced in the anaerobic digestion, based on a conversion rate of  $25 \text{ kg COD}/\text{m}^3\text{d}$ , a lower heating value of  $50.1 \text{ MJ}/\text{kg CH}_4$ , and an overall energy efficiency of 30%, is  $1,087 \text{ W}/\text{m}^3$ . So, while the performance of this scaled-up MFC in terms of power production is still a factor 5 away from anaerobic digestion, its energy efficiency is already comparable or higher. When comparing MFCs with anaerobic digestion with respect to power production, it should be noted, that the conversion rate in the MFC at a current density of  $4.2 \text{ A}/\text{m}^2$  was only  $3 \text{ kg COD}/\text{m}^3\text{d}$ , while the power produced in the anaerobic digester was based on a conversion rate of  $25 \text{ kg}$

COD/m<sup>3</sup>d. While in anaerobic digesters an increase in conversion rate results in an increase in power, this does not hold for MFCs, in which the balance between voltage and current determines at which conversion rate maximum power is reached.

Which issues need to be further addressed to bring application of MFCs closer?

First of all, there is need for a well-functioning cathode if MFC performance is to be further improved. This study again showed that the cathode resistance was considerably higher than the anode resistance, and until today, the limit of the bio-anode has not been reached. For this to happen, we need a strong cathode that can accept the electrons from the anode at a similar rate, or we need to increase the cathode surface area several times compared to the anode surface area. We showed that reduction of ferric iron resulted in superior performance compared to oxygen reduction. The scaled-up MFC with ferric iron reduction was operated during 37 days with continuous increase in performance. A further increase in iron concentration may result in higher cathode potential and improved MFC performance. On the other hand, higher iron concentrations may inhibit the iron oxidizers. Another limitation to ferric iron reduction may be the risk of precipitation. These issues need to be further studied and addressed. Besides the use of iron as electron acceptor, several other routes are possible to improve the cathode, for example the application of oxygen reducing biocathodes (Clauwaert et al., 2006; Freguia et al., 2009; Ter Heijne et al., 2010). Testing these alternatives in a scaled-up system will show their feasibility for practical application.

Secondly, this study aimed at characterization and improvement of a single cell, whereas as part of scaling-up, also stacking is an important point of attention to achieve high voltages. Still little research has been done on stacking. When stacking cells in series, cell reversal, which happens when one cell is not strong enough to maintain the current produced by the other cells, has been shown to be a major bottleneck (Dekker et al., 2009; Oh and Logan, 2007). Ways to overcome cell reversal need to be further studied, for example by analyzing flow characteristics and by testing strategies to keep an MFC running when cell reversal occurs.

Thirdly, it is important that these phenomena are studied in scaled-up systems, as these may reveal other limiting factors not encountered in lab-scale systems. These scaled-up MFCs should further demonstrate the applicability of MFCs in practice.

Finally, new challenges arise when using real wastewater as the substrate instead of acetate. These new challenges are related to the presence of particulate matter, hydrolysis of more complex substrates than acetate, fluctuating concentrations of organics, and the need for sufficient buffer capacity to reach the desired activity at the bio-anode.

## 7.4 Conclusions

In this continued study on scaling-up MFCs, the cathode reaction was improved by replacing oxygen reduction with ferric iron reduction. This resulted in a maximum power density of 200 W/m<sup>3</sup> at a current density of 4.5 A/m<sup>2</sup>. Analysis of anode and cathode resistances revealed that MFC performance increased as a result of development of the electroactive biofilm on the anode, and increase in Fe<sup>3+</sup> concentration in the cathode.

## 7.5 References

- Clauwaert, P.; Van Der Ha, D.; Boon, N.; Verbeken, K.; Verhaege, M.; Rabaey, K.; Verstraete, W. 2007. Open air biocathode enables effective electricity generation with microbial fuel cells. *Environ. Sci. Technol.* 41, 7564-7569.
- Clauwaert, P.; Aelterman, P.; Pham, T. H.; De Schampelaire, L.; Carballa, M.; Rabaey, K.; Verstraete, W. 2008. Minimizing losses in bio-electrochemical systems: The road to applications. *Appl. Microbiol. Biotechnol.* 79, 901-913.
- Dekker, A.; Ter Heijne, A.; Saakes, M.; Hamelers, H.V.M.; Buisman, C.J.N. 2009. Analysis and improvement of a scaled-up and stacked Microbial Fuel Cell. *Environ. Sci. Technol.* 43, 9038-9042.
- Freguia, S.; Rabaey, K.; Yuan, Z.; Keller, J. 2008. Sequential anode-cathode configuration improves cathodic oxygen reduction and effluent quality of microbial fuel cells. *Water Res.* 42, 1387-1396.
- Hamelers, H. V. M.; Ter Heijne, A.; Sleutels, T. H. J. A.; Jeremiasse, A. W.; Strik, D. P. B. T. B.; Buisman, C. J. N. 2010. New applications and performance of bioelectrochemical systems. *Appl. Microbiol. Biotechnol.* 85, 1673-1685.
- Logan, B. E.; Hamelers, B.; Rozendal, R.; Schröder, U.; Keller, J.; Freguia, S.; Aelterman, P.; Verstraete, W.; Rabaey, K. 2006. Microbial fuel cells: Methodology and technology. *Environ. Sci. Technol.* 40, 5181-5192.
- Menicucci, J.; Beyenal, H.; Marsili, E.; Veluchamy, R. A.; Demir, G.; Lewandowski, Z. 2006. Procedure for determining maximum sustainable power generated by microbial fuel cells. *Environ. Sci. Technol.* 40, 1062-1068.
- Nemati, M.; Harrison, S. T. L.; Hansford, G. S.; Webb, C. 1998. Biological oxidation of ferrous sulphate by thiobacillus ferrooxidans: A review on the kinetic aspects. *Biochem. Eng. J.* 1, 171-190.
- Oh, S.E.; Logan, B. E. 2007. Voltage reversal during microbial fuel cell stack operation. *J. Power Sources.* 167, 11-17.
- Rozendal, R. A.; Hamelers, H. V. M.; Rabaey, K.; Keller, J.; Buisman, C. J. N. 2008. Towards practical implementation of bioelectrochemical wastewater treatment. *Trends Biotechnol.* 26, 450-459.
- Ter Heijne, A.; Hamelers, H.V.M.; de Wilde, V.; Rozendal, R.A.; Buisman, C.J.N. 2006. A bipolar membrane combined with ferric iron reduction as an efficient cathode system in microbial fuel cells. *Environ. Sci. Technol.* 40, 5200-5205.

- Ter Heijne, A.; Hamelers, H. V. M.; Buisman, C. J. N. 2007. Microbial fuel cell operation with continuous biological ferrous iron oxidation of the catholyte. *Environ. Sci. Technol.* 41, 4130-4134.
- Ter Heijne, A.; Hamelers, H. V. M.; Saakes, M.; Buisman, C. J. N. 2008. Performance of non-porous graphite and titanium-based anodes in microbial fuel cells. *Electrochim. Acta* 53, 5697-5703.
- Ter Heijne, A.; Strik, D.P.B.T.B.; Hamelers, H.V.M.; Buisman, C.J.N. 2010. Cathode potential and mass transfer determine performance of oxygen reducing biocathodes in microbial fuel cells. *Environ. Sci. Technol.* In press.
- Sleutels, T. H. J. A.; Hamelers, H. V. M.; Rozendal, R. A.; Buisman, C. J. N. 2009. Ion transport resistance in microbial electrolysis cells with anion and cation exchange membranes. *Int. J. Hydrogen Energy.* 34, 3612-3620.
- Van Lier, J.B.; Mahmoud, N.; Zeeman, G. 2008. Anaerobic wastewater treatment, in: Heenze, M.; van Loosdrecht, M.C.M.; Ekama, G.A.; Brdjanovic, D. (Eds). *Biological wastewater treatment: principles, modeling and design.* IWA Publishing, London, pp. 415-456.
- Weiland, P. 2006. Biomass digestion in agriculture: A successful pathway for the energy production and waste treatment in Germany. *Eng. Life Sci.* 6, 302-309.

## Chapter 8

# General discussion and outlook

Chapter 8.2.1 and 8.2.2 are partly based on:

Hamelers, H. V. M.; Ter Heijne, A.; Sleutels, T. H. J. A.; Jeremiasse, A. W.; Strik, D. P. B. T. B.; Buisman, C. J. N. 2010. New applications and performance of bioelectrochemical systems. *Appl. Microbiol. Biotechnol.* 85, 1673-1685.

## 8.1 Introduction

This chapter will give an overview of the status of Microbial Fuel Cells (MFCs) and addresses the main limitations in MFC performance. As basis for the discussion, we will first summarize the findings of this thesis.

We started with investigation of the bioanode (Chapter 2). It was shown that bioanodes could produce considerable current densities up to 4.6 A/m<sup>2</sup>. This maximum current density was limited by bioanode activity. Then, several routes were followed to improve cathode performance.

First, a cathode where oxygen reduction was replaced by reduction of ferric iron (Fe<sup>3+</sup>) was tested (Chapter 3 and 4). This resulted in improved cathode performance and in higher MFC performance compared to uncatalyzed oxygen reduction at graphite. The bipolar membrane however, led to new limitations related to water splitting efficiency and energy losses.

Secondly, microorganisms were used as the catalyst for oxygen at the cathode (Chapter 5). This showed to be another successful approach for improving cathode performance compared to uncatalyzed oxygen reduction. In this case, it was shown that limitations arose as a result of both charge transfer and mass transfer of oxygen.

Thirdly, replacing oxygen reduction with reduction of Cu<sup>2+</sup> (Chapter 6) at pH=3 and with the use of a bipolar membrane, resulted in recovery of pure metallic copper while simultaneously, power was produced comparable to the power produced in other well-performing MFCs with catalyzed oxygen reduction. Here, cathode and MFC performance decreased in time as a result of depletion of Cu<sup>2+</sup>.

Finally, a scaled-up MFC was tested with a bipolar membrane and ferric iron reduction (Chapter 7). This scaled-up MFC produced 200 W/m<sup>2</sup> and showed that power densities in scaled-up systems can be similar to lab-scale systems. Still, the cathode was the most important factor limiting MFC performance.

In this final chapter, we will discuss the limitations that were encountered in this thesis. The maximum power production that is feasible in MFCs is estimated. Power density in combination with energy efficiency is used to compare MFCs to anaerobic digestion to discuss the future for MFCs for production of electricity from biomass.

## 8.2 Power production in MFCs

In the early stage of development of MFCs, just after the first mediator-less MFC was reported by Kim et al. (2002), power densities between 1 and 10 mW/m<sup>2</sup> were reported (Logan, 2009). Power density in MFCs has increased several orders of magnitude during the following years of research (Figure 1) and has reached values above 1 W/m<sup>2</sup> in 2005. This increase in power density resulted from improvements in system architecture and from improved understanding of how to extract power using bacteria more effectively (Logan, 2009). Whereas in the first years of MFC research, power density increased almost an order of magnitude per year, from 2005 on, the maximum power density reported in literature increased at lower pace. The highest power density reported until now, which is not included in Figure 1, is 6.86 W/m<sup>2</sup> (Fan et al., 2008). The reason that this value is not included in Figure 1, is that this power density was normalized to the anode surface area, and was reached with a cathode area 14 times larger than the anode surface area to overcome cathode limitations. When normalized to the cathode surface area, this power density would be only 0.49 W/m<sup>2</sup>. For comparison, the results of this thesis are included in the figure, as indicated by the filled circles.

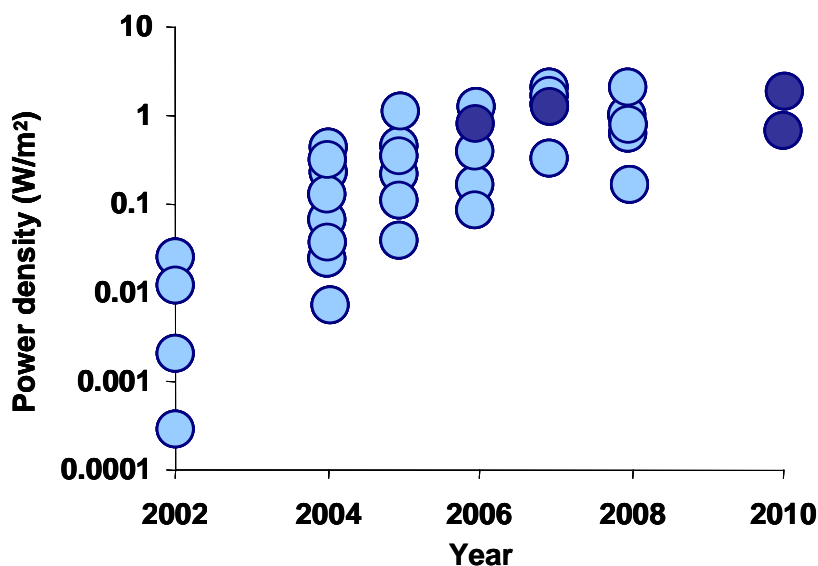


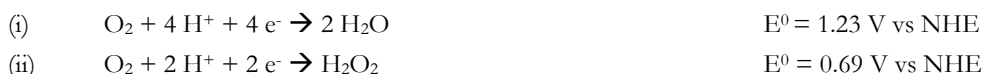
**Figure 1.** Development of power density in MFCs (based on Logan, 2009). Since 2005, the maximum power density achieved in MFCs has not increased considerably. The filled circles represent the results obtained in this thesis.

The question is if the power density in MFCs has already reached its limit, or if further reduction of energy losses will result in a further increase in power density. To discuss this, the limiting factors that have arisen in this thesis, being the cathode, bipolar membrane, mass transfer, and scaling up, will be addressed in the following paragraphs.

### 8.2.1 Energy losses for oxygen reduction at the cathode of MFCs

The oxygen reduction reaction is the most commonly used cathodic reaction in MFCs. Oxygen is an attractive oxidant because of its availability, its thermodynamic high redox potential of +0.805 V vs NHE at actual MFC conditions, and because the cathodic reaction product is pure water. The oxygen reduction reaction can follow two overall pathways: (i) the direct 4-electron pathway in which oxygen is reduced to water or hydroxide, and (ii) the peroxide pathway (Yeager, 1984).

The oxygen reduction reactions via the two pathways are:



Note that in both cases, the oxygen reduction rate and the potential at which oxygen is reduced is strongly dependent on the solution pH. This is important, because in MFCs, the catholyte pH generally increases in time as a result of cation transport through the cation exchange membrane (Rozendal et al., 2006).

In practice, the reduction of oxygen in MFCs turns out to be slow (irreversible) and to occur at much lower potentials than the thermodynamic potential, because a large part of the energy at the cathode is lost to drive the oxygen reduction at the desired rate. Open circuit potentials for uncatalyzed carbon materials are typically around 0 V vs Ag/AgCl (Logan et al., 2006). This potential is close to the theoretical potential for hydrogen peroxide instead of oxygen reduction to water. Because carbon materials are good catalysts for the reduction of oxygen to hydrogen peroxide (Rozendal et al., 2009), hydrogen peroxide may be produced as a product of oxygen reduction, instead of water. Because the electrode potential for reduction of oxygen to hydrogen peroxide is lower than for reduction of oxygen to water, the formation of hydrogen peroxide results in lower power densities and should thus be avoided when aiming at improving MFC performance.

To improve the reaction rate for oxygen reduction, many studies have been devoted to the development of metal- and non-metal catalysts to reduce overpotentials for oxygen reduction. Because Pt is an expensive catalyst, metal catalysts other than platinum have been examined, for example Fe(II) and Co-based catalysts (Lefebvre et al., 2009; Yu et al., 2009), and a possible catalytic action of copper for oxygen reduction was found (Ter Heijne et al., 2010).

Recently, increased attention is paid to the development of biological catalysts for the reduction of oxygen to water at the cathode. The advantages of biological catalysts are their ability to regenerate and their activity at ambient temperatures. These biocathodes can either operate indirectly via a mediating compound, or direct. Examples of indirect biocathodes are (i) the use of *A. ferrooxidans*, which oxidizes  $\text{Fe}^{2+}$  to  $\text{Fe}^{3+}$  while reducing oxygen. The formed  $\text{Fe}^{3+}$  is reduced at the (non-catalyzed) cathode at higher rate than oxygen (Ter Heijne et al., 2007), and (ii) the reduction of  $\text{MnO}_2$  to  $\text{Mn}^{2+}$  at the electrode, with simultaneous oxidation of  $\text{Mn}^{2+}$  to  $\text{MnO}_2$  by manganese oxidizing bacteria (Rhoads et al., 2005). Direct biocathodes can be based on enzymes (Topcagic and Minteer, 2006; Schaetzle et al., 2009) or contain microorganisms that are attached to the cathode and that accept electrons from the electrode while reducing oxygen. This last type of biocathodes has been studied in salt water as well as in freshwater (Bergel et al., 2005; Clauwaert et al., 2007). Although (bio-)catalyzed cathodes have been shown to catalyze oxygen reduction compared to the plain material, the open circuit potentials are still low: in the range of +0.2-0.3 V vs Ag/AgCl or sometimes higher: +0.42 V vs Ag/AgCl (Clauwaert et al., 2007). A detailed overview of open circuit cathode potentials for different cathode catalysts are reported in literature is given in Table 1. Open circuit cathode potentials range from -0.05 to +0.75 V vs Ag/AgCl. While open circuit potentials can be compared to the thermodynamic potential, the cathode potential decreases (i.e. cathode overpotential increases) when a current is flowing. The increase in overpotential with changing current density provides information on the performance of the cathode.

To be able to compare different systems, it is important to analyze cathode overpotential in combination with current density. The cathode overpotential divided by current density results in cathode resistance ( $\Omega\text{m}^2$ ) (Sleutels et al., 2009a). An overview of cathode resistances reported in literature is shown in Table 1. In this table, the cathode resistance was determined from the slope of the polarization curves. It can be seen that internal resistances of this small selection of cathodes vary between 22 and 630  $\text{m}\Omega\text{m}^2$ . For comparison, if a cathode energy loss of 10% of the maximum cell voltage would be acceptable (0.11 V) at a current density of 20  $\text{A}/\text{m}^2$ , the maximum cathode resistance should be as low as 5.5  $\text{m}\Omega\text{m}^2$ .

Table 1 furthermore shows, that in many studies, the cathode contributes considerably to the total internal resistance. It must be noted, that many studies that aim at improving the cathode do not report cathode potential vs current density. This makes elaborate comparison of cathode performance difficult.

**Table 1.** Performance of MFCs and cathodes reported in literature. Performance was analyzed in terms of current and power density, open circuit cathode potential, cathode resistance, and cell resistance. Power density and current density was normalized to the membrane surface area. Resistances were calculated from the slope of the polarization curve.

<i>Cathode material and catalyst</i>	<i>Open circuit cathode potential (V vs Ag/AgCl)</i>	<i>Cathode resistance (mΩ.m<sup>2</sup>)</i>	<i>Cell resistance (mΩ.m<sup>2</sup>)</i>	<i>Contribution of cathode to internal resistance (%)</i>	<i>Maximum power density (W/m<sup>2</sup>)</i>	<i>Current density at Pmax (A/m<sup>2</sup>)</i>	<i>Reference</i>
Cu <sup>2+</sup> and oxygen on graphite, pH=3	0.18	37	105	35	0.8	3.2	Ter Heijne et al., 2010a
Graphite with biocathode	0.38	481	n.a.	n.a.	n.a.	n.a.	Ter Heijne et al., 2010b
Pt-coated titanium with Fe <sup>3+</sup> /Fe <sup>2+</sup> , pH=1.6	0.5	85	125	69	2.0	4.2	Ter Heijne et al., 2010c
Pt coated carbon cloth	0.5	557	724	77	0.26	0.68	Fornero et al., 2010
Polypyrrole/carbon black composite	-0.05	56	n.a.	n.a.	0.4	1.8	Yuan et al., 2010
Graphite with Fe-EDTA	0.1	86	n.a.	n.a.	0.36	n.a.	Aelterman et al., 2009
Graphite fibre brush with biocathode	0.3	513	653	79	0.53	1.3	You et al., 2009
Graphite granules with HNO <sub>3</sub> activation	0.6	36	942	3.8	0.32	0.48	Erable et al., 2009a
Pt-coated titanium, pH=4	0.55	110	130	86	1.4	2.8	Dekker et al., 2009
Pt-coated carbon air cathode, pH=1	0.75	22	n.a.	n.a.	5.0	11	Erable et al., 2009b
Pt coated carbon fibre	n.a.	28	1,306	22	0.98	3.6	Fan et al., 2008
Carbon with CoTMPP	0.25	193	256	75	0.73	2.1	Zuo et al., 2008
Carbon felt pretreated MnO <sub>2</sub> +microorganisms	0.32	n.a.	193	n.a.	1.7	3.7	Clauwaert et al., 2007
Graphite with soluble Fe <sup>3+</sup> /Fe <sup>2+</sup> +iron oxidizers, pH=2.5	0.57	55	122	45	1.2	4.5	Ter Heijne et al., 2007
Graphite with soluble Fe <sup>3+</sup> /Fe <sup>2+</sup> , pH=2.5	0.45	40	221	18	0.86	4.5	Ter Heijne et al., 2006
Pyrolyzed FePc modified graphite foil	0.3	185	457	40	0.061	0.16	Zhao et al., 2006
Pt coated carbon cloth + PTFE	0.3	45	n.a.	n.a.	0.76	1.9	Cheng et al., 2006
Reticulated Vitreous Carbon + MnO <sub>2</sub>	0.55	n.a.	n.a.	n.a.	0.13 <sup>1</sup>	n.a.	Rhoads et al., 2005
CoTMPP coated carbon cloth, pH=3.3	0.5	37	85	44	2.35	3.8	Zhao et al., 2005
Stainless steel + biocathode	0.25	630	n.a.	n.a.	0.32 <sup>2</sup>	1.34 <sup>2</sup>	Bergel et al., 2005
Pt coated carbon cloth + PEM	0.2	180	n.a.	n.a.	0.49	1.22	Liu et al., 2004

n.a. = not analyzed

<sup>1</sup> no polarization curve was made to determine maximum performance

<sup>2</sup> anode oxidation reaction was hydrogen oxidation instead of a bio-anode

## 8.2.2 Bipolar membrane

In this thesis, we used a bipolar membrane in cases where neutral pH at the anode and low pH at the cathode was required. This was a Fumasep FBM bipolar membrane, produced by FuMA-tech GmbH, St. Ingbert, Germany. The suitability of a bipolar membrane for application in MFCs, was questioned by Harnisch et al. (2008). Their main arguments against use of a bipolar membrane were, that the bipolar membrane needs high current densities for water splitting to occur, and that the energy loss (polarization) as a result of water splitting is substantial. Here, we would like to challenge their arguments and to discuss arguments in favor of the use of bipolar membranes in MFCs. For this, first the general principle of the bipolar membrane will be explained. Then, the three main factors determining its applicability will be discussed: the energy required for water splitting, the limiting current density, and the proton transport number.

The bipolar membrane consists of an anion exchange layer (AEM) and a cation exchange layer (CEM) mounted together (Figure 2). When placed into a solution containing salts, the positively charged ions from the cathode ( $M^+$ ) and the negatively charged ions from the anode ( $X^-$ ) will diffuse into the membrane.

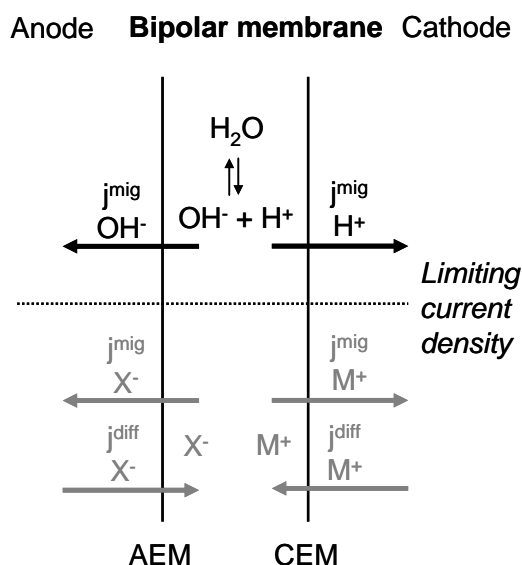


**Figure 2.** Principle of the bipolar membrane. The limiting current density represents the current density at which salt transport out of the membrane exceeds salt diffusion into the membrane so that water splitting occurs.

When an electric field is applied and a current flows, these salt ions will be transported out of the membrane. Water splitting will occur only when the current density increases to such a level that the rate of diffusion of salt ions out of the membrane exceeds the transport of salt ions into the membrane. In this case, no salt can be transported out of the membrane and in the transition region between anion and cation exchange membrane, water is split to produce protons and hydroxide anions. The protons will migrate through the cation exchange layer and the hydroxide anions will migrate through the anion exchange layer. In this way, the protons produced at the anode will be neutralized by the hydroxide anions, and the protons consumed at the cathode will be replenished by the protons produced in the membrane.

The energy needed for the water splitting reaction to occur is determined by the pH difference between the compartments. The voltage drop needed for water splitting is 0.83 V for a 100% selective bipolar membrane for the generation of a one molar acid and base solution at 298 K (Hurwitz et al., 2001) using:  $\Delta V = \frac{-2.3RT}{F} \Delta pH$ . This equation shows that the pH difference between anolyte and catholyte determine the voltage drop across the membrane and indicates the energy required for water splitting to occur.

At the same time, a certain current density is needed to start water splitting. This current density is called the limiting current density, i.e. the current density where salt transport out of the membrane exceeds salt diffusion into the membrane. This limiting current density is thus dependent on the salt concentration in the electrolytes, and is the prerequisite for water splitting to occur. The following equation has been derived for the limiting current density

(Wilhelm et al., 2001): 
$$i_{\text{lim}} = 2F \frac{D^m c_s^2}{s c_{\text{fix}}}$$

This equation shows that the limiting current density is directly dependent on the square of the solution concentration ( $c_s$  in mol/m<sup>3</sup>) and the average ion diffusion coefficient in the membrane ( $D^m$  in m<sup>2</sup>/s). They are inversely dependent on the thickness of the membrane ( $s$  in m) and the fixed charge density of the membrane ( $c_{\text{fix}}$  in mol/m<sup>3</sup>). Thus, the higher the solution concentration, the higher the current density required to exceed the rate of salt diffusion into the membrane in order to start water splitting.

Figure 3 shows the calculated limiting currents at different low solution concentrations, assuming a fixed charge density of 1.5 mol/L (Krol et al., 1998) and an ion diffusion coefficient of  $1.8 \cdot 10^{-9}$  m<sup>2</sup>/s (for K<sup>+</sup>, Krol, 1997), and a measured thickness of the bipolar membrane of 180 μm.

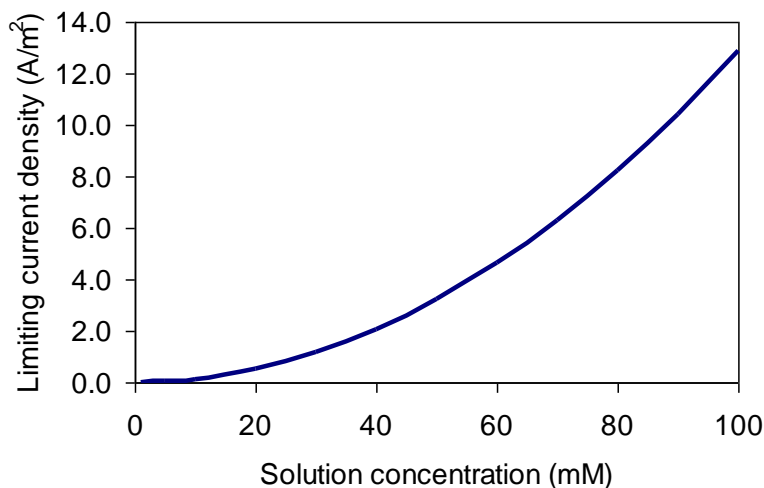


**Figure 3.** The current densities obtained in MFC studies up to 5 A/m<sup>2</sup> are sufficient to allow water splitting to occur, if solution concentrations are below 60 mM.

As MFCs usually operate under conditions of low salt concentration, this is actually advantageous for the use of a bipolar membrane in MFC, as the limiting current density needed to let the water splitting reaction occur is lower. Figure 3 shows that the current densities obtained in MFC studies in the range of 0-5 A/m<sup>2</sup> is indeed enough to start water splitting when the solution concentration is lower than 60 mM. At the same time, if a pH difference of 5 units is to be maintained, this will result in an energy loss of 300 mV. The question is if this energy loss is acceptable, and depends mainly on the extent to which cathode performance is improved.

Besides energy losses and limiting current density, the third factor determining the applicability of (bipolar) membranes is the proton transport number. The proton transport number indicates which part of the ions that are transported through the membrane consists of protons. Besides protons, other positively charged ions are present in the anolyte, and because these are often present in higher concentration, the other ions contribute to a large extent to the ion transport through the membrane (Rozendal et al., 2006). This is a problem, because it leads to pH gradients between anolyte and catholyte, as not all protons formed at the anode are transported to the cathode. As a result, the anolyte pH decreases and the catholyte pH increases. It is thus important that the proton transport number of a membrane is close to 1, meaning that all transport takes place in the form of protons. Especially in case of the bipolar membrane, that is used to maintain low pH in the cathode and neutral pH in the

anode, it is of major importance that the proton transport number is close to 1. Analysis of the proton transport number of a bipolar membrane from FuMA-tech (Chapter 4) showed that it was 0.65-0.76, and the other charge was transported mainly via  $K^+$  from anolyte to catholyte and via  $HSO_4^-/SO_4^{2-}$  from catholyte to anolyte. The other 24%-35% of the protons and hydroxides was externally supplied via addition of KOH and  $H_2SO_4$ . Two other studies determined the proton transport number of the same bipolar membrane under comparable conditions. Rozendal et al (2007) found a similar value of 0.72, whereas Harnisch et al. (2008) observed a decrease in proton transport number from 1 to 0.1 with increasing current density.

Methods need to be found to increase the proton transport number. Directions could be to operate MFCs at higher current densities, or to add  $CO_2$  to the system. Recent experiments in our lab indicated that addition of  $CO_2$  decreased the voltage loss across the bipolar membrane and resulted in an increase in MFC performance. Therefore, we hypothesize that the bipolar membrane may be able to produce protons not only from water splitting, but also from dissociation of  $H_2CO_3$ , as previously suggested for improvement of performance of anion exchange membranes (Torres et al., 2008a; Fornero et al., 2010). Replacing water splitting with dissociation of  $H_2CO_3$  may reduce the energy required for proton production, because  $H_2CO_3$  is a stronger acid than water ( $pK_a$  of  $H_2CO_3$  is 6.73, vs 14 for  $H_2O$ ). Furthermore,  $CO_2$  addition might positively influence the proton transport number. Further study is needed to optimize the experimental conditions in such a way, that the bipolar membrane has a low energy loss in combination with a high proton transport number.

### 8.2.3 Scaling-up

In MFC research, most studies are performed on lab-scale in systems varying in size from 20 mL to 2 L, with electrode surface areas ranging from 1  $cm^2$  to 300  $cm^2$ . Study on scaled-up systems has been lagging behind, despite its necessity for application of MFCs. Only recently, performance of a scaled-up system with 4 stacked cells, each with a projected surface area of 0.5  $m^2$  and a total volume of 20 L has been reported (Dekker et al., 2009). Dekker et al. (2009) found a maximum power density of 144  $W/m^3$  or 1.4  $W/m^2$ , which is comparable to the power obtained in small lab-scale systems. This is contrary to the observation that volumetric power density decreases with increasing system size (Dewan et al., 2008).

When scaling up, new challenges arise that are not observed in lab-scale systems. The most important issues as observed by Dekker et al. (2009) were, that flow characteristics are important to ensure good contact between electrolyte and electrode, that cell reversal is difficult to prevent especially in a bipolar stacked system, and that oxygen reduction at the

cathode even at low pH of 4 was contributing to more than 80% of the total internal resistance (Dekker et al., 2009).

Further study on this scaled-up system (Chapter 7 of this thesis) aimed at improvement of MFC performance. The approach was to improve the cathode by replacing oxygen reduction by reduction of  $\text{Fe}^{3+}$  to  $\text{Fe}^{2+}$ . Furthermore, flow characteristics were improved by a change in flow path. This resulted in a maximum power density of  $200 \text{ W/m}^3$  or  $2.0 \text{ W/m}^2$  for a single cell with an electrode size of  $0.5 \text{ m}^2$ . In this case, the cathode resistance was reduced compared to oxygen reduction. Still, the cathode contributed to 53% of the total internal resistance, while the anode contributed to only 5% of the internal resistance. This showed, that the cathode was still the main limiting factor in MFC performance.

Cell reversal is a factor that needs further research. In Dekker et al. (2009), the four cells were stacked in series by bipolar stacking, which means that the first cathode and the second anode are using the same bipolar plate. This was done to minimize internal losses by keeping short distances and having optimal contact. The disadvantage of bipolar stacking is that when one cell cannot produce the current of the other cells, and reverses polarity, it cannot simply be taken out: the current will still flow through this cell at the expense of cell voltage. Two possible routes can be followed. Firstly, flow characteristics should be good to ensure that oxidants (substrate) and reductants (oxygen or iron) are well-distributed over the electrodes and that they are present in high enough concentrations not to pose a limit on current production (Dekker et al., 2009). Secondly, stacking should be done in such a way, that a cell can be disconnected when cell reversal occurs, so that this cell does not use the energy produced by the other cells. Thus, a suitable operating strategy should be found. More operating experience will probably make it possible to ensure that all cells become reliable.

## 8.2.4 Mass transfer of oxygen

When considering the cathode, mass transfer of oxygen is the main limiting factor in MFC performance. In this thesis, three routes were followed to improve the cathode reaction with oxygen as the final electron acceptor. Each of these routes will finally run into similar limitations of mass transfer of oxygen, especially when dissolved oxygen is used as the electron acceptor.

Reduction of  $\text{Fe}^{3+}$  to  $\text{Fe}^{2+}$  instead of oxygen reduction resulted in better cathode performance, because of the higher solubility of ferric iron compared to oxygen: a concentration of  $17 \text{ mM}$  ( $1 \text{ g/L}$ ) of ferric iron was tested, while the maximum oxygen solubility in water at  $30 \text{ }^\circ\text{C}$  is only  $0.24 \text{ mM}$  ( $7.6 \text{ mg/L}$ ). This is also one of the reasons for the superior performance of  $\text{Fe}^{3+}$  reduction compared to oxygen reduction, the other reason being

the faster reaction of iron using a faster one electron transfer reaction than the four electron-four proton oxygen reduction reaction. However, as the produced  $\text{Fe}^{2+}$  needs to be re-oxidized to  $\text{Fe}^{3+}$  using oxygen, eventually, oxygen transfer will limit the amount of  $\text{Fe}^{3+}$  available. Similarly, oxygen transfer may become limiting for the possible catalytic action of  $\text{Cu}^{2+}/\text{Cu}$  for oxygen reduction. While performance is increased in the presence of oxygen, oxygen transfer will finally determine the rate of electron transfer.

In case of direct biocathodes, where the biofilm attached to the electrode catalyzes the reduction of oxygen, the situation is more complicated. Oxygen diffusion from bulk to the microorganisms takes place through three adjacent layers: the diffusion layer facing the bulk solution, the stagnant water layer attached to the biofilm, and the biofilm itself. In this case, oxygen transfer from bulk to biofilm needs to take place. Ways to improve oxygen transfer are increasing the linear flow rate, which improves oxygen transfer only through the outer diffusion layer. Besides, air cathodes with a biofilm combined with a thin water layer attached may be developed for better oxygen transfer. Oxygen diffusion inside the biofilm and the stagnant water layer however, cannot be influenced by flow rate. To improve oxygen transfer into the biofilm, several approaches are possible: use of pure oxygen (Dekker et al., 2009), pressurized air (Fornero et al., 2008), or photosynthetic microorganisms that can create oxygen concentrations up to 20 mg/L (Strik et al., 2010). Another direction to increase volumetric productivity is the use of 3D electrodes with a high specific surface area, like graphite felt or carbon granules (Logan et al., 2007). If the flow is well-directed through the porous electrode (Sleutels et al., 2009b), this can also further increase the oxygen transfer and thus the volumetric current production of biocathodes.

### 8.2.5 Factors limiting bioanode activity and MFC performance

Until now, the discussion on factors limiting MFC performance in this chapter focused on the cathode. Here, we would like to discuss three other limitations that may become more prominent when the cathode bottleneck is overcome, and that were observed in Chapter 2. These limitations are related to maximum bioanode performance as a result of limited buffer capacity and solution conductivity, and the use of membranes.

An important issue that arises when the anode and cathode are connected is the conductivity of the electrolytes. Often waste streams are used as substrate, while these typically have a low conductivity of 1-2 mS/cm (Rozendal et al., 2008). It has been shown that at these low conductivities, a limited anode compartment thickness is allowed to achieve high current densities (Rozendal et al., 2008). In lab-scale set-ups, often large amounts of salts and buffer are added to increase the conductivity and improve performance. In full-scale MFCs in a water

purification setting however, this is not possible, because of economical issues and discharge regulations. The fact that no buffer can be added on a larger scale, results in another limitation related to acidification. The electrochemically active microorganisms at the bio-anode produce considerable amounts of protons when oxidizing the organic materials. For each mol of acetate, 8 moles of electrons are produced. When protons cannot diffuse from anode to anolyte at high enough rate, the low local pH seriously limits bio-anode activity (Torres et al., 2008b). Examples of possible routes to prevent low local pH without external supply of buffer are enhancement of mass transport, for example by forced flow through porous electrodes (Sleutels et al., 2010a), or addition of caustic produced in the cathode (Rabaey et al., 2010). Other challenges arise at the bioanode when real wastewater are used as the substrate instead of acetate. These new challenges are related to the presence of particulate matter, hydrolysis of more complex substrates than acetate, and fluctuating concentrations of organics.

The advantage of using a membrane in an MFC is that the anode compartment and cathode compartment do not readily mix. For an MFC, this has the advantage that the coulombic efficiency is higher, as less oxidant can pass from the cathodic to the anodic compartment. The disadvantage of for example oxygen passing to the anode is, that it leads to unwanted oxidation of the substrate and thus lowers coulombic efficiency. A major disadvantage of using a membrane is that a pH gradient develops between the anode and cathode compartment (Rozendal et al., 2006). This pH gradient gives an additional overpotential at the electrodes as can be calculated using the Nernst equation. A way to prevent this pH gradient is either to take out the membrane (Call and Logan, 2008; Liu and Logan, 2004), to pump the anolyte to the cathode to guarantee mixing (Freguia et al., 2008), to use CO<sub>2</sub> in the catholyte (Fornero et al., 2010), or to use a bipolar membrane (Ter Heijne et al., 2006). Although it has been shown that these methods prevent the pH gradient to develop, some of the strategies may also cause substrate/product crossover giving unwanted side reactions and products. Another effect of use of a membrane is, that it will increase the resistance of the system (Sleutels et al., 2009a) resulting in a lower cell voltage. Depending on membrane properties like charge (negative or positive) and charge density, different species of ions and amounts of ions will be transported and this will have effects on voltage losses.

### **8.3 Production of electricity from wastewater by MFCs: perspectives**

All the above mentioned factors should be taken into account for further improvement of MFCs. If the major bottlenecks are overcome, what is then the maximum power that can be achieved in MFCs? In this chapter, we compare the currently achieved MFC performance with

the estimated maximum performance, and with the established technology of anaerobic digestion.

In this thesis, the maximum achieved performance was found in the scaled-up MFC with  $\text{Fe}^{3+}$  reduction at the cathode (Chapter 7). The power density was  $2.0 \text{ W/m}^2$  ( $200 \text{ W/m}^3$ ) at an overall energy efficiency of 28%.

Few attempts have been made to estimate the maximum possible power production of MFCs. In this respect, values of  $17 \text{ W/m}^2$  (Logan, 2009). and  $19 \text{ W/m}^2$  (Fan et al., 2008) have been proposed based on limitations in substrate diffusion and based on minimizing losses in system design. Based on the current density measured by Jeremiassé et al. (2010) by a bio-anode in a hydrogen producing Microbial Electrolysis Cell, we find a similar estimation for the maximum power density.

Jeremiassé et al. (2010) measured a maximum current density of  $22.8 \text{ A/m}^2$  at an anode potential of  $-0.36 \text{ V}$  vs  $\text{Ag/AgCl}$ . At this anode potential, overpotential was  $0.1 \text{ V}$  ( $\text{pH}=6.54$ , acetate= $4 \text{ mM}$ ,  $\text{HCO}_3^- = 10 \text{ mM}$  results in a thermodynamic anode potential of  $-0.46 \text{ V}$  vs  $\text{Ag/AgCl}$ ). This means that the energy losses at the anode would be almost 10% of the maximum theoretical cell voltage of  $1.09 \text{ V}$ . If we now assume that the cathode can perform equally well at this current density, so that cathode energy losses are 10%, and other internal losses (membrane and solution) contribute to another 10%, this would result in a cell voltage of  $0.7 \cdot 1.09 = 0.76 \text{ V}$ . In this case, power density would be  $17.3 \text{ W/m}^2$ , similar to the other two estimations. Besides power density normalized to surface area, the volumetric power density ( $\text{W/m}^3$ ) is an important measure, and this volumetric power density is dependent on the volumetric surface area. In our scaled-up MFC, we demonstrated that  $100 \text{ m}^2/\text{m}^3$  is feasible. Because there is still room for a further increase in surface area, we assume that an improvement to  $200 \text{ m}^2/\text{m}^3$  should be feasible. This would result in a maximum volumetric power density of  $3,460 \text{ W/m}^3$ . This of course is an estimated situation with low internal losses: a voltage loss of  $0.33 \text{ V}$  in combination with a current density of  $22.8 \text{ A/m}^2$  allows for a maximum total internal resistance of  $14 \text{ m}\Omega\text{m}^2$ , while for example the total internal resistance in the scaled-up MFC with iron reduction (Chapter 7) was still  $146 \text{ m}\Omega\text{m}^2$ , of which  $85 \text{ m}\Omega\text{m}^2$  was caused by the cathode. Thus, internal resistance should be further reduced with a factor 10 in order to achieve these results.

How does this power production relate to the electricity production of comparable biomass-to-electricity conversion technologies? The best candidate for comparison is anaerobic digestion, because both technologies have similar characteristics, as they both convert wet organic waste streams at ambient temperature. For comparison, we assume that all COD in the anaerobic digester is present in the form of acetate and that the desired product is electricity.

The energy content of the acetate can be calculated similarly to the MFC: with oxygen as the final electron acceptor (in combustion), the Gibb's free energy is -844 kJ/mol. The energy content of the formed CH<sub>4</sub> can then be calculated from the reaction  $\text{CH}_4 + 2 \text{O}_2 \rightarrow \text{CO}_2 + 2 \text{H}_2\text{O}$ , and is -810 kJ/mol. This means, that of the energy in acetate, -34 kJ/mol is lost in the conversion to CH<sub>4</sub>. This corresponds with an energy loss of roughly 5%. Furthermore, if we assume that 5% of the energy in acetate is incorporated in biomass (Van Lier et al., 2008), so that the efficiency of conversion of acetate into methane is 90%, and an average combustion efficiency of CH<sub>4</sub> of 33% (Weiland et al., 2006), we find an overall energy efficiency of acetate into electricity of 30%. The volumetric power density that can be produced in the anaerobic digestion, based on an organic loading rate of 25 kg COD/m<sup>3</sup>d, a lower heating value of 50.1 MJ/kg CH<sub>4</sub>, and an overall energy efficiency of 30%, is 1,087 W/m<sup>3</sup>.

The predicted maximum volumetric power density in an MFC is 3,460 W/m<sup>3</sup>: a factor 3 higher than achieved with anaerobic digestion at similar loading rate. From Table 2, it becomes clear that energy efficiency of the MFC is already comparable to anaerobic digestion. When maximum estimated performance is reached, the energetic efficiency will be as high as 63% compared to only 30% overall energy efficiency of anaerobic digestion.

Practical feasibility of the MFC will not only be determined by the maximum power produced and the energy efficiency, but also on the capital and operational costs of the final system. As operational costs are related to productivity, and thus to conversion rate, it is important to investigate the relationship between conversion rate (current density) and energy efficiency. Energy efficiency shows the combined Coulombic efficiency and voltage efficiency. Whereas voltage efficiency decreases with increasing current density as a result of increasing energy losses, Coulombic efficiency is likely to increase with higher anode potential, and thus increasing current density (Sleutels et al., 2010b). The balance between Coulombic efficiency and voltage efficiency determines if energy efficiency increases or decreases with increasing current density in an MFC. At the same time, increasing current density increases the productivity of the MFC, which is preferred from an application perspective, as it decreases capital cost and reduces the footprint of the MFC.

**Table 2.** Comparison of maximum volumetric power density produced by MFCs and via anaerobic digestion

	Loading rate (kg COD/m <sup>3</sup> /d)	Current density (A/m <sup>2</sup> )	Volumetric power density (W/m <sup>3</sup> )	Energetic efficiency (%)
Scaled-up Microbial Fuel Cell (Chapter 7) at maximum power density	8.1 <sup>1</sup>	4.2	200	28
Scaled-up Microbial Fuel Cell (Chapter 7) at maximum energy efficiency	5.0 <sup>1</sup>	2.6	180	41
Microbial Fuel Cell, estimated maximum	31.9 <sup>2</sup>	22.8	3,460 <sup>2</sup>	63 <sup>2</sup>
Anaerobic digestion	25	-	1,087 <sup>3</sup>	30 <sup>3</sup>

<sup>1</sup> Using the measured 65% Coulombic efficiency (Chapter 7)

<sup>2</sup> Assuming 90% Coulombic efficiency and assuming a specific surface area of 200 m<sup>2</sup>/m<sup>3</sup>

<sup>3</sup> Assuming 30% overall energy efficiency from acetate to electricity

The only way to combine these demands of high efficiency and high productivity is to lower losses of BESs. Therefore, a thorough analysis of the internal losses is a prerequisite (Sleutels et al. 2009a). Based on this analysis, further efforts should be done to design an energy efficient MFC. It should be kept in mind that besides efficient design, the use of cheap and renewable materials is required for further development of MFCs.

## 8.4 Concluding remarks

This final chapter described the development in performance of MFCs since 2002, based on their power density, and cathode performance. With further study and development of MFCs, it should be possible to improve MFC performance with a factor 10 to approach the estimated maximum power density of 17.3 W/m<sup>2</sup> at an efficiency of 63%. This estimated maximum power density and energy efficiency would make MFCs more attractive than anaerobic digestion for electricity production from biomass.

For reaching this estimated power density, further studies should focus on the cathode as it remains the main limiting factor, leading to largest part of the energy losses in the MFC. Finally, MFCs should prove their feasibility when converting real wastewaters at larger scale.

## 8.5 References

- Aelterman, P.; Versichele, M.; Genettello, E.; Verbeken, K.; Verstraete, W. 2009. Microbial fuel cells operated with iron-chelated air cathodes. *Electrochim. Acta.* 54, 5754-5760.
- Bergel, A.; Féron, D.; Mollica, A. 2005. Catalysis of oxygen reduction in PEM fuel cell by seawater biofilm. *Electrochem. Commun.* 7, 900-904.
- Call, D.; Logan, B. E. 2008. Hydrogen production in a single chamber microbial electrolysis cell lacking a membrane. *Environ. Sci. Technol.* 42, 3401-3406.
- Cheng, S.; Liu, H.; Logan, B. E. 2006. Increased performance of single-chamber microbial fuel cells using an improved cathode structure. *Electrochem. Commun.* 8, 489-494.
- Clauwaert, P.; Van Der Ha, D.; Boon, N.; Verbeken, K.; Verhaege, M.; Rabaey, K.; Verstraete, W. 2007. Open air biocathode enables effective electricity generation with microbial fuel cells. *Environ. Sci. Technol.* 41, 7564-7569.
- Dekker, A.; Ter Heijne, A.; Saakes, M.; Hamelers, H. V. M.; Buisman, C. J. N. 2009. Analysis and improvement of a scaled-up and stacked microbial fuel cell. *Environ. Sci. Technol.* 43, 9038-9042.
- Dewan, A.; Beyenal, H.; Lewandowski, Z. 2008. Scaling up microbial fuel cells. *Environ. Sci. Technol.* 42, 7643-7648.
- Erable, B.; Duteanu, N.; Kumar, S. M. S.; Feng, Y.; Ghangrekar, M. M.; Scott, K. 2009a. Nitric acid activation of graphite granules to increase the performance of the non-catalyzed oxygen reduction reaction (ORR) for MFC applications. *Electrochem. Commun.* 11, 1547-1549.
- Erable, B.; Etcheverry, L.; Bergel, A. 2009b. Increased power from a two-chamber microbial fuel cell with a low-pH air-cathode compartment. *Electrochem. Commun.* 11, 619-622.
- Fan, Y.; Sharbrough, E.; Liu, H. 2008. Quantification of the internal resistance distribution of microbial fuel cells. *Environ. Sci. Technol.* 42, 8101-8107.
- Fornero, J. J.; Rosenbaum, M.; Cotta, M. A.; Angenent, L. T. 2008. Microbial fuel cell performance with a pressurized cathode chamber. *Environ. Sci. Technol.* 42, 8578-8584.
- Fornero, J. J.; Rosenbaum, M.; Cotta, M. A.; Angenent, L. T. 2010. Carbon dioxide addition to microbial fuel cell cathodes maintains sustainable catholyte pH and improves anolyte pH, alkalinity, and conductivity. *Environ. Sci. Technol.* 44, 2728-2734.
- Freguia, S.; Rabaey, K.; Yuan, Z.; Keller, J. 2008. Sequential anode-cathode configuration improves cathodic oxygen reduction and effluent quality of microbial fuel cells. *Water Res.* 42, 1387-1396.
- Jeremiasse, A.; Hamelers, H.V.M.; Saakes, M.; Buisman, C.J.N. 2010. Continuous microbial electrolysis cell with a nickel foam cathode. Submitted.
- Harnisch, F.; Schröder, U.; Scholz, F. 2008. The suitability of monopolar and bipolar ion exchange membranes as separators for biological fuel cells. *Environ. Sci. Technol.* 42, 1740-1746.
- Hurwitz, H. D.; Dibiani, R. 2001. Investigation of electrical properties of bipolar membranes at steady state and with transient methods. *Electrochim. Acta.* 47, 759-773.
- Kim, H.J.; Park, H.S.; Hyun, M.S.; Chang, I.S.; Kim, M.; Kim, B.H. 2002. A mediator-less microbial fuel cell using a metal reducing bacterium, *Shewanella putrefaciens*. *Enzyme Microb. Technol.* 30, 145-152.

- Krol, J. J. 1997. Monopolar and bipolar ion exchange membranes. PhD thesis, University of Twente.
- Krol, J. J.; Jansink, M.; Wessling, M.; Strathmann, H. 1998. Behaviour of bipolar membranes at high current density water diffusion limitation. *Sep. Purif. Technol.* 14, 41-52.
- Lefebvre, O.; Ooi, W.K.; Tang, Z.; Abdullah-Al-Mamun, M.; Chua, D.H.C.; Ng, H.Y. 2009. Optimization of a Pt-free cathode suitable for practical applications of microbial fuel cells. *Bioresour. Technol.* 100, 4907-4910.
- Liu, H.; Logan, B. E. 2004. Electricity generation using an air-cathode single chamber microbial fuel cell in the presence and absence of a proton exchange membrane. *Environ. Sci. Technol.* 38, 4040-4046.
- Logan, B.E. ; Hamelers, B.; Rozendal, R. ; Schröder, U. Keller, J. ; Freguia, S. ; Aelterman, P. ; Verstraete, W. ; Rabaey, K. 2006. Microbial fuel cells: Methodology and technology. *Environ. Sci. Technol.* 40, 5181-5192.
- Logan, B.; Cheng, S.; Watson, V.; Estadt, G. 2007. Graphite fiber brush anodes for increased power production in air-cathode microbial fuel cells. *Environ. Sci. Technol.*, 41, 3341-3346.
- Logan, B. E. 2009. Exoelectrogenic bacteria that power microbial fuel cells. *Nature Rev. Microbiol.* 7, 375-381.
- Rabaey, K.; Bützer, S.; Brown, S.; Keller, J.; Rozendal, R. A. 2010. High current generation coupled to caustic production using a lamellar bioelectrochemical system. *Environ. Sci. Technol.* 44, 4315-4321.
- Rhoads, A.; Beyenal, H.; Lewandowski, Z. 2005. Microbial fuel cell using anaerobic respiration as an anodic reaction and biomineralized manganese as a cathodic reactant. *Environ. Sci. Technol.* 39, 4666-4671.
- Rozendal, R. A.; Hamelers, H. V. M.; Buisman, C. J. N. 2006. Effects of membrane cation transport on pH and microbial fuel cell performance. *Environ. Sci. Technol.* 40, 5206-5211.
- Rozendal, R. A.; Hamelers, H. V. M.; Molenkamp, R. J.; Buisman, C. J. N. 2007. Performance of single chamber biocatalyzed electrolysis with different types of ion exchange membranes. *Water Res.* 41, 1984-1994.
- Rozendal, R. A.; Hamelers, H. V. M.; Rabaey, K.; Keller, J.; Buisman, C. J. N. 2008. Towards practical implementation of bioelectrochemical wastewater treatment. *Trends Biotechnol.* 26, 450-459.
- Schaetzle, O.; Barriere, F.; Schröder U. 2009. An improved microbial fuel cell with laccase as the oxygen reduction catalyst. *Energy Environ. Sci.* 2, 96-99.
- Sluutels, T. H. J. A.; Hamelers, H. V. M.; Rozendal, R. A.; Buisman, C. J. N. 2009a. Ion transport resistance in microbial electrolysis cells with anion and cation exchange membranes. *Int. J. Hydrogen Energy.* 34, 3612-3620.
- Sluutels, T. H. J. A.; Lodder, R.; Hamelers, H. V. M.; Buisman, C. J. N. 2009b. Improved performance of porous bio-anodes in microbial electrolysis cells by enhancing mass and charge transport. *Int. J. Hydrogen Energy.* 34, 9655-9661.
- Sluutels, T. H. J. A.; Hamelers, H. V. M.; Buisman, C. J. N. 2010a. Effect of mass and charge transport speed and direction in porous anodes on microbial electrolysis cell performance. *Bioresource Technology*, in press.
- Sluutels, T. H. J. A.; Hamelers, H. V. M.; Buisman, C. J. N. 2010b. Influencing Coulombic efficiency in bioelectrochemical systems.

- Strik, D. P. B. T. B.; Hamelers, H. V. M.; Buisman, C. J. N. 2010. Solar energy powered microbial fuel cell with a reversible bioelectrode. *Environ. Sci. Technol.* 44, 532-537.
- Ter Heijne, A.; Hamelers, H.V.M.; de Wilde, V.; Rozendal, R.A.; Buisman, C.J.N. 2006. A bipolar membrane combined with ferric iron reduction as an efficient cathode system in microbial fuel cells. *Environ. Sci. Technol.* 40, 5200-5205.
- Ter Heijne, A.; Hamelers, H.V.M.; Buisman, C.J.N. 2007. Microbial fuel cell operation with continuous biological ferrous iron oxidation of the catholyte. *Environ. Sci. Technol.* 41, 4130-4134.
- Ter Heijne, A.; Liu, F.; Van der Weijden, R.; Weijma, J.; Buisman, C. J. N.; Hamelers, H. V. M. 2010a. Copper recovery combined with electricity production in a microbial fuel cell. *Environ. Sci. Technol.* 44, 4376-4381.
- Ter Heijne, A.; Strik, D.P.B.T.B.; Hamelers, H.V.M.; Buisman, C.J.N. 2010b. Cathode potential and mass transfer determine performance of oxygen reducing biocathodes in microbial fuel cells. *Environ. Sci. Technol.* In press.
- Ter Heijne, A.; Liu, F.; Van Rijnsoever, L.S.; Saakes, M.; Hamelers, H. V. M.; Buisman, C. J. N. 2010c. Improvement of the cathode of a scaled-up Microbial Fuel Cell.. Prepared for submission.
- Topcagic, S.; Minter, S.D. 2006 Development of a membraneless ethanol/oxygen biofuel cell. *Electrochim. Acta.* 51, 2168-2172.
- Torres, C. I.; Lee, H.; Rittmann, B. E. 2008a. Carbonate species as OH<sup>-</sup> carriers for decreasing the pH gradient between cathode and anode in biological fuel cells. *Environ. Sci. Technol.* 42, 8773-8777.
- Torres, C. I.; Marcus, A. K.; Rittmann, B. E. 2008b. Proton transport inside the biofilm limits electrical current generation by anode-respiring bacteria. *Biotechnol. Bioeng.* 100, 872-881.
- Van Lier, J.B.; Mahmoud, N.; Zeeman, G. 2008. Anaerobic wastewater treatment, in: Heenze, M.; van Loosdrecht, M.C.M.; Ekama, G.A.; Brdjanovic, D. (Eds). *Biological wastewater treatment: principles, modeling and design*. IWA Publishing, London, pp. 415-456.
- Weiland, P. 2006. Biomass digestion in agriculture: A successful pathway for the energy production and waste treatment in Germany. *Eng. Life Sci.* 6, 302-309.
- Wilhelm, F. G.; Pünt, I.; Van Der Vegt, N. F. A.; Wessling, M.; Strathmann, H. 2001. Optimisation strategies for the preparation of bipolar membranes with reduced salt ion leakage in acid-base electrodialysis. *J. Membr. Sci.* 182, 13-28.
- Yeager, E. 1984. Electrocatalysts for O<sub>2</sub> reduction. *Electrochim. Acta.* 29, 1527-1537.
- You, S.; Ren, N.; Zhao, Q.; Wang, J.; Yang, F. 2009. Power generation and electrochemical analysis of biocathode microbial fuel cell using graphite fibre brush as cathode material. *Fuel Cells.* 9, 588-596.
- Yu, E.H.; Cheng, S.; Logan, B.E.; Scott, K. 2009. Electrochemical reduction of oxygen with iron phthalocyanine in neutral media. *J. Appl. Electrochem.* 39, 705-711.
- Yuan, Y.; Zhou, S.; Zhuang, L. 2010. Polypyrrole/carbon black composite as a novel oxygen reduction catalyst for microbial fuel cells. *J. Power Sources.* 195, 3490-3493.
- Zhao, F.; Harnisch, F.; Schröder, U.; Scholz, F.; Bogdanoff, P.; Herrmann, I. 2005. Application of pyrolysed iron(II) phthalocyanine and CoTMPP based oxygen reduction catalysts as cathode materials in microbial fuel cells. *Electrochem. Commun.* 7, 1405-1410.

- Zhao, F.; Harnisch, F.; Schröder, U.; Scholz, F.; Bogdanoff, P.; Herrmann, I. 2006. Challenges and constraints of using oxygen cathodes in microbial fuel cells. *Environ. Sci. Technol.* 40, 5193-5199.
- Zuo, Y.; Cheng, S.; Logan, B. E. 2008. Ion exchange membrane cathodes for scalable microbial fuel cells. *Environ. Sci. Technol.* 42, 6967-6972.

**Summary**

**Samenvatting**

## Summary

### **Microbial Fuel Cells are a promising technology for efficient conversion of biomass into electricity**

There is a huge and increasing energy demand in the world. As described in **Chapter 1**, production of energy from fossil sources has major drawbacks related to accessibility of sources, climate change, air pollution, and political instability. Renewable sources are the alternative for fossil sources, as they can offer advantages regarding social and environmental impacts. Of the renewable energy sources, biomass is most important, contributing to 9.8% of the total primary energy supply in 2007. Electricity is a desired form of energy, as access to electricity is a key driver for social and economical development. In developing countries, it would thus be beneficial if biomass can be used for electricity production to improve energy accessibility, whereas in industrialized countries, production of electricity from biomass will be more oriented towards climate change mitigation. There is thus a need for simple and cost-effective technologies to efficiently convert biomass into electricity.

Microbial Fuel Cells are a promising technology for conversion of wet organic waste streams into electricity, because they can produce electricity from biomass in one efficient step, they operate at ambient temperatures, they are robust, and they are environmentally sustainable. This thesis aims at efficient electricity production in Microbial Fuel Cells by improving the reduction reaction at the cathode, because the cathode is the main limiting factor in power production in Microbial Fuel Cells.

### **First crucial part: the electron producing bioanode**

Microbial Fuel Cells are a new technology in which microorganisms convert biomass into electricity. The Microbial Fuel Cell consists of two electrodes: an anode and a cathode. At the anode, microorganisms convert organic material (biomass) into electrons, protons, and CO<sub>2</sub>. The produced electrons flow via an electrical circuit to the other electrode, the cathode, meanwhile releasing their energy. The anode with microorganisms attached is called the bioanode. The bioanode is the first crucial part of the Microbial Fuel Cell as it is the location where electrons are produced. In **Chapter 2**, performance of bioanodes on different electrode materials was studied using different characterization techniques. Bioanode performance was different for each material, which could not be explained solely by differences in specific surface area. The microorganisms were capable of producing considerable current densities up

to 4.6 A/m<sup>2</sup> on a flat graphite electrode. This limiting current density reflected the maximum biomass activity.

## Second crucial part: the electron accepting cathode

In order to produce electricity, the electrons must flow from the bioanode to the cathode, where a reduction reaction takes place. Oxygen is the most desired electron acceptor because of its unlimited availability and its high potential. To drive the oxygen reduction reaction at the desired rate however, a catalyst is needed. The mostly used catalyst for oxygen reduction is Pt, however, its high cost requires development of other cost-effective and renewable catalysts. We followed three strategies to improve cathode performance.

In the first strategy, the oxygen reduction was replaced by reduction of Fe<sup>3+</sup> to Fe<sup>2+</sup> as described in **Chapter 3 and 4**. The formed Fe<sup>2+</sup> was simultaneously reoxidized to Fe<sup>3+</sup> by the microorganism *Acidithiobacillus ferrooxidans*, using oxygen as the final electron acceptor. Because Fe<sup>3+</sup> is only soluble at low pH (<2.5), and the bioanode operates at near neutral pH, a bipolar membrane was used to maintain this pH difference. Inside this bipolar membrane, water is split into H<sup>+</sup> and OH<sup>-</sup>. The formed H<sup>+</sup> can migrate to the low pH cathode compartment, while the formed OH<sup>-</sup> can migrate to the neutral pH anode compartment to neutralize the formed protons. The maximum power density was 1.2 W/m<sup>2</sup> at a current density of 4.5 A/m<sup>2</sup>. Replacing oxygen with Fe<sup>3+</sup> improved cathode performance considerably. Challenges related to the bipolar membrane were the energy required for water splitting and the transport of other ions than H<sup>+</sup> and OH<sup>-</sup>.

In the second strategy, described in **Chapter 5**, microorganisms were grown on the cathode to catalyze the reduction of oxygen. These microorganisms originated from nitrifying sludge and were grown at three different potentials. In all cases, an oxygen reducing biofilm developed, while the produced current density was different for each potential. The current density produced by the biofilm was considerably higher than on the control bare graphite electrode. Limitations rose as a result of the cathode potential (charge transfer), and mass transfer of oxygen.

In the third strategy, described in **Chapter 6**, we studied the reduction of Cu<sup>2+</sup> to metallic Cu. The advantages were twofold: Cu was recovered in its pure form, which makes this a process of possible interest for recovery of copper from waste streams, and Cu<sup>2+</sup>/Cu seemed to act as a catalyst for oxygen reduction, as cathode performance increased in presence of oxygen. The bipolar membrane was used to maintain low pH at the cathode to prevent precipitation of Cu<sup>2+</sup>. The maximum power achieved was 0.8 W/m<sup>2</sup>, comparable to other well-performing MFCs.

## First step towards application: scaling-up

While most Microbial Fuel Cell studies are performed in small-scale lab setups, it is of utmost importance that experience is obtained with Microbial Fuel Cells on a larger scale, as new limitations may arise that are not encountered on a small scale. We continued the study on the first reported scaled-up MFC in the world in **Chapter 7**. This MFC had a membrane surface area of 0.5 m<sup>2</sup> and a total volume of 5 L. To overcome the previously encountered cathode limitations, we replaced oxygen reduction by reduction of Fe<sup>3+</sup> to Fe<sup>2+</sup> and simultaneous biological iron oxidation. In order to maintain the low pH to keep Fe<sup>3+</sup> soluble, a bipolar membrane was used. The scaled-up MFC was operated during 37 days and reached a maximum power density of 2.0 W/m<sup>2</sup>, which is a factor 1.4 higher than obtained with oxygen in previous study. Analysis of the internal resistance revealed that both anode and cathode resistance decreased with a factor 10 during the 37 days operation period. Despite the improvement in cathode performance by replacing oxygen reduction with reduction of Fe<sup>3+</sup>, the cathode remained the limiting factor, contributing to 58% of the total internal resistance.

## Maximum estimated power production in Microbial Fuel Cells

In the beginning of Microbial Fuel Cell research in 2002, the reported power densities increased from 1 to 10 mW/m<sup>2</sup> roughly by a factor 10 each year. Since 2005, however, the reported maximum power densities have stabilized at a level of about 2 W/m<sup>2</sup>, although the number of groups studying Microbial Fuel Cells has increased. The question that is raised in **Chapter 8** is, if the power density in Microbial Fuel Cells has reached its limit, or if further reduction of energy losses will result in a further increase in power density. We show that there is still a factor 10 to gain in power density, as the estimated maximum power density that can be achieved in Microbial Fuel Cells is 17.3 W/m<sup>2</sup> or 3,460 W/m<sup>3</sup>. This is a factor 3 higher than produced in an anaerobic digester at a similar loading rate of 25 kg COD/m<sup>3</sup>/d. At this estimated maximum performance, the energy efficiency in a Microbial Fuel Cell will be 63%, whereas the energy efficiency in anaerobic digestion is 30%. For reaching this estimated power density, further studies should focus on the cathode as it remains the main limiting factor, leading to largest part of the energy losses in the MFC. Finally, MFCs should prove their feasibility when converting real wastewaters at larger scale.

# Samenvatting

## De biobrandstofcel is een veelbelovende technologie voor efficiënte omzetting van biomassa in elektriciteit

De wereldwijde vraag naar energie is enorm en neemt toe. Zoals beschreven in **Hoofdstuk 1**, heeft de energieproductie uit fossiele brandstoffen grote nadelen met betrekking tot winning, klimaatverandering, luchtvervuiling, en politieke instabiliteit. Hernieuwbare bronnen zijn het alternatief voor fossiele bronnen, omdat zij voordelen bieden op maatschappelijk en milieugebied. Van de hernieuwbare bronnen is biomassa de meest belangrijke. In 2007 maakte biomassa 9,8% uit van de totale energievoorziening. Electriciteit is een aantrekkelijke vorm van energie, omdat elektriciteit een belangrijke drijfveer is voor sociale en economische ontwikkeling. In ontwikkelingslanden heeft gebruik van biomassa voor elektriciteitsproductie het voordeel dat de toegang tot elektriciteit verbeterd wordt, terwijl elektriciteitsproductie uit biomassa in geïndustrialiseerde landen meer gericht zal zijn op vermindering van klimaatverandering. Er zijn dus simpele, goedkope technologieën nodig om biomassa met hoge efficiëntie om te zetten in elektriciteit.

De biobrandstofcel is een veelbelovende technologie voor de omzetting van natte organische reststromen in elektriciteit, omdat de omzetting naar elektriciteit plaatsvindt in één efficiënte stap, de reactie plaatsvindt bij omgevingstemperatuur, en de technologie robuust en milieuvriendelijk is. Dit proefschrift richt zich op efficiënte elektriciteitsproductie in de biobrandstofcel door het verbeteren van de reductiereactie aan de kathode, omdat de kathode op het moment de belangrijkste limiterende factor is in de energieproductie.

## Eerste cruciale onderdeel: de elektronenproducerende anode

De biobrandstofcel is een nieuwe technologie waarin microorganismen biomassa omzetten in elektriciteit. De biobrandstofcel bestaat uit twee elektrodes: een anode en een kathode. Aan de anode zetten microorganismen organisch materiaal (biomassa) om in elektronen, protonen en CO<sub>2</sub>. De geproduceerde elektronen stromen via een elektrisch circuit naar de andere elektrode, de kathode, terwijl zij hun energie afgeven. De anode met daarop de microorganismen heet de bio-anode en is het eerste cruciale onderdeel van de biobrandstofcel omdat daar de elektronen geproduceerd worden. In **Hoofdstuk 2** werd de stroomproductie van bioanodes op verschillende elektrodematerialen bestudeerd met verschillende karakterisatietechnieken. Elk materiaal resulteerde in een andere stroomdichtheid, die niet alleen verklaard kon worden door verschillen in specifiek oppervlak. De microorganismen

produceerden aanzienlijke stroomdichtheden tot  $4.6 \text{ A/m}^2$  op een vlakke grafietelektrode. Deze limietstroom gaf de maximale biomassa-activiteit weer.

## **Tweede cruciale onderdeel: de elektronenaccepterende kathode**

Om elektriciteit te produceren, moeten de elektroden van de bioanode naar de kathode stromen. Aan de kathode vindt een reductiereactie plaats. Zuurstof is de meest aantrekkelijke elektronenacceptor vanwege de beschikbaarheid en de hoge potentiaal. Om de zuurstofreductiereactie op aanvaardbare snelheid te laten plaatsvinden, is echter een katalysator nodig. De meest gebruikte katalysator voor zuurstofreductie is Pt, maar vanwege de hoge kosten zijn er andere goedkope en duurzame katalysatoren nodig. Om het functioneren van de kathode te verbeteren, hebben we drie strategieën gevolgd.

De eerste strategie was het vervangen van zuurstofreductie door de reductie van  $\text{Fe}^{3+}$  naar  $\text{Fe}^{2+}$ , zoals beschreven in **Hoofdstuk 3 en 4**. Het gevormde  $\text{Fe}^{2+}$  werd tegelijkertijd geoxideerd naar  $\text{Fe}^{3+}$  door de bacterie *Acidithiobacillus ferrooxidans*, met zuurstof als elektronenacceptor. Omdat  $\text{Fe}^{3+}$  alleen oplosbaar is bij lage pH ( $<2.5$ ) en de bioanode bij neutrale pH werkt, was een bipolair membraan gebruikt om het pH verschil in stand te houden. In dit bipolair membraan wordt water gesplitst in  $\text{H}^+$  en  $\text{OH}^-$ . De gevormde  $\text{H}^+$  migreert naar de kathode zodat de lage pH gehandhaafd wordt, terwijl het gevormde  $\text{OH}^-$  naar de anode bij neutrale pH migreert om de daar gevormde protonen te neutraliseren. De maximale vermogensdichtheid was  $1.2 \text{ W/m}^2$  bij een stroomdichtheid van  $4.5 \text{ A/m}^2$ . Het vervangen van zuurstof door  $\text{Fe}^{2+}$  verbeterde de prestaties van de kathode aanzienlijk. Uitdagingen met betrekking tot het bipolair membraan waren de energie die nodig is om water te splitsen en het transport van andere ionen dan  $\text{H}^+$  en  $\text{OH}^-$ .

De tweede strategie, zoals beschreven in **Hoofdstuk 5**, was het groeien van microorganismen op de kathode om zuurstofreductie te katalyseren. Deze microorganismen kwamen uit nitrificerend slib en groeiden bij drie potentialen. In alle gevallen ontwikkelde zich een zuurstofreducerende biofilm, terwijl de stroomproductie verschillend was bij iedere potentiaal. De stroomdichtheid geproduceerd door de biofilm was aanzienlijk hogere dan op een grafietelektrode zonder biofilm. Limitaties onstonden ten gevolge van de kathodepotentiaal (ladingsoverdracht) en massatransport van zuurstof.

De derde strategie, zoals beschreven in **Hoofdstuk 6**, bestudeerde de reductie van  $\text{Cu}^{2+}$  naar metallisch Cu. De voordelen waren tweeledig: puur Cu werd herwonnen, wat dit een mogelijk aantrekkelijk proces maakt voor winning van koper uit afvalstromen, en  $\text{Cu}^{2+}/\text{Cu}$  leek als een katalysator te fungeren voor zuurstofreductie, omdat de kathode beter functioneerde in de aanwezigheid van zuurstof. Het bipolair membraan werd gebruikt om de lage pH aan de

kathode te handhaven en neerslag van  $\text{Cu}^{2+}$  te voorkomen. De maximale vermogensdichtheid was  $0.8 \text{ W/m}^2$ , vergelijkbaar met andere goed functionerende biobrandstofcellen.

### **Eerste stap naar praktische toepassing: opschalen**

Terwijl de meeste studies naar de biobrandstofcel gedaan worden in kleine lab-schaal reactoren, is het uitermate belangrijk dat ervaringen worden opgedaan op grotere schaal, omdat nieuwe limitaties kunnen ontstaan die op kleine schaal niet naar voren komen. We hebben de studie naar de eerste opgeschaalde biobrandstofcel in de wereld voortgezet in **Hoofdstuk 7**. Deze biobrandstofcel had een membraanoppervlak van  $0.5 \text{ m}^2$  en een totaal volume van 5 L. Om de eerder gevonden kathodelimitaties te verminderen, gebruikten we de reductie van  $\text{Fe}^{3+}$  naar  $\text{Fe}^{2+}$  met tegelijkertijd biologisch oxidatie van  $\text{Fe}^{2+}$ . Het bipolair membraan werd gebruikt om de lage pH aan de kathode te handhaven zodat  $\text{Fe}^{3+}$  in oplossing zou blijven. De opgeschaalde biobrandstofcel werd 37 dagen getest en bereikte een maximale vermogensdichtheid van  $2.0 \text{ W/m}^2$ , een factor 1.4 hoger dan met zuurstof in vorige studie. Analyse van de interne weerstand liet zien dat zowel anode als kathodeweerstand met een factor 10 afnam gedurende de 27 dagen dat de biobrandstofcel bedreven werd. Ondanks de verbetering van de kathode door het vervangen van zuurstof met  $\text{Fe}^{3+}$ , bleef de kathode de limiterende factor, en droeg bij aan 58% van de totale interne weerstand.

### **Maximale geschatte vermogensproductie in de biobrandstofcel**

In het begin van het onderzoek naar de biobrandstofcel, in 2002, namen de gerapporteerde vermogensdichtheden toe vanaf  $1\text{-}10 \text{ mW/m}^2$  met ruwweg een factor 10 per jaar. Sinds 2005 lijken de vermogensdichtheden te stabiliseren op een niveau van ongeveer  $2 \text{ W/m}^2$ , terwijl het aantal groepen dat onderzoek doet naar de biobrandstofcel enorm is gestegen. De vraag die in **Hoofdstuk 8** gesteld wordt is of de vermogensdichtheid in de biobrandstofcel de limiet bereikt heeft, of dat verdere vermindering van energieverliezen nog kan resulteren in een toename in vermogensdichtheid. We laten zien dat er nog een factor 10 in vermogen te winnen is, en dat de geschatte maximum vermogensdichtheid in de biobrandstofcel  $17.3 \text{ W/m}^2$  of  $3,460 \text{ W/m}^3$  is. Dit is een factor 3 hoger dan geproduceerd in een anaerobe vergister bij vergelijkbare belasting van  $25 \text{ kg COD/m}^3/\text{d}$ . Bij deze geschatte maximale prestatie is de energie-efficiëntie 63%, terwijl de energie-efficiëntie van anaerobe vergisting 30% is. Om deze geschatte vermogensdichtheid te bereiken, moet verder onderzoek zich richten op de kathode omdat dit nog steeds de limiterende factor is voor het grootste deel van de energieverliezen zorgt. Uiteindelijk moet de haalbaarheid van de biobrandstofcel bewezen worden bij het omzetten van echte afvalwaters op grotere schaal.



# List of publications

## Publications

- Ter Heijne, A.; Liu, F.; van Rijnsoever, L.S.; Saakes, M.; Hamelers, H.V.M.; Buisman, C.J.N. Improvement of the cathode of a scaled-up Microbial Fuel Cell. Submitted.
- Michaelidou, U.; Ter Heijne, A.; Euverink, G.J.; Hamelers, H.V.M.; Stams, A.J.M.; Geelhoed, J.S. Electrochemical performance and microbial communities of titanium-based anodic electrodes in a Microbial Fuel Cell. Submitted.
- Hamelers, H.V.M.; Ter Heijne, A.; Stein, N.; Rozendal, R.A.; Buisman C.J.N. 2011. Butler-Volmer-Monod model for describing bio-anode polarization curves. *Bioresource Technology*, 102 (1), 381-387.
- Ter Heijne, A.; Strik, D.P.B.T.B.; Hamelers, H.V.M.; Buisman, C.J.N. 2010. Cathode potential and mass transfer determine performance of oxygen reducing biocathodes in Microbial Fuel Cells. *Environmental Science & Technology*, 44 (18), 7151-7156.
- Ter Heijne, A.; Liu, F.; Van der Weijden, R.; Weijma, J.; Buisman, C.J.N.; Hamelers, H.V.M. 2010. Copper recovery combined with electricity production in a Microbial Fuel Cell. *Environmental Science & Technology*, 44 (11), 4376-4381.
- Hamelers, H.V.M.; Ter Heijne, A.; Sleutels, T.H.J.A.; Jeremiasse, A.W.; Strik, D.P.B.T.B.; Buisman, C.J.N. 2010. New applications and performance of bioelectrochemical systems. *Applied Microbiology and Biotechnology*, 85 (6), 1673-1685.
- Dekker, A.; Ter Heijne, A.; Saakes, M.; Hamelers, H.V.M.; Buisman, C.J.N. 2009. Analysis and improvement of a scaled-up and stacked Microbial Fuel Cell. *Environmental Science & Technology*, 43 (23), 9038-9042.
- Ter Heijne, A.; Hamelers, H.V.M.; Saakes, M.; Buisman, C.J.N. 2008. Performance of non-porous graphite and titanium-based anodes in microbial fuel cells. *Electrochimica Acta* 53 (18), 5697-5703.
- Strik, D.P.B.T.B.; Ter Heijne, A.; Hamelers, H.V.M.; Saakes, M.; Buisman, C.J.N. 2008. Feasibility study on Electrochemical Impedance Spectroscopy for Microbial Fuel Cells: measurement modes & data validation. *ECS Transactions* 13 (21), 27-41.

Ter Heijne, A.; Hamelers, H.V.M.; Buisman, C.J.N. 2007. Microbial fuel cell operation with continuous biological ferrous iron oxidation of the catholyte. *Environmental Science & Technology* 41 (11), 4130-4134.

Ter Heijne, A.; Hamelers, H.V.M.; de Wilde, V.; Rozendal, R.A.; Buisman, C.J.N. 2006. A bipolar membrane combined with ferric iron reduction as an efficient cathode system in microbial fuel cells, *Environmental Science & Technology*, 40 (17), 5200 – 5205.

## **Patent**

Ter Heijne, A.; Hamelers, H.V.M.; Buisman, C.J.N. 2007. Device comprising a new cathode system and method for generating electrical energy with use thereof (WO/2007/094658). Filing date: February 13, 2007.



# Acknowledgements

## Acknowledgements

Although I am the author of this book, I realize that it would never be finished in this form without the contributions of many others. On these pages I would like to thank everyone around me, and mention some people specifically.

First of all I would like to thank my supervisors.

Bert, I admire your involvement in both my research as my personal development. You have always been able to increase my enthusiasm and you keep on amazing me with your knowledge, ideas, and insights. It is great that you have well-thought answers to all questions. I enjoyed all our discussions and learned many things from you.

Cees, I highly appreciate your openness to (almost) all initiatives. Your vision and involvement made my research and the department nice topics for inspiring discussions with you.

Michel, your knowledge and experience has greatly helped my progress in research. Your Tuesdays in Wageningen were a good moment to look in detail at my results and to make many calculations and schematics. Your input resulted in decent lab setups and measurement equipment and methods.

Vinnie, thanks for all your help. At the start of my research you made sure that I could build my first microbial fuel cell. I always enjoyed our discussions and your practical solutions were very valuable.

Special thanks go out to the (MSc) students that helped me to study and improve the Microbial Fuel Cell: Fei, Arjan, Tim, Xinying, Lucas, Jingjing, and Laura. I enjoyed working with you and I have learned a lot from you.

When I started my research, the bioenergy group in Wageningen consisted of Bert, Vinnie, René, Jan, Kirsten and me, and we had just started the microbial fuel cell and bio-energy research. Meanwhile, we have grown to a large group of enthusiastic researchers. David, Kirsten, Tom, Nienke, Ruud, Adriaan, Tim, Marjolein, Mieke, Ralph, Alexandra, Doga, Bruno, Fei and Michel, thanks for the nice discussions and chats. My 'buddy' Tom: thanks for reading all my writings so critically, for your always striking remarks. It was great to be in the same stage of our PhD together.

Thanks to the people and companies that supported the bio-energy theme at Wetsus. I would like to especially thank the theme managers Maarten van Riet and Pieter Hack, and Marcel Geers, Kristan Goeting and Niels Groot, but also everyone else, for their enthusiasm and their critical and constructive questions and comments. Besides, I would like to thank

Urania for sharing our thoughts. At Wetsus, I have enjoyed the hours with the SEM first with Janneke, later with Astrid. All colleagues at Wetsus: I enjoyed the talks to you all.

I am very happy with my paranimphs Alex and Kirsten and that they are supporting me during my defense. We started almost at the same time with our project and we have shared many important moments in each others life. Thank you both for your support.

There are so many people at the department that I need to thank, that I will not list everyone here as I am afraid to forget someone. I enjoy the open atmosphere and the nice coffee breaks (with or without cake) with you all. Special thanks go out to my office mates Roel (I enjoyed our morning coffee ritual) and Marjolein (for the nice chats and discussions), to Darja (for all the chats about our pregnancy and our little girls), to Simon (for the good discussions during lunch walks), to Olivier (for impedance and all discussions), to Jan K. (for the vegetable garden talks), to Christel, Mieke, and Tânia (for the good chats), to Maarten (for your ideas and input), to Nora (for helping me to translate the propositions), and to Martijn B. (for the dinners with colleagues). Furthermore, I would like to thank the analytical staff and Liesbeth, Anita, and Patricia.

Besides a good working environment, my personal environment is of course very important. I would like to mention my closest friends here for they are very important to me. Dear Iris, Nynke, Marleen, Karin, Suzanne, Janneke, Sara, Vera, and Anda, I enjoy spending time with you. Grindhorst housemates Cosy, Jannie, Nico, Hermen, Bas, Chris, Renske, Vera, Tim, Joyce, Annemarie, Harke, Hanneke, Maaïke, Niklas, Nienke, Madeleine, Steven, Kim, Sjors, Idger, and Sunny, I have special memories of you and the typical Grindhorst discussions during dinner.

My family-in-law, thanks for being there.

I dedicated this thesis to my parents. Dear ‘papa en mama’, thank you for your neverending support and interest in what I am doing, and for always taking care of me and my family when I am in need. My sister Marlien, the same holds for you. You have helped me a lot during the last few years.

And, saving the best for last...

Thank you Dirk, love of my life, and Tilia, our little big girl. I love you.



## About the author

Annemiek ter Heijne (1982) was born in Enschede, The Netherlands. She obtained her BSc in Environmental Sciences at Wageningen University in 2003. After her BSc, she spent one fulltime year as a board member of the Wageningen Student Union, where the support of students in educational boards was one of her main tasks. During her Masters program, she spent four months in Sogndal, Norway studying geology and ecology to broaden her perspective. In 2006, she graduated with honors for her MSc in Environmental Sciences at Wageningen University. Her MSc thesis aimed at improving the cathode of the Microbial Fuel Cell and resulted in a patent and one of the publications in this PhD thesis. After graduation, she continued the research on Microbial Fuel Cells as a PhD student at Wageningen University within the Wetsus framework. Besides the research itself, she enjoyed to supervise MSc students, to assist with courses, to join the activities at the department, and to follow new courses to develop her personal and professional skills. She is currently involved in identifying innovative technologies for a sustainable biobased economy.









Netherlands Research School for the  
Socio-Economic and Natural Sciences of the Environment

# C E R T I F I C A T E

The Netherlands Research School for the  
Socio-Economic and Natural Sciences of the Environment  
(SENSE), declares that

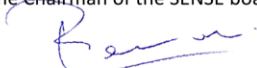
***Annemiek ter Heijne***

born on 23 March 1982 in Enschede, The Netherlands

has successfully fulfilled all requirements of the  
Educational Programme of SENSE.

Wageningen, 3 December 2010

the Chairman of the SENSE board



Prof. dr. Rik Leemans

the SENSE Director of Education



Dr. Ad van Dommelen

The SENSE Research School has been accredited by the Royal Netherlands Academy of Arts and Sciences (KNAW)



K O N I N K L I J K E N E D E R L A N D S E  
A K A D E M I E V A N W E T E N S C H A P P E N



The SENSE Research School declares that **Mrs. Annemiek ter Heijne** has successfully fulfilled all requirements of the Educational PhD Programme of SENSE with a work load of 51 ECTS, including the following activities:

#### SENSE PhD courses

- o Environmental Research in Context
- o Research Context Activity: Co-organization of MSc course on 'Renewable Energy: Sources, Technology & Applications' (Wageningen, March-April 2007).
- o Physical Modelling
- o Uncertainty Analysis

#### Other PhD and MSc courses

- o Environmental Biotechnology
- o PhD competence assessment
- o Teaching and supervising thesis students

#### Research and Management Skills

- o Writing PhD research proposal
- o Co-organization of Masterclass Sustainable Bio-energy and Innovation (2009)
- o Organization of Bio-Energy meetings (Wageningen/Wetsus)

#### Oral Presentations

- o Microbial fuel cells for electricity production, SENSE symposium Sensible Water Technology, 12-13 April 2007, Leeuwarden, The Netherlands
- o Performance of non-porous graphite and titanium-based anodes in Microbial fuel cells. Mini-Microbial fuel cell symposium, 19-20 November 2007, Lyon, France.
- o Analysis of bio-anode kinetics using a minimal model, Microbial fuel cells: First International Symposium, 26-29 May 2008, Pennsylvania, USA
- o Experiences with scaling-up the Microbial fuel cell, Wetsus Congress, 6 October 2009, Leeuwarden, The Netherlands

SENSE Coordinator PhD Education and Research

Mr. Johan Feenstra

Cover design by my father Eddy ter Heijne

This thesis was printed on recycled paper and with vegetable oil-based inks to minimize harm to the environment, by drukkerij Macula bv: [www.macula.nl](http://www.macula.nl).